Invited review article

Water-fluxed melting of the continental crust: A review

Roberto F. Weinberg [a,*], Pavlína Hasalová [b,c]

[a] School of Earth, Atmosphere and Environment, Monash University, Clayton, VIC 3800, Australia
[b] Centre for Lithospheric Research, Czech Geological Survey, Klárov 3, Prague 1, 11821, Czech Republic
[c] Institute of Geophysics ASCR, v.v.i., Boční II/1401, Prague 4, 14131, Czech Republic

ARTICLE INFO

ABSTRACT

Water-fluxed melting, also known as fluid- or water-present melting, is a fundamental process in the differentiation of continents but its importance has been underestimated in the past 20 years during which research efforts focused mostly on dehydration melting reactions involving hydrate phases, in the absence of a separate aqueous phase. The presence of a free aqueous phase in anatectic terranes influences all major physical and chemical aspects of the melting process, from melt volumes, viscosity and ability to segregate from rock pores, to melt chemical and isotopic composition. A review of the literature shows that melting due to the fluxing of aqueous fluids is a widespread process that can take place in diverse tectonic environments. Active tectono-magmatic processes create conditions for the release of aqueous fluids and deformation-driven, transient high permeability channels, capable of fluxing high-temperature regions of the crust where they trigger voluminous melting. Water-fluxed melting can be either congruent in regions at the water-saturated solidus, or incongruent at suprasolidus, P–T conditions. Incongruent melting reactions can give rise to peritectic hornblende, or to nominally anhydrous minerals such as garnet, sillimanite or orthopyroxene. In this case, the presence of an aqueous phase is indicated by a mismatch between the large melt fraction generated and the much smaller fractions predicted in its absence.

The relatively small volumes of aqueous fluids compared to that of rocks imply that melting reactions are generally rock buffered. Fluids tend to move upwards and down temperature. However, there are cases in which pressure gradients drive fluids up temperature, potentially fluxing suprasolidus terranes. Crustal regions at conditions equivalent to the water-saturated solidus represent a natural impediment to the up-temperature migration of aqueous fluids because they are consumed in melting reactions. In this case, continued migration into supra-solidus terranes take place through the migration of water-rich melts. Thus, melts become the transport agent of water into supra-solidus terranes and responsible for water-fluxed melting. Other processes, such as the relatively rapid fluid migration through fractures, also allow regional aqueous fluids to by-pass the water-saturated solidus fluid trap and trigger melting above solidus conditions. When aqueous fluids or hydrous melts flux rocks at supra-solidus conditions, they equilibrate with the surroundings through further melting, decreasing water activity and giving rise to undersaturated melts. It is in these conditions that hornblende or anhydrous peritectic phases are stabilized. Unlike dehydration melting, the melt fraction generated in this case is not limited by the water contained in hydrous minerals but by the volume of water added to the system. Unlike melting at the water-saturated solidus, these melts are capable of rising without freezing and do give rise to upper crustal granitic bodies.

Contents

* Corresponding author. Tel.: +61 3 990 54902; fax: +61 3 990 54903.
E-mail addresses: roberto.weinberg@monash.edu (R.F. Weinberg), pavlina.hasalova@geology.cz (P. Hasalová).

1. Introduction

"Water is the driving force for all Nature", Leonardo da Vinci.

Water even in very small quantities influences dramatically a variety of physical and chemical properties of geological materials such as melting temperatures, melt chemistry, viscosity and density, phase equilibria, and reaction kinetics. Therefore water affects fundamental magmatic processes ranging from anatexis to magma ascent, and crystallization to eruption. Migration of granitic anatectic magmas is the main process of crustal differentiation controlling the thermal and chemical structure of continents (Brown, 2013; Sandiford and McLaren, 2002) and ultimately the origin of continents (Campbell and Taylor, 1983).

Crustal melting may involve the presence of a free H_2O phase. This is referred to as water-present, water-assisted or water-fluxed melting. Alternatively melting may involve the breakdown of a hydrous phase, such as biotite, muscovite or amphibole, and is referred to as dehydration melting, hydrate-breakdown melting, or vapour or fluid-absent melting. Water-present melting can be either congruent or incongruent. The latter may occur in the presence of low water activity fluids but it may also occur in the absence of an aqueous fluid phase, where water is supplied by the breakdown of hydrous minerals. Whilst water-fluxed melting is expected to be limited because of low porosity of the crust at depth, the presence of a water-rich fluid phase lowers the solidus temperature so that melting can take place at amphibolites facies conditions, with the potential to produce voluminous melt (e.g. Yardley and Barber, 1991a).

The dominant paradigm until the 1980s was that an aqueous fluid phase was generally present throughout the crust, controlling metamorphic reactions, including melting (Tuttle and Bowen, 1958; Wyllie, 1977). By the end of that decade this perception had shifted, driven by the realization that the low porosity of high-grade rocks meant that lower to mid-crustal regions will only contain small volumes of free H_2O. This perception shift was perhaps led by three seminal papers published in the mid-1980s (Clemens and Vielzeuf, 1987; Powell, 1983; Thompson, 1983). These papers concluded that anatexis of lower to mid-crustal regions is likely characterized by fluid-absent

melting. Research efforts then turned towards the control of dehydration-melting reactions in the generation of crustal magmas (e.g. Johannes and Holtz, 1991; Patiño Douce and Johnston, 1991; Vielzeuf and Holloway, 1988).

A number of arguments were put forward to explain why water-fluxed melting would be a process of minor importance. These arguments focused around three main issues (e.g. Berger et al., 2008; Brown, 2013; Clemens and Vielzeuf, 1987; Vernon and Clarke, 2008): (i) There are only small volumes of water stored in stable lower or middle crust, limiting access of significant fluid volumes to rocks (Ramberg, 1952; Yardley, 2009; Yardley and Valley, 1997). Whilst it was accepted that active tectonics could modify this, it was argued that fluids are likely to be channelled into fractures where they will have little interaction with the surroundings (Clemens and Vielzeuf, 1987). (ii) Water-saturated melts are unable to rise because decompression leads to solidification. Thus, such melts do not impact on the thermal and chemical structure of the crust and explain magmas that remained close to the source (Collins et al., 1989; Finger and Clemens, 1995; Wickham, 1987). (iii) Water-saturated solidus conditions in the crust form a trap for aqueous fluids where they are consumed by melting reactions. In this case, the volume decrease accompanying water-saturated melting causes a pressure drop attracting more fluids into the area in a positive feedback and trapping the melts. The question then becomes how does water flow into rocks that are at or above the water-saturated solidus?

Combined, these issues have created the perception that water-fluxed melting is unimportant as clearly expressed by Brown (2007) when referring to the beginning of crustal melting: "Heat generally will be the principal rate control at the crustal scale, whereas deformation as a result of regional stress will be the enabling mechanism." In this paper, we review the literature to argue that water-fluxing is a common process, even if only transient, and that our understanding of the processes involved remains relatively limited. In most cases of water fluxing, there is insufficient water to saturate large rock volumes and so the system is rock-dominated and melts generated are the water-deficient melts of Clemens and Droop (1998), where small volumes of free water may result in voluminous generation of water-undersaturated melts. We will argue that it is in the nature of active tectonics and magmatism, particularly of crustal shortening events and underplating of mafic magmas, to force the flow of water-rich fluids into hot crust.

We start this paper by an introductory section where we expand on the three main issues listed above and used to argue for the minor importance of water-fluxed melting and advance some possible solutions. This is followed by a broad review of the literature focusing first on the melt products and their physical and chemical properties, and then on natural examples of water-fluxed melting. This is followed by a discussion of structural control on water-fluxed melting, including the role of shear zones and then examples of possible recycling of magmatic fluids are described. Finally, we address the three main issues, discuss the literature and conclude that a number of active processes in migmatitic terrane overcome the apparent limitations of water-fluxed melting explaining why this is a widespread process that plays a crucial role in the evolution of many anatectic terranes, the genesis of granitic terranes and ultimately in the evolution of the crust.

1.1. Terminology

In this paper we use mineral abbreviations from Kretz (1983). We use the term aqueous fluids to refer to fluids with only small quantities of other volatiles such as CO_2, and we use water as general H_2O, independently of its state (vapour or liquid). Melt here refers to silicate melts. Metatexite refers to partially molten rocks that have maintained coherence, as opposed to diatexite where melt fraction was sufficient to disaggregate the solid framework (Brown, 1973). In migmatites, neosome refers to the rock modified by melting

and composed of leucosome, referring to "quartzo-feldspathic material related to melting but not necessarily preserving liquid compositions" (Brown, 2013), and a melt-depleted melanosome, being the predominantly solid residuum after melting and melt segregation. Water-saturated melt has water activity of one, $aH_2O = 1$, whereas water-undersaturated melts have $aH_2O < 1$.

Melting reactions in the presence of a general aqueous fluid phase, and those in their absence, have been referred to in a number of ways in the search for a precise way of describing the processes and differentiating between them. The issue with the terminology is that water is always present and plays a fundamental role in lowering the solidus temperature of rocks in both types of melting reactions. We use the terms water-fluxed melting or water-present melting to refer to the general case where aqueous fluids form a free phase. These are simple and widely used terms. We use water-fluxed melting specifically for natural systems dominated by the ingress of external water, and water-present melting, when referring to static situations, such as experiments. In the absence of an aqueous fluid, melting takes place through dehydration melting reactions involving hydrate phases, such as muscovite, biotite, or amphibole. These reactions have typically been referred to as dehydration-melting reactions, hydrate-breakdown melting, vapour-absent or water-absent reactions. In this paper we will use the term dehydration melting reaction.

2. Issues with water-fluxed melting

2.1. Small volumes of aqueous fluids stored in the lower or middle crust

Thompson (1983) made a concise case against the long-term presence of aqueous fluids during most dynamic processes, concluding that "there is actually little compelling evidence to suggest that the presence of aqueous fluids is common during metamorphism of the middle and lower crust, and the mantle, for the duration of most dynamic processes, including partial melting." He argued that the hot crust is unlikely to see pervasive fluid flow due to very low porosity in the ductile crust (Ramberg, 1952; Yardley and Barber, 1991b). However, Ingebritsen and Manning (2010) discussed evidence for dynamic responses of permeability, where it greatly increases above the long-term crustal mean average in response to dewatering and aqueous fluid production on short time scales. Thompson (1983) also argued that excess fluids are likely to develop widely spaced channelways through the crust (Fyfe et al., 1978) as evidenced for example by the preservation of pre-metamorphic isotopic heterogeneities (e.g. Butler et al., 1997; Valley and O'Neil, 1984). Clemens and Vielzeuf (1987) added that fluids channelled into structural discontinuities, such as faults, will have minor effect on the surroundings. However, we will see below that this is not always the case (e.g. the Karakoram Shear Zone; Reichardt and Weinberg, 2012a).

2.2. How to extract water-rich melt from the source and form plutons and batholiths?

Clemens and Vielzeuf (1987) noted that magmas in the upper crust are markedly undersaturated in water, from which they inferred that they were generated by dehydration melting. Whilst water-saturated melts solidify upon decompression, many natural examples of water-fluxed melting have not generated water-saturated melting (see Section 5). These melts formed in the presence of free water in what Clemens and Droop (1998) termed water deficient environments. Experimental studies on the anatexis of metapelites (Holtz and Johannes, 1991) determined that at temperatures between 700 and 800 °C melt remained water-undersaturated even though aqueous fluids were needed to trigger melting. Significantly, water-fluxed melts that are undersaturated are also upward mobile, with the potential to form plutonic intrusions.
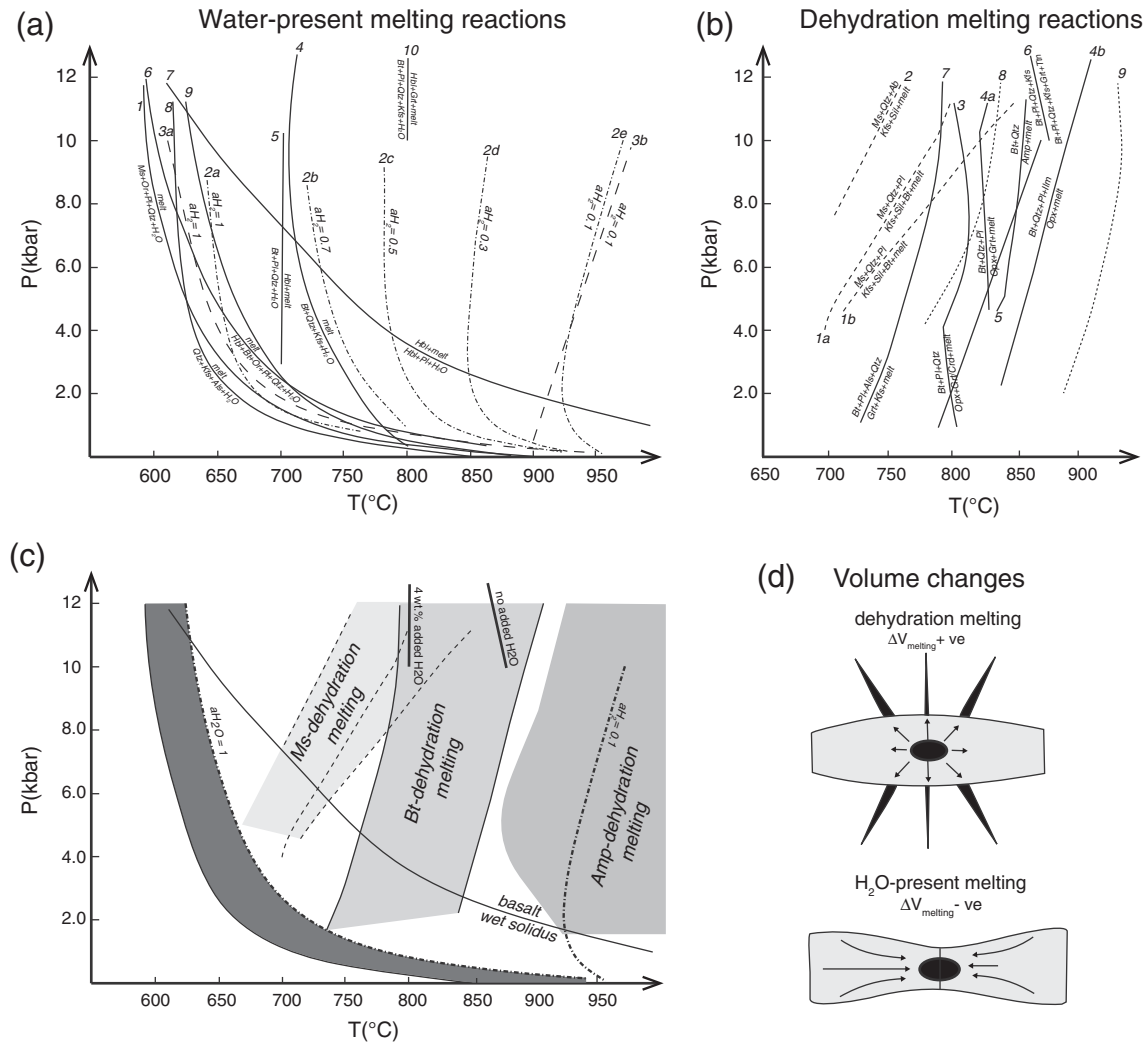
Fig. 1. Experimentally determined water-present melting reactions (a) and dehydration melting reactions (b). (a) 1 − H$_2$O saturated Ms-granite solidus from Huang and Wyllie (1973); 2 − H$_2$O saturated solidus in Qtz + Or + Ab + H$_2$O system from Johannes (1985) with melt aH$_2$O = 1 (2a), aH$_2$O = 0.7 (2b), aH$_2$O = 0.5 (2c), aH$_2$O = 0.3 (2d) and aH$_2$O = 0.1 (2e); 3 − melting reaction Qtz + Pl + Kfs + H$_2$O = melt from Stevens and Clemens (1993) with aH$_2$O = 1 (3a) and aH$_2$O = 0.1 (3b); 4 − Bt + Qtz + Kfs + H$_2$O = melt melting reaction from Peterson and Newton (1989); 5 − H$_2$O-saturated melting of tonalite Bt + Pl + Qtz + H$_2$O = Hbl + melt from Büsch et al. (1974); 6 − tonalite H$_2$O-saturated solidus from Yoder and Tilley (1962); 7 − wet basalt solidus from Green (1982); 8 − H$_2$O-saturated melting reaction Qtz + Kfs + Als + H$_2$O = melt from Johannes and Holtz (1996); 9 − H$_2$O-saturated granite solidus (Qtz + Ab + Or + H$_2$O = melt) from Ebadi and Johannes (1991); 10 − melting reaction (Bt + Pl + Qtz + Kfs + H$_2$O = Hbl + Grt + melt) of gneiss with 4 wt.% added H$_2$O from Gardien et al. (2000). For comparison see position of similar reaction 6 in (b) with no added water. (b) 1 − Ms-dehydration melting of muscovite–biotite schist (1a) and muscovite schist (1b) from Patiño Douce and Harris (1998); 2 − Ms-dehydration melting from Pëto (1976); 3 − Bt-dehydration melting of metagreywacke from Vielzeuf and Montel (1994); 4a,b − Bt-dehydration melting of metagreywacke/gneiss from Patiño Douce and Beard (1995, 1996); 5 − Bt-dehydration melting in MASH system from Vielzeuf and Clemens (1992); 6 − Bt-dehydration melting of gneiss from Gardien et al. (2000); 7 − Bt-dehydration melting of metapelite from Le Breton and Thompson (1988); 8 − Amphibole dehydration melting of amphibolite from Rushmer (1987); 9 − amphibolite dehydration melting of basalt from Rushmer (1989). (c) Summarizing diagram comparing H$_2$O-present and absent melting reactions. Note different slopes and solidus T. Thick solid lines represent similar melting reactions with no added water and with 4 wt.% added water (from Gardien et al., 2000). (d) Schematic diagram depicting difference in volume changes during water-present and dehydration melting (from Clemens and Droop, 1998). Water-present melting results in negative volume change, in contrast to dehydration melting which results in positive volume change and brittle failure and melt expulsion into the host. Rock volume is represented by grey deformed rectangles, melt is black.

2.3. How does water invade rocks at conditions above their solidus?

There are numerous ways in which fluids can be delivered to hot lower and middle crust and circumvent the solidus isotherm trap: (i) intrusion and crystallization of water-rich magmas releasing water to its surroundings (e.g. Annen and Sparks, 2002; Finger and Clemens, 1995; Pattison and Harte, 1988; Symmes and Ferry, 1995; Yardley and Barber, 1991a); (ii) pervasive intrusion of water-rich magmas out of equilibrium with their dry (low water activity) surroundings triggering melting; (iii) diffusion or advection of fluids from a rock undergoing sub-solidus dehydration reaction to another above its water-saturated solidus (Droop and Brodie, 2012; White and Powell, 2010; White et al., 2011b, 2005); or (iv) influx of fluids released at depth by

underthrusted water-rich rocks (Cloos, 1984; Le Fort et al., 1987) rising through zones of localized high-strain (e.g. Berger et al., 2008; Genier et al., 2008; Johnson et al., 2001) or fracture systems (Sawyer, 2010; Ward et al., 2008).

3. Water-fluxed melting: reactions, composition and physical characteristics

Water-fluxed melting reactions are significantly different from dehydration melting reactions (Fig. 1, Tables 1 and 2; e.g. Patiño Douce and Harris, 1998). The differences are so significant that Clemens and Watkins (2001) suggested that "dehydration melting reactions occurring at temperatures of the granulite facies are the only

Table 1
Key dehydration melting reactions. For comparison see Table 2 where water-present melting reactions are listed.

	Peritectic mineral	Melt composition	PT conditions	Protolith type	Reference
Ms-dehydration melting					
Ms + Pl + Qtz = Als + Kfs + melt	Als, Kfs	Kfs-rich melt	MP MT	metapelite	Thompson, 1983; Pĕto, 1976; Spear, 1993
Bt-dehydration melting					
Bt + Als + Qtz = Grt/ Crd + Kfs + melt	Grt, Crd, Kfs	Kfs-rich melt	Crd will form at LP, Grt at HP, both at intermediate T	metapelite (no Pl)	Le Breton and Thompson, 1988; Spear, 1993
Bt + Pl + Als + Qtz = Grt/ Crd + Kfs + melt	Grt, Crd, Kfs	Kfs + Pl in melt	Crd will form at LP, Grt at HP, both at intermediate T	metapelite	Le Breton and Thompson, 1988; Spear, 1993
Bt + Pl + Qtz = Opx (+Cpx + Grt) + melt	Opx, Cpx, Grt (depends on rock composition)	Kfs + Pl in melt	variable, type of peritectic mineral depends on rock composition and PT	metapsammite, metagranitoids, metatonalite	Thompson, 1982; Vielzeuf and Holloway, 1988; Vielzeuf and Montel, 1994; Patiño Douce and Beard, 1995, 1996
Amp-dehydration melting					
Hbl + Qtz = Pl + Opx + Cpx (+Grt) + melt Hbl + Pl = Cpx (+Grt + Opx + Amp) + melt	Pl, Opx, Cpx, Grt	Pl-rich melt	variable, type of peritectic mineral depends on rock composition and PT	metabasalt K-poor/Ca-rich amphibolite	Thompson, 2001; Moyen and Stevens, 2006; Wolf and Wyllie, 1994

Abbreviations: MP = medium pressure; MT = medium temperature; HP = high pressure; LP = low pressure; P = pressure; T = temperature

way that large volumes of granitic magma can be generated in the continental crust." The major differences between them are: (i) presence, type and composition of peritectic minerals and melts (Tables 1 and 2; Fig. 2); (ii) melting temperatures (Fig. 1); (iii) slope of the solidus curve (Fig. 1c) related to volume changes during melting (Fig. 1d); and (iv) initial water content of the melt. In this section, we start with a comparison of these two types of melting reactions and explore the impact of water. Then we describe the nature of peritectic minerals resulting from water-present melting. This is followed by a review of the geochemical signature of water-present melting. We finish the section with a discussion of the limitations of melting experiments in comparison to both natural observations and thermodynamic modelling.

3.1. Melting reactions

In dehydration melting reactions all water is derived from hydrous minerals (Table 1), and the melt produced is water undersaturated. By contrast, in the presence of an aqueous fluid phase, water is only limited by the rate of influx, and melting may produce water-rich or even water-saturated melts. Water-present melting reactions may be either congruent (generally at low T; reactions [1]–[14] in Table 2; all mineral reactions are quoted here with numbers in hard brackets corresponding to numbers in Table 2; Thompson, 1990; Yardley and Barber, 1991a; Stevens and Clemens, 1993; Patiño Douce and Harris, 1998; Vernon and Clarke, 2008) or incongruent at higher temperatures (Table 2) where melts generated are water undersaturated.

Water-present incongruent melting reactions form peritectic minerals, most commonly amphibole (e.g. reactions [15]–[21]; Büsch et al., 1974; Conrad et al., 1988; Mogk, 1992; Escuder-Viruete, 1999; Gardien et al., 2000), but also garnet and/or cordierite (e.g. reactions [22]–[33]; Otamendi and Patiño Douce, 2001; Patiño Douce and Harris, 1998; Yardley and Barber, 1991a), pyroxenes (e.g. reactions [34], [37] and [38]; Clemens, 1984; Gardien et al., 2000) and alumino-silicates (e.g. reactions [35] and [36]; Clemens, 1984; Icenhower and London, 1995; Thompson and Tracy, 1979).

The most common dehydration melting reactions involve muscovite, biotite or amphibole as the hydrous reacting phase. Ms-dehydration melting reactions occur at ~650–750 °C, are mildly P-dependent (Fig. 1b), and produce peraluminous granitic melts with high K/Na ratio. They typically produce peritectic alumino-silicates and K-feldspar (Table 1; e.g. Patiño Douce and Harris, 1998; Storre, 1972; Storre and Karotke, 1972). Biotite-dehydration melting reactions

of quartzo-feldspathic rocks begin at ~750–850 °C and are mildly P-dependent (Fig. 1b). Melts vary in their chemistry depending on protolith composition. Typical peritectic minerals are Grt, Opx, Crd, Kfs, Ttn, Ep (Table 1; e.g. Le Breton and Thompson, 1988; Patiño Douce and Johnston, 1991; Skjerlie and Johnston, 1993; Vielzeuf and Montel, 1994). Amphibole dehydration melting occurs at T ~850–900 °C, typically producing peritectic Opx, Cpx and/or Grt (Fig. 1b and Table 1; e.g. Rushmer, 1987; Wyllie and Wolf, 1993; Wolf and Wyllie, 1994). Melts vary in geochemical characteristics, depending on protolith composition and temperature, and generally are dioritic to granodioritic and peralkaline to metaluminous in composition, and have lower K/Na ratio than other melts.

Melt inclusions in minerals are potentially useful indicators of the nature of melting reactions (e.g. Acosta-Vigil et al., 2010; Bartoli et al., 2013a, 2013b; Höller and Hoinkes, 1996). Bartoli et al. (2013b) measured between 3.1 and 7.6 wt.% H_2O in S-type granites, interpreted as indicative of an initial melting at water-saturated conditions progressing into mica-breakdown and lower water content. However, there is still significant discussion about the integrity of melt inclusions and questions about the interpretation of their origin and significance (e.g. Clemens, 2009; Vernon, 2007).

3.2. Role of water in melting reactions

Increasing water activity progressively decreases the melting temperature of granitic rocks (e.g. Becker et al., 1998; Castro et al., 2000; Ebadi and Johannes, 1991; Maaloe and Wyllie, 1975; Naney, 1983; Naney and Swanson, 1980). Ebadi and Johannes (1991) estimated the solidus T at aH_2O between 0 and 1 at 10 kbar for quartzo-feldspathic rocks and found that it decreases considerably when aH_2O increases slightly from zero. Water-present melting experiments on granodiorite and tonalite (Wyllie et al., 1976) show that K-feldspar is the first phase to disappear from the palaeosome (also found by Sawyer, 1998, in a natural example). In this case the volume of granite melt that could have been generated at a given temperature is limited by the amount of K-feldspar in the protolith.

Water also greatly enhances reaction rates during melting (Acosta-Vigil et al., 2006; Rubie, 1986). Brearley and Rubie (1990) studied experimentally the effect of H_2O on reaction pathways during breakdown of muscovite. Surprisingly, they found that in H_2O-saturated experiments, a metastable paragenesis developed that reduced the free-energy of the system reducing the driving force for the

Table 2
Summary of the main water-present melting reactions as determined from experimental and natural studies.

	Melting reaction	P–T conditions	Rock type	Reference
No peritectic mineral				
[1]	$Qtz + Pl (Ab) + Kfs (Or) + H_2O = melt$			e.g. *Johannes (1985); Ebadi and Johannes (1991); Stevens and Clemens (1993); Sawyer (1998); Vernon et al. (2003)*
[2]	$Bt + Sil + Kfs + Qtz + H_2O = melt$	650–750°C/4–5.5kbar	KFMASH system, pelite	*Yardley and Barber (1991a)*
[3]	$Kfs + Sil + Bt + Grt + Qtz + H_2O = melt$	650–750°C/4–5.5kbar	KFMASH system, pelite	*Yardley and Barber (1991a)*
[4]	$Pl + Kfs + Qtz \pm Sil + H_2O = melt$	700°C/4–5kbar	Metapelite	*Jung et al. (2000)*
[5]	$Bt + Qtz + Kfs + H_2O = melt$	700–720°C/10kbar	KMASH	*Peterson and Newton (1989)*
			Orthogneiss	*Sawyer (2010)*
[6]	$Hbl/Bt + Qtz + Kfs/Pl + H_2O = melt$	~680–690°C/6bar	TTG	*Watkins et al. (2007)*
[7]	$Hbl + Bt + Qtz + Or + Pl + H_2O = melt$		Tonalite	*Yoder and Tilley (1962)*
[8]	$Qtz + Kfs + Als + H_2O = melt$			*Johannes and Holtz (1996)*
[9]	$Ms + Pl + Qtz + H_2O = melt$	700–800°C/5–8kbar	Metagreywacke, metasedimentary rocks	*Fornelli et al. (2002)*
		~700–900°C/>6kbar	Ms–schist (HHC)	*Patiño Douce and Harris (1998)*
[10]	$Ms + Pl + Kfs + Qtz + H_2O = melt$		Metapelite	*Thompson (1990); Huang and Wyllie (1973)*
[11]	$Ms + Sil + Pl + Qtz \pm Grt \pm Bt + H_2O = melt$		MnNCKFMASH, metapelite	*Johnson et al. (2003a)*
[12a]	$Kfs + Pl + Bt + Crd + Qtz + H_2O = melt$	<700°C/3kbar	Metapelite	*Johnson et al. (2003b)*
[12b]	$Kfs + Pl \pm Bt + Crd \pm Grt + Qtz + H_2O = melt$	~725°C/3kbar	Metapelite	
[13]	$Ms + Bt + Kfs + Pl + Qtz + H_2O = melt$		Metapelite	e.g. *Storre and Karotke (1972); Vielzeuf and Schmidt (2001)*
[14]	$Kfs + Qtz \pm Pl \pm Bt \pm Crd + H_2O = melt$	650–680°C/3kbar	Semipelite, pelite	*Pattison and Harte (1988)*
Peritectic Hbl				
[15]	$Bt + Pl_1 + Qtz + Ep + H_2O = Hbl + Pl_2 + melt (Kfs rich)$	670–780°C/8–10kbar	TTG	*Mogk (1992)*
		670°C/7kbar	Metagranitoid	*Berger et al. (2008)*
[16]	$Bt + Pl (An_{28}) + Qtz + (H_2O) = Hbl + Pl (An_{32-34}) + Ttn + melt^*$	675–750°C/6–8kbar	Feldspathic gneiss	*Lappin and Hollister (1980); Kenah and Hollister (1983)*
		~700°C/6–8kbar	Calc–alkaline granitoids	*Reichardt and Weinberg (2012b)*
[17a]	$Bt + Pl + Qtz + H_2O = Hbl + melt$	750–800°C/9–11kbar	Tonalite	*Büsch et al. (1974)*
		~ 750–850°C/9–12kbar	Dioritic gneiss	*Slagstad et al. (2005)*
		675–750°C/4–6kbar	Dacite	*Conrad et al. (1988)*
		~ 700°C/5–10kbar >760°C/>10kbar	CKFMASH, tonalitic gneiss	*Escuder–Viruete (1999)*
			Gneiss	*McLellan (1988)*
			Amp+Bt gneiss	*Cherneva and Georgieva (2007)*
		675–750°C/6–8kbar	Calc–alkaline granitoids	*Reichardt et al. (2010); Reichardt and Weinberg (2012b)*
[17b]	$Bt + Pl + Qtz + H_2O = Hbl + Kfs + melt$	675–750°C/6–8kbar	Calc–alkaline granitoids	*Reichardt et al. (2010); Reichardt and Weinberg (2012b)*
[18a]	$Bt + Pl + Qtz + Kfs \pm Ap \pm Ttn \pm Ep + H_2O = Hbl + Grt + Ap \pm Ttn + melt$	<800°C/10kbar	Bt+Pl+Qtz banded gneiss	*Gardien et al. (2000)*
[18b]	$Bt + Pl + Qtz + Kfs \pm Ap \pm Ttn \pm Ep + H_2O = Hbl + Cpx + Grt \pm Ap \pm Ttn + melt$	900°C/20kbar	Bt+Pl+Qtz banded gneiss	*Gardien et al. (2000)*

[19]	$Pl + Qtz + Bt + H_2O = Amp + Pl \pm Ttn + melt$		Orthogneiss	Sawyer (2010)
[20]	$Amp_1 + Pl + Qtz + H_2O = Hbl + melt$	700-730°C/4.7-5.5kbar	Metaigneous rocks	Lee and Cho (2013)
[21a]	$Hbl_1 + Pl\,(An_{40}) + Bt + Qtz\,(+ H_2O) = Hbl_2 + Pl\,(An_{48}) + Qtz + melt*$	675-750°C/6-8kbar	Amphibolite	Lappin and Hollister (1980); Kenah and Hollister (1983)
[21b]	$Hbl + Qtz\,(+ H_2O) = Hbl + melt*$	675-750°C/6-8kbar	Amphibolite	Lappin and Hollister (1980)
	Peritectic Grt and/or Crd			
[22]	$Sil + Bt + Qtz + H_2O = Crd + Grt + melt$	650-750°C/4-5.5kbar	KFMASH system, pelite	Yardley and Barber (1991a)
[23]	$Bt + Qtz + Pl + Als + H_2O = Grt + melt$			Stevens and Clemens (1993)
[24]	$Qtz + Pl + Bt \pm Sil + H_2O = melt \pm Kfs + Grt/Crd + Ilm$	650-950°C/7-8kbar	Bt-Grt gneiss experiment	Otamendi and Patiño Douce (2001)
[25]	$Bt \pm Crd + Pl + Sil + Qtz + H_2O = Grt \pm Kfs + melt$	700°C/4-5kbar	Metapelite	Jung et al. (2000)
[26]	$Hbl + Pl + Qtz + H_2O = Grt + Cpx + Ttn + melt$	800-850°C/8-10kbar	Amphibolite	Storkey et al. (2005)
[27]	$Bt\,(Mg_{40}) + Als + Pl + H_2O = Grt + Crd \pm Kfs + melt$		Metapelite	Clemens (1984)
[28]	$Bt + Pl + Qtz + H_2O = Grt + Ms + melt$	700°C/10kbar	Ms-schist (HHC) experiment	Patiño Douce and Harris (1998)
[29]	$Bt + Sil + Qtz + H_2O = Crd + melt$	650-750°C/4-5.5kbar	KFMASH system, pelite	Yardley and Barber (1991)
[30]	$Bt + Qtz + Pl + H_2O = Crd + Grt + melt$	700-750°C/5kbar	Metasedimentary	Ward et al. (2008); Kisters et al. (2009); Brown (2013)
[31]	$Bt + Kfs + Pl + Qtz + H_2O = Grt + melt$	690-730°C/4-6kbar	Metaigneous rocks	Jung et al. (2009)
[32]	$Kfs + Als + Bt + Qtz + H_2O = Crd + melt$	650-750°C/4-5.5kbar	KFMASH system, pelite	Yardley and Barber (1991)
		670-730°C/3.5-4kbar	Metapelite, metapsammite	Ellis and Obata (1992)
[33]	$Bt + Qtz + Sil + Pl + H_2O = Crd/Sp + melt$		Metapelite	Butler et al. (1997)
	Other peritectic minerals			
[34]	$Bt + Qtz + H_2O = En + melt$	780-790°C/10kbar	KMASH; experiment	Peterson and Newton (1989)
[35]	$Ms + Qtz + Pl + H_2O = Als + melt$	750°C/10-12kbar	Metasediment	Kalsbeek et al. (2001)
			Metapelites	Clemens (1984)
		~625°C/2kbar	Metapelite	Icenhower and London (1995)
[36]	$Ms + Pl + Qtz + H_2O = Sil + Bt + melt$			Thompson and Tracy (1979)
		<800°C/4-7kbar	Metasedimentary	Milord et al. (2001)
[37a]	$Hbl + Qtz + H_2O = Cpx + Opx \pm Grt + melt$	680-700°C/6kbar	TTG	Watkins et al. (2007)
[37b]	$Bt + Qtz + Pl + H_2O = Opx \pm Grt \pm Kfs + melt$	680-700°C/6kbar	TTG	
[38]	$Bt\,(Mg_{60}) + Qtz + Pl + H_2O = Opx \pm Kfs + melt$		Metasedimentary	Clemens (1984)
[39]	$Pl + Qtz + Bt + H_2O = Ttn + melt$		Orthogneiss	Sawyer (2010)
[40]	$Qtz + Kfs + Pl + H_2O = Pl + melt$	630-670°C/2-4kbar	Metagreywacke	Genier et al. (2008)

* H_2O in brackets has been added explicitly to the reactions. The original assumed water was present ($P_{H2O} \sim P_{total}$).

nucleation and growth of the stable assemblage. In contrast, water-undersaturated experiments led to the more rapid development of the stable mineral assemblage. Melts produced close to the solidus T are controlled by interface reaction. In contrast, melt compositions at T well above solidus are determined by the diffusive transport properties of melt and the extent of equilibrium with surrounding minerals (Acosta-Vigil et al., 2006). Disequilibrium melting impacts significantly on melt composition and could be important in geological situations where variables, such as P and T or water content change rapidly (e.g. contact aureoles). Prince et al. (2001) used these findings to argue that aqueous fluid ingress into an unmelted rock at conditions above the water-saturated solidus could shift conditions rapidly potentially causing chemical disequilibrium.

3.3. Peritectic minerals

At its simplest, water-fluxed melting may be distinguished from dehydration melting by their peritectic minerals (Tables 1 and 2). As stated by Brown (2013): "Mica- and hornblende-bearing leucosomes without anhydrous minerals in mica- and hornblende bearing hosts are more likely to be the product of fluid-present melting, whereas leucosomes that carry nominally anhydrous (peritectic) minerals, such as garnet or pyroxene, are more likely to be a product of fluid-absent hydrate-breakdown melting." Whilst this is a rough guide in the field, there are several examples where water fluxing triggers incongruent melting producing anhydrous peritectic minerals (Table 2). Numerous experimental studies were performed in order to understand the

difference in peritectic mineral composition and stability during dehydration melting and water-present melting.

3.3.1. Amphibole

Already in the 1960s a series of experiments on natural igneous rocks (granite to tonalite) at 1–3 kbar under water-saturated conditions (15–25 wt.% H_2O added) generated eutectic melts with peritectic Hbl (e.g. Gibbon and Wyllie, 1969; Piwinskii, 1968). More recent experiments found that at low aH_2O, peritectic amphibole is stable only near the solidus (~850 °C; Conrad et al., 1988). Peritectic hornblende is stable at a minimum of ~4 wt.% H_2O (at 2 kbar) and 2.5 wt.% H_2O (at 8 kbar) indicating that stability shifts to lower aH_2O with increasing P (Naney, 1983; Naney and Swanson, 1980). Gardien et al. (2000) showed that amphibole was stabilized above the water-saturated solidus only upon addition of 2–4 wt.% of H_2O (at ≥10 kbar). Also melting experiments at 10 kbar on Westerly granite (Johnston and Wyllie, 1988) showed that amphibole is present only if 10 wt.% of H_2O is added. Combined, these experiments indicate that the presence of Hbl indicates addition of external aqueous fluids during partial melting.

3.3.2. Garnet

Increasing aH_2O reduces garnet stability (Conrad et al., 1988; Gardien et al., 2000). However, the experiments of Alonso Perez et al. (2009) on Si-rich melts indicated rather the opposite, i.e. that stability of igneous garnet slightly increases with increasing H_2O in melt. Also with increasing dissolved H_2O contents, garnet composition becomes more Ca-rich (Alonso Perez et al., 2009; Conrad et al., 1988; Gardien et al., 2000) whereas X_{Mg} of Grt is independent of water content.

3.3.3. Cordierite

This mineral is involved in a number of melting reactions in the presence of water as documented by many field studies (Tables 2 and 3). However, there is a lack of experimental investigations of its behaviour during water-present melting. Melting experiments of Crd-bearing gneiss at 5–15 kbar and 900 °C (Koester et al., 2002) showed that water-present melting produces Crd + Bt + Pl + Qtz + Fe-oxides + melt. However, cordierite is not produced at this T in water-absent experiments, which suggests that the addition of H_2O stabilized cordierite. Cordierite can contain variable amounts of H_2O and CO_2 incorporated in its structure, thus it can record the nature of the volatile regime at the time of its formation. Lower H_2O content in cordierite could reflect equilibration with H_2O-undersaturated melts and vice-versa (Carrington and Harley, 1996). However, water can also be lost easily and thus small amounts of water in Crd do not always reflect H_2O-undersaturated conditions of formation. Harley and Carrington (2001) suggested that high to moderate aH_2O (0.4–1) are characteristic of cordierites in zones of fluid infiltration/pegmatites and also in migmatites that underwent extensive melt loss/segregation. By contrast, granulite facies migmatite terranes typically have lower H_2O content in cordierite ($aH_2O = 0.1$–0.4) reflecting dehydration melting reactions.

3.3.4. Ortho- and clinopyroxene

Pyroxene stability is controlled by T, P, rock composition and H_2O content (Carroll and Wyllie, 1990; Naney, 1983; Patiño Douce, 1996). Patiño Douce (1996) showed in experiments on a synthetic biotite gneiss that increased water content favoured Opx at the expense of Grt–Bt–Pl shifting melt compositions away from granitic towards granodioritic and tonalitic. Experimental melting of tonalite with 2.5–10 wt.% added H_2O at 15 kbar and 850–1100 °C (Carroll and Wyllie, 1990) shows that Cpx is stable only with water contents below 3 wt.%. With increasing water content, the peritectic mineral changes from Cpx to Grt and to Hbl ($H_2O > 9$ wt.%). In the experiments of Gardien et al. (2000), Cpx occurred only at 20 kbar, 900 °C and 4 wt.% added water with no Cpx at lower pressures. Naney (1983) showed that at high pressures

(>8 kbar) Opx stability is restricted to water-absent conditions, by contrast to low P (<2 kbar) when Opx is stable at both water-present and water-absent conditions. Similarly, Cpx is stable at P > 8 kbar only at low water contents (<5 wt.%). This suggests that melting in the presence of small amounts of water (or in its absence) favours Opx or Cpx formation over amphibole. X_{Mg} of orthopyroxene is similar in both H_2O-saturated and undersaturated conditions at similar T.

3.3.5. K-feldspar

K-feldspar is a typical peritectic phase resulting from muscovite and biotite dehydration melting reactions (Table 1; e.g. Clemens and Vielzeuf, 1987; Spear, 1993; Thompson, 1983; Vernon and Clarke, 2008). The amount of K-feldspar depends on protolith composition. Most metapelites that are typically K-rich have excess K_2O resulting from dehydration melting reactions that cannot be accommodated in the melt and forms peritectic Kfs at low pressure (e.g. Carrington and Watt, 1995). However, at higher pressure this may not be the case (Brown, 2013). By contrast, water-present melting not involving micas in melting reactions will not produce peritectic K-feldspar (Table 2). This is supported by experimental result of Patiño Douce and Harris (1998) where K-feldspar is present in all dehydration melting experiments and is absent from all experiments to which water was added.

3.4. Melt composition: geochemical signature of water-fluxed melting

The melting reaction and volume of melt produced by a given protolith depend critically on the presence of an aqueous fluid phase. In this way, water plays a key role in controlling the geochemistry of granitic melts. A large variety of silicate melt compositions can be obtained from melting similar protoliths under variable aH_2O conditions (e.g. Conrad et al., 1988; Holtz and Barbey, 1991; Patiño Douce, 1996; Patiño Douce and Harris, 1998). The most significant difference between melt compositions resulting from dehydration melting and water-present melting is in the proportion of Ab, An and Or (Fig. 2a–b; Becker et al., 1998; Patiño Douce, 1996; Pichavant et al., 1992). At high aH_2O, melts become richer in An and Ab and poorer in Or (Fig. 2a). Therefore added water produces more tonalitic to trondhjemitic melts, by contrast to granitic melts produced by Ms-dehydration melting (Castro, 2013; Patiño Douce and Harris, 1998). Patiño Douce and Harris (1998) melted High Himalayan Crystalline metasedimentary rocks (a Ms-schist and a Tur–Ms–Bt schist both lacking Kfs) without added H_2O and with 1–4 wt.% added H_2O. They found that melting of these K-rich metasedimentary rocks generated trondhjemitic melts in experiments with added water, because of a decrease in the melting temperature of plagioclase + quartz, in the stability field of muscovite (see also Conrad et al., 1988; Patiño Douce, 1996). Melting in this case leaves a residue rich in mica and quartz, and depleted in plagioclase. By contrast, the same rocks generated granitic melts in experiments without added water, reflecting the breakdown of muscovite. This is similar to the results of Gardien et al. (2000) who found that K_2O in melt decreases in melting experiments with added H_2O. A further impact of water influx is that it stabilizes Opx at the expense of Grt (+Bt + Pl) causing melts to tend towards granodioritic to tonalitic composition (Fig. 2a-b; Patiño Douce, 1996).

The ferromagnesian content of granitic melts is generally very small, but is very distinctive for different melting reactions (Fig. 2b; e.g. Carroll and Wyllie, 1990; Patiño Douce, 1996). At constant P–T, MgO and FeO concentrations in granitic melts increase with increased water content or water activity (e.g. Conrad et al., 1988; Holtz and Johannes, 1991; Patiño Douce, 1996). Therefore, melts become more mafic (at constant P–T) with increasing water content (Patiño Douce, 1996).

Water increases the solubility of Al in the melt, thus impacts on the aluminium saturation index (ASI) of melts. Independently of temperature, Al_2O_3 increases at 0.04 to 0.10 mol in the melt per mole of H_2O (Acosta-Vigil et al., 2003). Consequently melt produced by water-

fluxed melting will have higher ASI values than those produced by muscovite or biotite dehydration melting (Acosta-Vigil et al., 2003) where excess aluminium goes into forming peritectic phases such as sillimanite.

Pichavant et al. (1992) evaluated the role of pressure and water content for solidus composition in the H_2O-saturated ($aH_2O = 1$) and undersaturated ($aH_2O < 1$) conditions in Qtz–Ab and Qtz–Or system. They showed that increasing the water content of melt at 2 kbar lowers the eutectic T more in the Qtz–Ab system than in the Qtz–Or system (but the eutectic composition remains similar). When P is increased to 5 kbar, the eutectic composition in the Qtz–Ab system becomes more albitic. This is attributed to higher water solubility in Na-bearing melt than in K-bearing melts. Similar results were also reported by Holtz et al. (1992a, 1992b).

Experimental studies on the anatexis of a quartz–feldspars gneiss at 3–5 kbar and 700–800 °C and various aH_2O (reflecting between 1 and 7 wt.% added H_2O; Holtz and Johannes, 1991) showed that melt remained H_2O-undersaturated ($aH_2O = 0.5$) even though external fluids were needed to trigger melting. They suggest that the control of aH_2O on melt composition is as significant as T and P. The average aH_2O of 0.5 in melt is similar to values estimated by Clemens and Wall (1981) for Australian S-type granites.

Water influx also plays an important role in the melting of mafic rocks. There is a large number of water-absent melting experiments on mafic protoliths (e.g. Rushmer, 1991 – basalt; Wolf and Wyllie, 1994 –

amphibolite; Patiño Douce and Beard, 1995 – amphibolite) and some water-present melting experiments (e.g. Beard and Lofgren, 1991; Springer and Seek, 1997 – metabasalt; Zamora, 2000 – ophiolite). Beard and Lofgren (1991) performed melting experiments of amphibolites at 800–1000 °C at 1–6.9 kbar in the absence or presence of free water. Melts produced by dehydration melting coexist with Pl + Cpx + Opx + Mag restites and have granodioritic to trondhjemitic compositions, similar to low-K island arc magmas. In contrast, water-saturated melting experiments produced strongly peraluminous, low iron melts unlike most silicic igneous rocks, and amphibole-rich, plagioclase-poor residues (Beard and Lofgren, 1991). These authors concluded that whilst dehydration melting of amphibolites can generate low-potassium silicic rocks typical of magmatic arcs, water-saturated melting cannot. In the water-present melting experiments (1 wt.% water added and some CO_2) of metamorphosed cumulate gabbros (Springer and Seek, 1997), melt composition changes from trondhjemitic to tonalitic to quartz dioritic with increasing T and degree of melting.

There is currently a lively debate concerning the nature of melting of metamorphosed ocean basalts and the origin of Archean trondhjemites–tonalites–granodiorites (TTGs, e.g. Drummond and Defant, 1990; Sen and Dunn, 1994; Prouteau et al., 1999; Moyen and Stevens, 2006). Experimental studies have found that dehydration melting of metamorphosed oceanic basalt produces trondhjemitic–tonalitic–dacitic melts, but at temperatures exceeding 1000 °C, over a wide range of P but
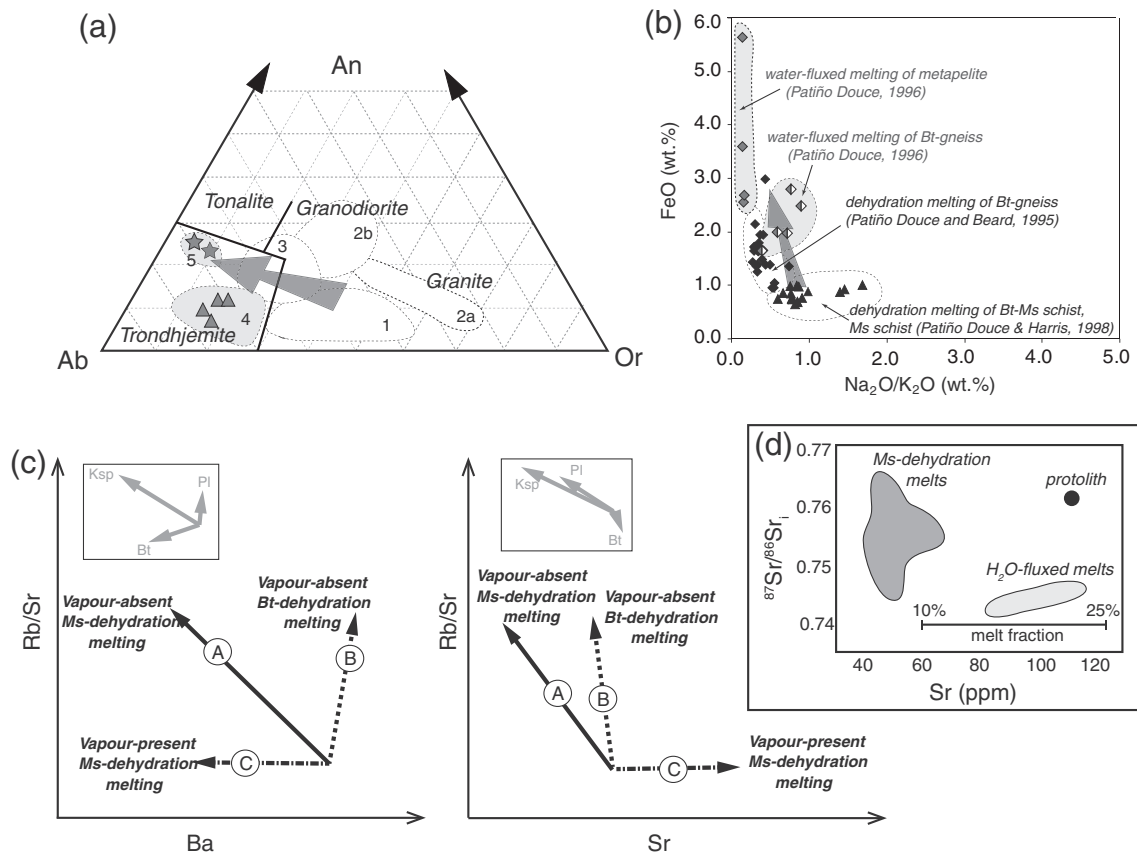
Fig. 2. (a) An–Ab–Kfs normative triangle of distinct melt compositions for dehydration melting reactions (white fields) and water-present melting reactions (grey fields) (fields after Barker, 1979). 1 - dehydration melting of tonalite from Patiño Douce (2005) and dehydration melting of Bt-Ms schist from Patiño Douce and Harris (1998); 2a,b - dehydration melting of Bt-gneiss and Qtz amphibolite from Patiño Douce and Beard (1995); 3 – H_2O undersaturated melting of dacite/greywacke from Conrad et al. (1988); 4 - H_2O present melting of Bt-Ms schist from Patiño Douce and Harris (1998); 5 - H_2O saturated melting of dacite/greywacke from Conrad et al. (1988). (b) Na_2O/K_2O vs FeO diagram of melt compositions for different melting reactions. Grey arrows point in the direction of melt composition change from dehydration melting to water-present melting. (c) Distinct behaviour of Rb, Sr and Ba for different melting reactions: Ms-dehydration (A), Bt-dehydration (B), and aqueous fluid-saturated Ms-dehydration (C). Breakdown of muscovite in the absence of aqueous fluids leads to increased Rb/Sr and a decrease in Sr and Ba (A). Aqueous fluid-saturated muscovite melting leads to considerable decrease in Ba and increase in Sr with little change in Rb/Sr (B). Bt-dehydration melting shows a strong increase in the Rb/Sr ratio with little effect on either Ba or Sr (C). Black arrows represent the different melting reactions. Grey arrows in insets represent 10% crystallization of phases. Length of the vectors is maximum melt % produced from average metapelite (after Inger and Harris, 1993). (d) Comparison of Sr isotope composition of melts produced by Ms-dehydration melting and H_2O-fluxed melting (example from Manaslu intrusive complex, data from Knesel and Davidson, 2002). Protolith schist is marked by black circle. Produced melt fraction is labelled.

commonly above 15 kbar (see Moyen and Stevens for review, 2006). By contrast to these findings, Prouteau et al. (1999) found that in order to explain the origin of high-Sr dacitic magmas, such as adakites and Archean TTGs, low-T slab melting triggered by the presence of free water is necessary. In particular, high water content in the melt is necessary to prevent plagioclase from crystallizing early in the history and remove Sr through fractionation.

3.4.1. Trace elements

Concentrations of Rb, Sr, Ba, and Eu are controlled by major mineral phases contributing to the melting reaction and have been used as possible indicators of the melting reaction (Fig. 2c–d; e.g. Harris and Inger, 1992; Inger and Harris, 1993; Knesel and Davidson, 2002; McDermott et al., 1996). Micas are rich in Rb and poor in Sr, and plagioclase is rich in Sr and poor in Rb (Inger and Harris, 1993). Thus, melts derived from mica-dehydration reactions have high Rb/Sr ratios whereas water-fluxed melting has low Rb/Sr ratio. This basic difference has been used to determine the relative involvement of the different minerals and constrain the melting reaction. Harris et al. (1993) found through geochemical modelling of melting of a wide range of metasedimentary compositions "that Rb/Sr ratios will vary between 4 and 10 during equilibrium melting and vapour-absent conditions, but are less than 3.5 during vapour-present melting." Inger and Harris (1993) modelled the behaviour of Rb/Sr versus Sr and Ba for three different melting reactions: Ms-dehydration, Bt-dehydration, and aqueous fluid-saturated Ms-dehydration (Fig. 2c). They also incorporated the behaviour of Ba because it is highly compatible with K-feldspar and a good measure of its involvement in the melting reactions (Zeng et al., 2005b). They showed how breakdown of muscovite in the absence of an aqueous fluid phase leads to increased Rb/Sr and a decrease in Sr and Ba (Fig. 2c). This contrasts with the water-present case that leads to considerable decrease in Ba and increase in Sr with little change in Rb/Sr (Fig. 2c–d). It contrasts also with Bt-dehydration melting, which shows a strong increase in the Rb/Sr ratio with little effect on either Ba or Sr, because these are hosted mainly by Pl (Fig. 2c–d). Ba decrease with increasing Rb/Sr is interpreted as resulting from Ms-dehydration breakdown producing a restite richer in K–feldspar which is typically Ba-rich.

Previous studies of anatectic terranes have shown that the behaviour of Eu in felsic melt is controlled mainly by K-feldspar (e.g. Nabelek and Glascock, 1995; Watt and Harley, 1993). Hence crystallization and/or removal of K-feldspar from a felsic melt produces a negative Eu anomaly in the melt. A similar negative Eu anomaly is generated during partial melting of a rock in which the feldspar is retained in the source rock. Both, muscovite and biotite dehydration melting typically form K-feldspar as a peritectic phase (Table 1; Fig. 1b), by contrast to water-present melting where peritectic K-feldspar is typically missing (Table 2 and Fig. 1a). Thus, K-feldspar generated by dehydration melting will sequester Eu and produce a negative Eu anomaly in coexisting peritectic phases and in the melt, whereas high positive Eu anomaly in the melt indicates of water-fluxed melting (McDermott et al., 1996).

Trace element behaviour during melting was used by Koester et al. (2002) and Butler et al. (1997) to argue for different melting reactions underlying the origin of different granites. Knesel and Davidson (2002) defined two groups of Himalayan leucogranites based on differences in Sr contents and Sr isotopic signatures and suggested that one group resulted from Ms-dehydration melting and the other from water-fluxed melting (Fig. 2d). Zeng et al. (2005a, 2005b) investigated the partial melting of a pendant of pelite engulfed by granites of the southern Sierra Nevada batholith. They used trace element and Sr and Nd isotopic data of leucosomes to suggest that they were derived from water-fluxed melting. Prince et al. (2001) concluded that water fluxing into rocks at temperatures above the water-present solidus but below 650 °C caused relatively rapid melting and extraction, leading to disequilibrium melting, explaining a high Eu anomaly and unusually low Rb/Sr ratios in deformed leucogranites.

There are however some significant issues in the use of LILE to distinguish between melting reactions. This is because their contents and ratios depend on source composition, which is often unknown, and on the amount of water available, and thus is only detectable at high melt fractions (see discussion in Aikman et al., 2012). Furthermore, the composition of primary melts derived from modelling may be modified by feldspar fractionation, or by melting under disequilibrium conditions (Harris et al., 1993) or by melts carrying varying proportions of restitic feldspar and mica (Kalsbeek et al., 2001). Aikman et al. (2012) concluded that it is not unambiguously possible to identify the main melting mechanism from LILE covariance diagrams alone.

3.4.2. $\delta^{18}O$

Different unmetamorphosed protoliths may have distinct characteristic $\delta^{18}O$ values (e.g. Hoefs, 1980; Sawyer, 2010). Metasedimentary rocks in some metamorphic terranes have similar $\delta^{18}O$ to their protoliths (Cartwright, 1994; Valley et al., 1990) and typically, dehydration melting preserves the protolith's $\delta^{18}O$ values as there is no external input of $\delta^{18}O$ (Baker, 1990; Cartwright and Buick, 1998; Kohn et al., 1997). The influx of water with oxygen isotopes different to that of the melt source modifies the isotopic composition of the melt and therefore can be used in deciphering the presence and origin of fluids during melting (e.g. Cartwright et al., 1995; Sawyer, 2010). Water-present melting is characterized either by significant decrease of $\delta^{18}O$ (Cartwright et al., 1995; Rye et al., 1976; Tartèse et al., 2012; Wickham and Taylor, 1985) or by $\delta^{18}O$ homogenisation (Jung et al., 2000; Sawyer, 2010; Scaillet et al., 1990; Tartèse et al., 2012). This depends on the timing of fluid influx – during, before or after anatexis – as well as on the fluid source (meteoric, magmatic or metamorphic). If there is no shift in $\delta^{18}O$, the infiltrating fluid has similar $\delta^{18}O$ to the protolith and is most likely of metamorphic origin, derived from dehydration reactions of similar rocks (Jung et al., 2000; Sawyer, 2010; Tartèse et al., 2012). On the other hand, a significant decrease in $\delta^{18}O$ reflects interaction with isotopically light meteoric water or sea water (Cartwright et al., 1995; Tartèse et al., 2012; Wickham and Taylor, 1985) or magmatic fluid.

3.5. Experiments vs. nature

In the previous subsections we described insights into crustal anatexis derived largely from experiments. However, experiments have limitations which are discussed here. White et al. (2011b) summarized the advantages and pitfalls of the experimental approach and compared experimental results with thermodynamic modelling. They concluded that despite both methods being simplified proxies of the natural systems, the results of both replicate well natural observations from migmatitic terranes and tell a consistent story about crustal melting processes.

One of the main advantages of experiments on natural rocks compared to thermodynamic modelling is that they can deal with the full chemical complexity of rocks (including trace elements) and thus can provide direct constrains on rock fertility, P–T conditions of melting, melt and peritectic minerals composition. Experiments can be performed at variable P–T conditions, in the presence or absence of fluids of different composition, simulating the range of conditions appropriate for crustal anatexis. Melting experiments also incorporate kinetic factors such as diffusion, nucleation or crystal growth. Major pitfalls are (White et al., 2011b): (i) in experiments there is no melt loss, which tends to overestimate melt production compared to cases when melt removal is efficient; (ii) kinetics of reactions are slow; (iii) possible redistribution of elements within the charge can cause local re-equilibration (especially along retrograde paths); (iv) under dehydration melting conditions the oxidation state in the experiment cannot be directly controlled, which can lead to reduction of estimated water amount, growth of oxide minerals and conversion of ferrous to ferric iron; and (v) melting experiments do not allow for bulk compositional changes. All these have to be taken in account when interpreting experimental data, aware that experiments

cannot accurately represent crustal anatexis. Recently, Webb et al. (2014) argued that experiments typically exaggerate the amount of water available at the solidus, which leads to higher melt fraction estimates in comparison to nature. They suggest that significant amounts of water in nature are already lost during prograde dehydration of hydrous minerals resulting into lower melt fraction at typical crustal melting conditions. This cannot be duplicated in experiments that do not allow for water loss during the experiment.

4. Physical properties

In this section, we review the many physical properties of granitic melt that are modified by the presence of aqueous fluids. Understanding how these properties respond to changes in water content forms the basis for exploring the behaviour of natural systems.

4.1. Melting temperature, slope of solidus curve, volume changes and rates of melting

4.1.1. Melting temperature

Water-present melting of common crustal rocks such as pelites, psammites, and granitic rocks, starts at upper amphibolites facies at temperatures around 620–650 °C at crustal pressures (Fig. 1a), approximately 50–100 °C lower than the start of Ms-dehydration at granulite facies (e.g. Patiño Douce and Harris, 1998), and more than 100–150 °C lower than Bt-dehydration reactions (Fig. 1b, c; e.g. Castro et al., 2000; Holtz et al., 2001; Wyllie et al., 1976). Another significant difference is that water-present solidus curves are not particularly sensitive to rock composition for felsic to intermediate rocks (compare curves 6 for tonalite and 1 for granite in Fig. 1a; Clemens and Vielzeuf, 1987; Wyllie, 1977), and melt composition is not as strongly regulated by rock paragenesis (Rubatto et al., 2009). The implication is that multiple lithologies melt at similar conditions and the composition of low-T eutectic melts is similar for a variety of granitic and metasedimentary rocks (Clemens and Droop, 1998; Rubatto et al., 2009). In the presence of water, metabasic rocks melt at around 700–750 °C at high P and around 650 °C (at 6–10 kbar) (summary in Moyen and Stevens, 2006). Amphibole-dehydration melting of amphibolites at crustal pressures occurs at 850–900 °C (e.g. Rushmer, 1989). At P above 10 kbar, the peritectic mineral changes from clinopyroxene to garnet and causes a significant decrease in the solidus T of the dehydration melting solidus curve, that drops to T similar to water-saturated solidus (Wyllie and Wolf, 1993).

4.1.2. Use of T estimates in recognizing water-fluxed melting

Melting temperatures are commonly constrained from residual minerals using phase petrology and thermodynamic modelling (e.g. Spear, 1993). This can be combined with recently developed thermometers based on Zr or Ti solubility in melt in the presence of zircon and rutile, as well as thermometers based on Ti concentration in zircon, and Zr concentration in rutile (e.g. Ferry and Watson, 2007; Harrison et al., 2007; Hayden and Watson, 2007; Watson and Harrison, 2005; Zack et al., 2004). These temperature estimates can assist in determining the presence or absence of an aqueous fluid phase during melting. Watson and Harrison (2005) used Ti-in-zircon thermometer to estimate temperatures of ~700 °C for the origin of the 4–4.35 Ga Hadean zircon in Jack Hills, Australia, and suggested that they formed in melt that resulted from water-present melting. Water-present melting has been inferred in many cases from T estimates that are too low to allow for dehydration melting reaction or too low to produce the large melt fractions documented (Table 3; e.g. Genier et al., 2008; Jung et al., 2000; Mogk, 1992; Sawyer, 2010).

4.1.3. Slope of solidus curve and volume change

A further difference between water-present and dehydration melting is the slope of the solidus curve in P–T space (Fig. 1). The slope of the curve reflects the volume changes with melting where increased pressure favours volume decrease. Dehydration melting reactions, which lead to volume increase, have solidus curves with positive slopes (Fig. 1b, c) and are favoured by decompression (Fig. 1d). Water-present melting generally has a negative slope due to volume decrease (Fig. 1a, c) and is favoured by increased pressure (Fig. 1d). Significantly, the negative slope turns positive at high P (e.g. Vielzeuf and Schmidt, 2001).

Volume change during melting impacts on the pressure in the source, and therefore on the processes of melt segregation and extraction (Clemens and Droop, 1998). Volume increase during dehydration melting may lead to increased pressure. If the rate of melt production exceeds the rate of melt escape, then increased pressure may lead to melt-enhanced embrittlement of the crust (Brown et al., 1995; Rutter and Neumann, 1995) and melt extraction driven by buoyancy. A possible example of this process is given in Droop and Brodie (2012), who calculated the volume increase during water-absent melting and argued for hydrofracturing in a low-P thermal aureole. By contrast, assuming no significant regional differential stresses, volume decrease associated with water-present melting may lead to tension in the source, microcracking and possible initiation of ductile fractures (Fig. 1d).

There is a natural feedback between volume change during melting and the evolution of anatexis that is seldom acknowledged (see Powell et al., 2005). Increased pressure during dehydration melting inhibits further melting by moving the system away from the solidus curve. Melting will be inhibited until such overpressures are relaxed by fracturing due to the embrittlement mentioned above, or by viscous flow. Similarly, a pressure drop associated with water-fluxed melting has two significant effects: (a) like for dehydration melting, this will inhibit further melting by moving the system away from the water-saturated solidus, and (b) it will generate pressure gradients that attract aqueous fluids or melts from the surroundings (Fig. 1d; Clemens and Droop, 1998), leading to melt accumulation in zones of high melt production. In this case too, melting rates are controlled by relaxation of these pressure differences, and by the rate of melt/fluid influx.

As argued by Clemens and Droop (1998), pressure drop in the source may inhibit extraction of melt resulting from water-fluxed melting by inhibiting the embrittlement that may occur in rocks undergoing dehydration melting (Rutter and Neumann, 1995). However, this effect is partly counteracted by the lower density of hydrous melts compared to those derived from dehydration melting (Clemens and Droop, 1998) and by the tendency of melt to accumulate in the low pressure regions generated by volume decrease due to melting. This accumulation of low density melt can lead to magma extraction by: (a) mechanisms that require large magma buoyancy, such as diapirism (Weinberg and Podladchikov, 1994), or (b) ductile fracturing due to tensile stresses generated by contraction (Weinberg and Regenauer-Lieb, 2010).

4.1.4. Rates of melting

The rate of melt production by dehydration melting reactions is controlled by kinetics as well as heat flux into the rock, typically by thermal diffusion, and by the rate of pressure variation. Water-fluxed melting is controlled also by water advection, where the rate of water influx and its distribution throughout the rock mass, control the rate of melt production. The total water volume added to the rock is the main control the total melt fraction produced, unless a solid reactant is consumed first (Rubatto et al., 2009; Sawyer, 2010). This implies that the melt fraction generated cannot be calculated based on rock mineralogy and P–T only (Rubatto et al., 2009). Furthermore, because influx of aqueous fluids tend to vary in time and space, depending on the geometries of high permeability pathways, the volumes of melt and the physical behaviour of the anatectic terranes will vary considerably. For example, White et al. (2005) suggested that the degree of disaggregation of the Hores gneiss in Broken Hill could be related to different volumes of water influx.
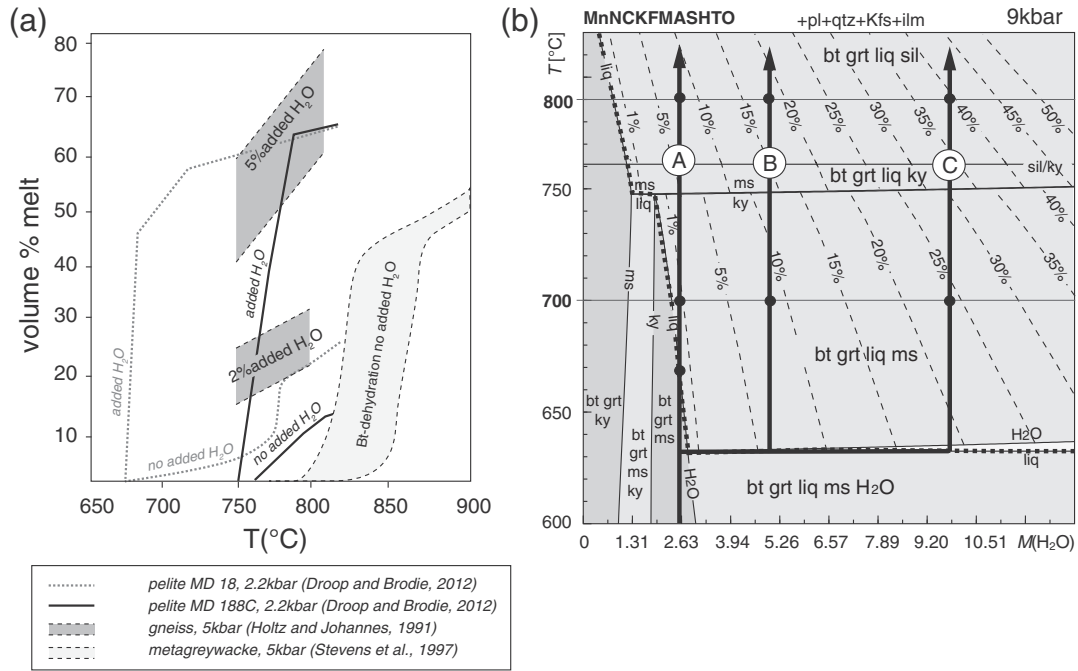
Fig. 3. Comparison of melt productivity. (a) Melt productivity by dehydration melting and water-present melting of pelitic rocks at 2.2 and greywacke at 5 kbar. Note increase in melt production when water is added. Grey dashed lines: melting of pelite (Qtz-bearing at solidus, sample MD18 of Droop and Brodie (2012)) at 2.2 kbar. Solid black line: melting of pelite (Qtz-absent at solidus, sample MD188C of Droop and Brodie (2012)) at 2.2 kbar. Light grey field: Bt-dehydration melting of metagreywacke with no added H_2O at 5 kbar (from Stevens et al., 1997). Dark grey field: melting experiment of gneiss with 2 wt.% and 5 wt.% of added H_2O at 5 kbar (data from Holtz and Johannes, 1991). (b) Results of thermodynamic modelling: T–M(H_2O) pseudosection illustrating melting of Bt–Ms granite (composition: SiO_2 = 75.30, Al_2O_3 = 10.24, CaO = 2.05, MgO = 1.65, FeO = 2.75, K_2O = 3.69, Na_2O = 2.97, TiO_2 = 0.4, MnO = 0.06, O = 0.02; data from Hasalová et al., 2008). MH_2O represents mol% of H_2O in the rock. Diagram is contoured for mol% melt (dashed lines). The three different paths labelled A, B and C are possible melt production paths during heating reflecting different amount of added H_2O.

4.2. Volume of melt produced

Thompson and Connolly (1995) estimated that residual free water from subsolidus dehydration reactions remaining in pores produces less than 0.5% granitic melt at the H_2O-saturated solidus. Both experiments and thermodynamic modelling of melting assume minimal melting at the H_2O-saturated solidus and that melting effectively starts by dehydration melting reactions, which is characterized initially by very low melt productivity at the dehydration melting solidus (Berger et al., 2008; Hasalová et al., 2008; Johnson et al., 2008).

A number of studies investigated melt productivity of common crustal rocks in the absence of free water (e.g. Brown and Korhonen, 2009; Johnson et al., 2008; Patiño Douce and Beard, 1995; Powell et al., 2005). They demonstrate that at amphibolite facies conditions small amounts of melt (<5%) is produced by Bt-dehydration melting and temperatures well into granulite facies are needed to produce larger amounts of melt (>10%). In metapelites, Ms-dehydration melting typically produces low melt volumes but may reach up to ~ 15% melt (e.g. Brown and Korhonen, 2009).

By contrast, the addition of even small amounts of water (1–2%) will have large impact on melt productivity (Fig. 3; Johannes and Holtz, 1996 p. 53). In melting experiments of Bt–Pl–Qtz gneiss, Gardien et al. (2000) demonstrated that <4 wt.% melt will be produced at 900 °C with no added H_2O. When 4 wt.% H_2O was added, melt production increased to 50–60% even at T as low as 800 °C (Gardien et al., 2000). Hasalová et al. (2008) modelled melting of Ms–Bt granite and showed that with no added H_2O (other than the ~2.6 mol% of H_2O in the rock; path A, Fig. 3b), melting is controlled only by mica-breakdown and starts at 670 °C (at 9 kbar), and at 700 °C and 800 °C, 1% melt and ~7.5% melt are formed, respectively (path A, Fig. 3b). When 5 mol% of external H_2O is added, ~8% melt is generated at 700 °C and ~18% at 800 °C (path B in Fig. 3b). Addition of 10 mol% of H_2O generates ~24% melt at 700 °C and 40% melt at 800 °C (path C in Fig. 3b). This is consistent with observations of White et al. (2005) who have shown for the

Hores gneiss in Broken Hill that at 700 °C and 4.2 kbar, the addition of 5 mol% of H_2O generates ~15 mol% melt, and the addition of 10 mol% H_2O ~35 mol% melt.

4.3. Maximum and minimum water contents in melts

The initial water content in magmas is related to the melting reaction and P–T conditions of magma generation (e.g. Clemens and Watkins, 2001; Johannes and Holtz, 1996). During dehydration melting the amount of dissolved water in the melt is determined by temperature and the amount of melt depends on water availability. By increasing temperature, melt fraction increases and water content in the melt decreases. For example, melt produced by dehydration melting of metasedimentary rocks by muscovite breakdown at 750 °C and 4 kbar will be more hydrous (5–6 wt.% H_2O) than melts produced by biotite breakdown at 850 °C and 4 kbar (2 wt.% H_2O; Castro, 2013; Castro et al., 2000; Patiño Douce and Beard, 1995; Patiño Douce and Harris, 1998). By contrast, the water content in magmas generated by water-fluxed melting is controlled by the minimum amount required to stabilize melts (e.g. Holtz et al., 2001) and the maximum solubility of water in the melt.

Here, we follow the definition of Johannes and Holtz (1996) where the solidus curve is defined by the first melt appearance, and this will always be on the water-saturated curve (Fig. 4), except in the total absence of free water. The solidus temperature is independent of the amount of water available because even a very small amount of H_2O available to establish the water activity of 1 is sufficient to create the first melt (Johannes and Holtz, 1996, p.50). Liquidus curves as defined by Johannes and Holtz (1996) are curves of minimum water content necessary to stabilize melt (Fig. 4). In haplogranites, these curves represent the amount of water in a melt in equilibrium with crystals of feldspar and quartz: if water drops below this value some of the melt solidifies to regain the minimum value, if water content increases, melting occurs to regain that minimum value (Holtz et al., 2001).
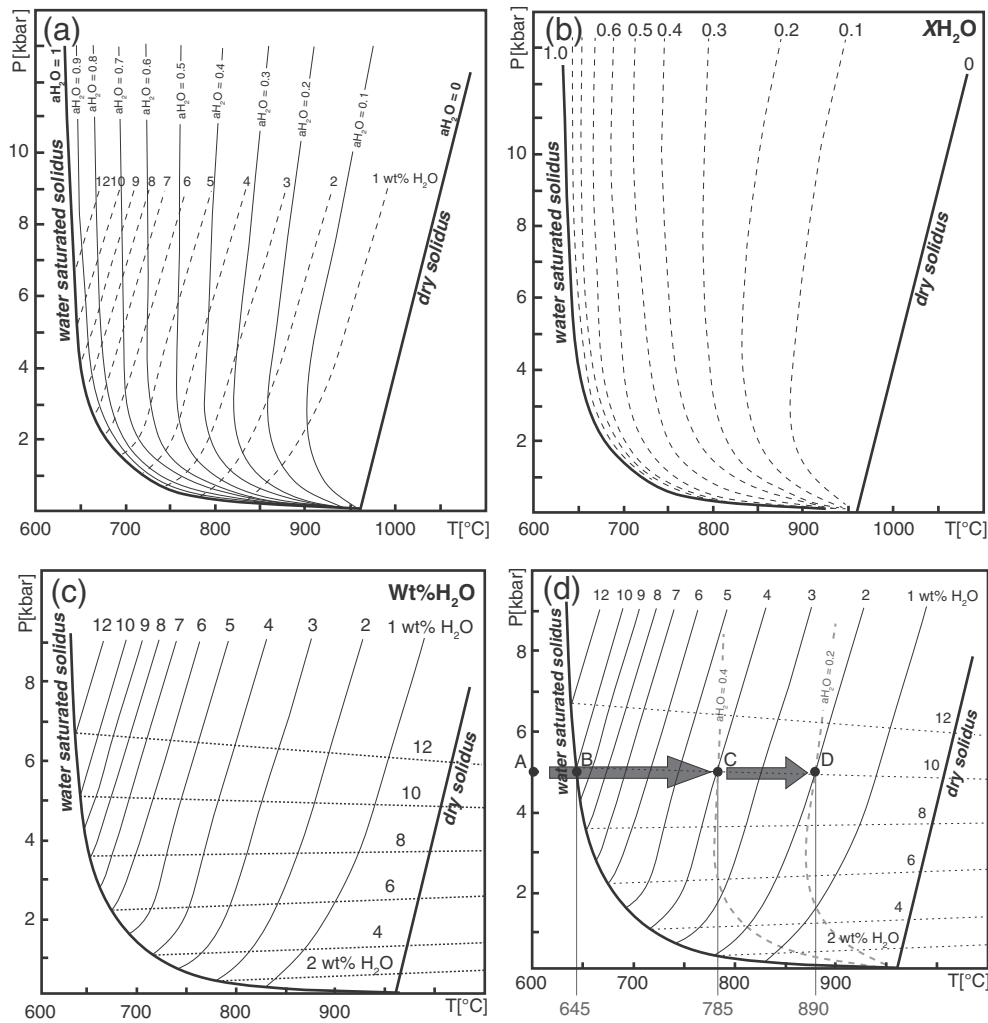
Fig. 4. P–T diagrams showing key curves for the Ab–Or–Qtz–H_2O–CO_2 system for: (a) solidus curves for different water activities (aH_2O) and liquidus curves or curves of minimum wt.% H_2O in melts (dashed lines), (b) solidus curves for different $XH_2O = H_2O/(H_2O + CO_2)$, and (c) liquidus curves (or minimum water content curves; continuous lines) and maximum water content curves (dotted sub-horizontal lines) in wt.% H_2O. Diagrams after Johannes and Holtz (1996). (d) Evolution of a haplogranite undergoing isobaric heating (see also p. 53 in Johannes and Holtz, 1996). Point A indicates a haplogranitic rock with 2 wt.% added H_2O at 600 °C. Heating causes water saturated melting at 645 °C and melt would have 10 wt.% dissolved H_2O (point B), given by the intersection of the liquidus curve and the solidus curve, and therefore only 20% of the rock can melt. When the rock reaches 785 °C, the liquidus curve for 4 wt.% H_2O is reached and therefore 50% of the rock will be molten with a water activity $aH_2O = 0.4$ (point C), as marked by the light grey, dashed line. Complete melting will be reached at 890 °C where the liquidus curve for 2 wt.% H_2O is reached with $aH_2O = 0.2$ (point D).

Maximum H_2O content curves separate the melt field from the field where melt and an aqueous fluid coexist. These curves correspond to the water solubility in silicate melts and it increases with pressure (horizontal dashed lines in Fig. 4c; Robertson and Wyllie, 1971; Holtz et al., 2000) with only little temperature effect. Fig. 4a–c shows the water-saturated solidus, liquidus and the maximum solubility curves in P–T space for the haplogranite system (Qtz–Ab–Or). Minimum and maximum H_2O contents are similar on the water saturated solidus and H_2O contents of melts formed by dehydration melting also lie at the minimum value for the given P–T conditions. These values have been experimentally constrained (Fig. 4) and are used to predict rock fertility.

The maximum solubilities of H_2O in melts in Qtz–Ab, Qtz–Or systems have been widely studied (e.g. Holtz and Johannes, 1994; Holtz et al., 1992b, 1996, 2001; Johannes and Holtz, 1990; Pichavant et al., 1992). Maximum water contents are dependent on melt composition and decrease slightly with decreasing Ab–Or ratios, and sharply with increasing Qtz content (e.g. Holtz et al., 1996, 2000). At low temperatures and moderate to high pressures, large amounts of water are required to completely melt a haplogranite of eutectic composition (Fig. 4c).

At specified P–T conditions above the water-saturated solidus (also known as the wet solidus), hydrous silicate melt can in principle have H_2O content anywhere between the maximum water solubility and the minimum H_2O content (i.e., the liquidus), as long as it is chemically isolated from the solid. This is fundamental for understanding the behaviour of the system: during melting, melt will interact chemically with the solid, the system will typically be rock-dominated (rock-buffered), and so melts generated above the wet solidus will tend to have the minimum water content, dictated by the liquidus for the prevailing P–T conditions. Thus, water-fluxing of rock-buffered systems will generate undersaturated melts with water activities determined by the P–T conditions of melting.

Figure 4d illustrates the heating of a haplogranite with pore aqueous fluids. Upon reaching the solidus (point B), fluids and thermal energy are consumed to produce water-saturated melt. Continued heating of the anatectic terrane moves it into suprasolidus conditions (points C and D) where the original water-saturated melt equilibrates with the surroundings by melting in order to dilute the water in the melt and reach the water content dictated by the liquidus curves. Thus, as T increases, melt fraction increases and the water content of the melt and

its activity drop. This process shifts the melt composition away from the water-saturated solidus, freeing it to rise.

4.4. Water and thermal diffusion

Water diffusivity in silicate melts increases linearly with water contents below 3 wt.%, but exponentially at higher water contents (e.g. Behrens and Nowak, 1997; Nowak and Behrens, 1997). This sudden change in diffusivity behaviour is attributed to depolymerization of the melt by incorporation of OH groups. Importantly, water diffusivity in silicate melts is four to six orders of magnitude lower than thermal diffusivity (Ni and Zhang, 2008). This difference implies that magmas reach thermal equilibrium orders of magnitude faster than water equilibrium. Acosta-Vigil et al. (2012) reviewed experimental studies on rates of chemical diffusion of major components in H_2O-saturated granite melts at anatectic conditions in the continental crust. They found a steep increase in element diffusivity with water content.

4.5. Viscosity

Melt viscosity decreases dramatically with increasing temperature and water content (e.g. Holtz et al., 1996) whereas pressure has only a small effect (Clemens and Petford, 1999; Scaillet et al., 1996; Schulze et al., 1996). The largest viscosity decrease is at low H_2O concentrations (Schulze et al., 1996). For instance, the viscosity of granitic melts decreases by several orders of magnitude when water content increases from 0 to 2 wt.% H_2O. Giordano et al. (2004) suggested decreases of up to four orders of magnitude, Schulze et al. (1996) by 2 to 4 orders of magnitude (depending on T). Dingwell et al. (1996) measured viscosities of haplogranitic melts at 2 kbar and 800–1040 °C and showed a drastic drop in viscosity

with the addition of 0.5 wt.% H_2O (from ~10^{12} Pa.s to ~10^{10} Pa.s), whereas only a small decrease is observed at larger water contents.

Viscosities of samples of High Himalayan Leucogranites were measured at different water contents (Scaillet et al., 1996; Whittington et al., 2004). Whittington et al. (2004) estimated viscosity of 10^{11} Pa.s for anhydrous granite at 750 °C, dropping to $10^{6.5}$ Pa.s when 3 wt.%. H_2O is added. By contrast, Scaillet et al. (1996) measured a viscosity of ~$10^{4.5}$ Pa.s for water contents of ~7 wt.% at T ~750 °C or ~4 wt.% at T ~ 850 °C. This viscosity, they suggested, is the leucogranite viscosity during emplacement, and is typical for melts resulting from Ms-dehydration. Clemens and Petford (1999) emphasized that for dehydration melting reactions, water content of the melt and T are co-dependent and their effect on viscosity counteract one another so as to decrease the viscosity range: at low temperatures melts are water-rich and as temperature increases, viscosity drop is counteracted by a decrease in water content, leading to viscosities between $10^{3.2}$ to $10^{6.3}$ Pa.s for leucogranite to tonalite melts.

4.6. Morphology of neosome

Neosomes formed by water-fluxed melting and dehydration melting have distinct morphologies (Fig. 5). Sawyer (2008, 2010) summarized characteristics typical of neosome formed by water-fluxed melting: (i) leucosome has diffuse boundaries with host rock (Fig. 5a–b); (ii) microstructure of the protolith in the outer part of the neosome, where no melt segregation occurred, is preserved; (iii) if neosome forms when an aqueous fluid enters the protolith via a fracture, then they may form net-like arrays or stringers of neosomes (Fig. 5a, b); (iv) commonly no melanosome or mafic selvedges are associated with neosomes (Fig. 5); and (v) water will partially or completely alter anhydrous minerals in the proximity of leucosomes. In contrast leucosomes formed by
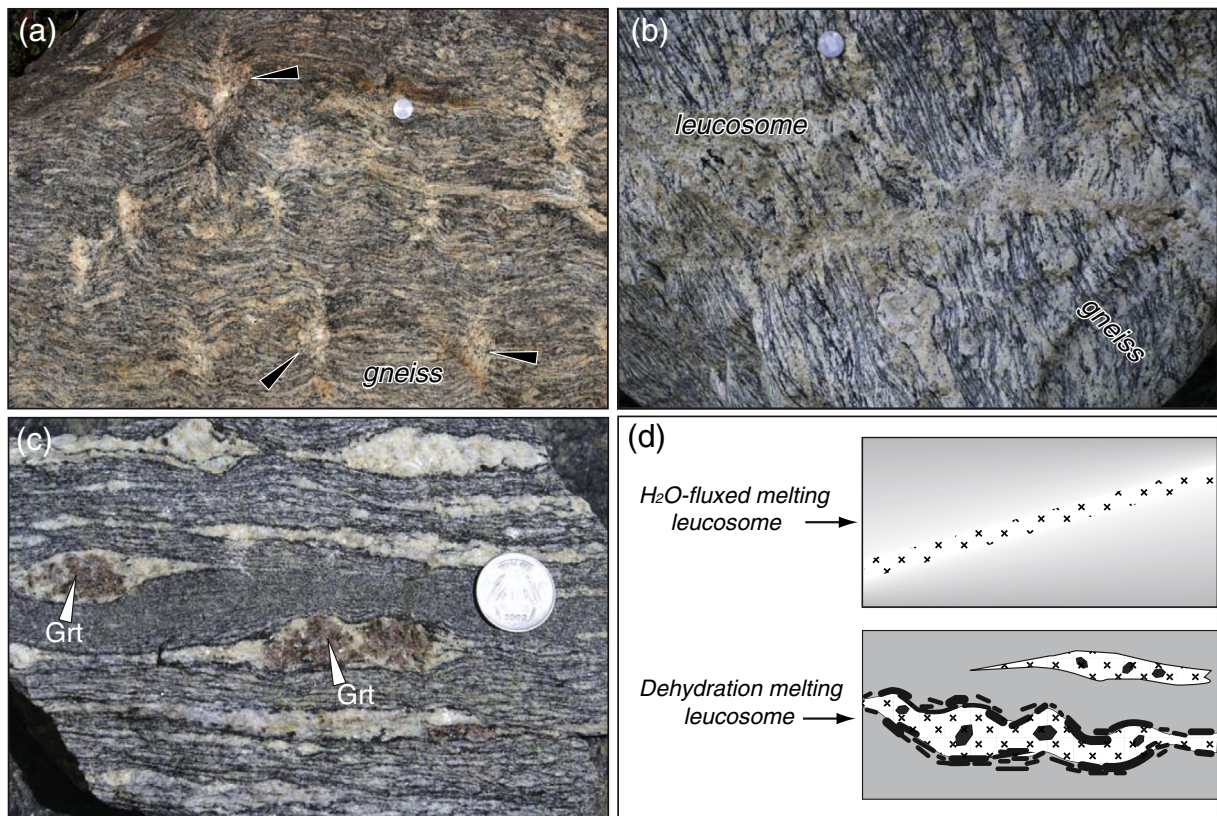
Fig. 5. Photographs (a–c) and sketch (d) depicting differences between leucosomes formed by water-fluxed melting and dehydration melting of the same Bt + Pl + Kfs + Qtz ± Grt orthogneiss in Zanskar, NW, Himalaya. (a–b) Leucosomes formed by water-fluxed melting. These have diffuse boundaries, lack both peritectic minerals and melanosome. (a) Records incipient water-fluxed melting with in situ melt patches (black arrows). In (b) leucosomes created an interconnected network with diffuse boundaries to host rock. (c) Bt-dehydration melting of the same orthogneiss. Leucosome has large peritectic Grt, sharp boundary to host orthogneiss and a melanosome rim. (d) Comparison between the two styles of leucosomes.
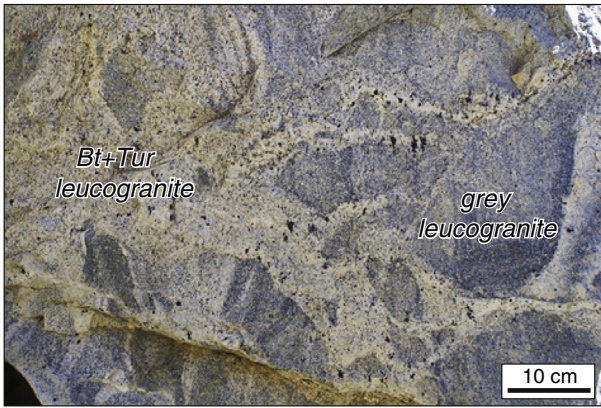
Fig. 6. A possible example of remelting of early, grey leucogranite to give rise to a white, coarser Bt–Tur leucogranite (Zanskar, NW Himalaya).

dehydration melting typically have: (i) sharp contacts with the host rock, with clearly defined melanosome rim; (ii) the leucosome does not retain the microstructure of the protolith at its margins; and (iii) the leucosome network is variable in appearance (Fig. 5c, d).

Acosta-Vigil et al. (2006) showed experimentally that melting of aplitic leucogranite in the presence of excess water results in an interconnected melt network at even very low degrees of melting (<5 vol.%). Melt occupies all grain boundaries and triple points in the rock. This is consistent with the finding that an increase in water content results in slight decrease of the wetting angles of melt (Laporte, 1994). Water-present melting should therefore be characterized by lower wetting angles that promotes melt interconnectivity enabling effective melt segregation and more efficient diffusion of elements throughout the interconnected silicate melt. This contrasts with dehydration melting where incipient melt typically forms isolated pools in triple point junction or films along grain boundaries or fractures (e.g. Sawyer, 2001). An exception might be Ms-dehydration melting which is associated with high dilation strains, producing high melt pore pressures and subsequent interconnected fracture network already at the onset of melting (Rushmer, 2001).

4.7. Remelting of granitic rocks

Water-fluxed melting can also lead to multiple melting events or to melting of rocks side-by-side at different times, during the same thermal cycle, because of heterogeneous and varying water-fluxing through time and space (Rubatto et al., 2009; Sawyer, 2010). Furthermore, leucosomes formed by water-fluxed melting, with compositions close to eutectic, may be remelted by subsequent fluid influx (Fig. 6). This contrasts with dehydration melting, where leucosomes will typically lack hydrate minerals and therefore are unlikely to remelt unless external water is added. In these systems new melt production will be limited to the source rock, which is more refractory than the original protolith. Thus, as concluded by Rubatto et al. (2009): "During fluid-induced melting, melt will form and readily crystallize at any time when the H_2O-rich fluid is consumed, partly independently of how the rock evolves in P–T." This gives rise to zircon populations recording long periods of crystallization (Rubatto et al., 2009), as well as multiple pulses of water-fluxed melting, explaining multiple cross-cutting relationships between in source leucogranite dykes and leucosomes (Finch et al., 2014; Weinberg et al., 2013).

5. Natural examples of water-fluxed melting

We review natural examples of water-fluxed melting in four subsections. We first describe examples of water-fluxed melting at low temperatures, typically lacking anhydrous minerals. Then, we describe

examples interpreted to have occurred above the water-saturated solidus and in which peritectic minerals are present. We present first cases with peritectic hornblende, followed by cases with nominally anhydrous peritectic minerals. In these, melt is water undersaturated, and the presence of aqueous fluids is inferred from a combination of low metamorphic peak temperatures, large melt volumes produced, and similarity with experimental results. In the last subsection we review examples of melting in the presence of low water activity fluids. All examples described and others are summarized in Table 3.

5.1. Melting at water-saturated solidus lacking anhydrous peritectic minerals

Sawyer (1998, 2010) described large regions of diatexites and voluminous anatectic granites in the *Opatica Subprovince, Superior Province, Canada*. Here, felsic "grey gneisses", melted at amphibolite–facies conditions to produce diatexites and granites. The low biotite content of the protolith, the relatively low peak metamorphic T and the large volumes of melt indicate water-fluxed melting of Qtz + Pl + Kfs, rather than Bt-dehydration melting, and melt volume was limited by the amount of K-feldspar in the gneisses (Sawyer, 1998). This is an example of the regional significance of water-fluxed melting where magmatic products escaped the source and rose through 20 km of crust to form plutons.

The transfer of fluids between rocks with different solidus temperatures and how these trigger melting during prograde melting is well-exemplified in *Broken Hill, Australia*. Here, White et al. (2005) documented water-fluxed melting of a granitic gneiss at upper amphibolite facies. Metapelitic rocks undergoing subsolidus muscovite breakdown released water that fluxed neighbouring gneiss, with slightly lower solidus temperatures. The early influx of relatively small water volumes resulted in the production of large amounts of melt as temperature increased. Heterogeneous water influx caused local variations in melt productivity and transitions from coherent metatexites to disaggregated diatexites with increasing volumes of fluids. Other examples of the presence of small volumes of a free-fluid phase in the early stage of prograde melting have also been documented (see Table 3; e.g. Escuder-Viruete, 1999; Nedelec et al., 1993).

Cartwright et al. (1995) and Cartwright and Buick (1998) studied changes in stable isotope ratios in metapelites and marbles during regional metamorphism in *Mount Lofty Ranges, South Australia*. Peak metamorphic conditions increased from 350 to 400 °C to 700 °C (migmatite) at 5 kbar, over ~50 km parallel to lithological strike. Increase in metamorphism was accompanied by a large decrease in $\delta^{18}O$ values in both, metapelites and marbles, suggesting widespread fluid–rock interaction during regional prograde metamorphism. They envisaged up-temperature fluid flow along strike, originated from

Fig. 7. Water-fluxed remelting of arc plutonic rocks of the St Peter Suite (after Symington et al., 2014). Diorite has undergone partial melting with Hbl in leucosome patches (light irregular patches on left hand side, white arrows). Diorite has wispy mingled contact with tonalite.

Table 3
Summary of natural examples of water-fluxed melting described in the literature.

Locality	Melting	Observations/argument for water-present melting	PT conditions	Fate of magmas	Reference
MELTING AT WATER-SATURATED SOLIDUS LACKING ANHYDROUS PERITECTIC MINERALS					
Opatica Subprovince, Superior Province, Canada	Water-fluxed melting of "grey gneisses" to produce diatexites and granites. Melting reaction [5].	Melt fraction produced too high (25-30%) for PT conditions and modal proportion of biotite. Bt stable. Metamorphic fluids released from Hbl breakdown from surrounding amphibolites (inferred from δ^{18}O).Water entered along network of fractures.			Sawyer (1998)
Opatica Subprovince, Superior Province, Canada	Water-fluxed melting of orthogneiss by reaction [5] where Kfs is the limiting reactant and incongruent water-fluxed Hbl-producing reactions [19] and [39].	Proportion of leucosome too high (25-30%), and estimated temperature too low, for dehydration melting. Biotite stable during melting. K-feldspar consumed creating monomineralic domains of plagioclase. Average whole rock δ^{18}O for the protolith and migmatites are similar indicating a fluid of metamorphic origin that used back-thrusts as main channelways.	720-755°C / 4-7kbar	Magmas escaped source. Diatexites occur in north-verging back-thrusts, and metatexites in between thrust planes.	Sawyer (2010)
Broken Hill, Australia	Water-fluxed melting of granitic gneiss. Melt fraction varies (25-60% of melt) over short distances revealing spatial variation of fluid influx.	Transfer of fluids from metapelites undergoing sub-solidus dehydration reactions to rocks at supra-solidus conditions.	~750°C / 4-kbar	Essentially in situ.	White et al. (2005)
Mount Lofty Ranges, South Australia	Congruent water-present melting of metapelites.	Aqueous fluids released by dehydration reactions (inferred from δ^{18}O isotopes) and migrating up-temperature. Melt fraction too high (up to 40%) for given PT conditions.	Variable T up to ~700°C /5kbar (migmatite zone)		Cartwright et al. (1995) Cartwright and Buick (1998)
St. Malo, France	Diatexites surrounded by metatexites derived from anatexis of greywacke.	No peritectic Grt or Crd. Amount of mica in protolith (<10%) too small to produce substantial amount of melt at estimated PT conditions.	650−750°C / 4−8 kbar	Essentially in situ.	Brown (1979) Milord et al. (2001)
Wuluma granite, Central Australia	Congruent melting of gneiss during regional retrogression from granulite- to amphibolite-facies.	Water-fluxing inferred from low % of micas in source for volume of melt produced. Pegmatite intrusions possible fluid source.		Essentially in situ.	Collins et al. (1989)
Trois Seigneurs Massif, Pyrenees, France	Water-fluxed melting of pelitic metasedimentary rocks. Melting locally produce peritectic Crd.	Shallow crustal melting in very steep geothermal gradient above hot terrane. Fluid source: groundwater (marine fluids inferred from δ^{18}O isotopes).	~ 700°C and 10−12 km depth	Leucogranites close to source.	Wickham (1987) Wickham and Taylor Jr (1985)
Aiguilles-Rouges Massif, Western Alps, France and Switzerland	Water-fluxed melting of metagreywacke in 500m wide vertical shear zone. Melting reaction [40].	Water-fluxing inferred from high melt proportion (15-20%) at given PT conditions. Addition of 1wt% of external water calculated. Fluid source: from overthrusted tectonic units underlying the metagreywackes.	630−670°C/2−4kbar	Extensive melting restricted to vicinity of shear zone.	Genier et al. (2008)
Serre, Southern Italy	Congruent Ms water-present melting of metagreywacke and metapelite producing sodic melts. Melting reaction [9].	Subsequent Bt-dehydration melting produced mobile melts that escaped source.	700-800°C / 5-8kbar	Melt extracted but remained in source.	Fornelli et al. (2002)
Garhwal Himalaya, High Himalaya Crystallines (HHC), India	Water-present melting of metasedimentary rocks HHC during prograde metamorphism followed by dehydration melting forming voluminous leucosomes.	Water-present melting inferred from granite geochemistry and existence of wide range of produced granite compositions − reflecting different aH$_2$O. Small volumes of two-mica leucogranites produced. Fluid source: underlying cold metasedimentary rocks.	< 650°C /~7kbar	Essentially in-situ. Leucogranites from dehydration melting are mobile and escaped from source.	Prince et al. (2001)

Zanskar, NW Himalaya, India	Bt and Ms-dehydration melting of orthogneiss (and minor paragneiss) followed by extensive water-present melting.	Water-fluxed melting inferred from high melt % for given protolith and PT conditions. Water from underlying cold metasedimentary rocks.	650-720°C/ 4-7kbar	Magma escaped the source.	Pognante (1992) Finch et al., (2014)
WATER-FLUXED MELTING WITH PERITECTIC HORNBLENDE					
Central Alps, Switzerland	Water-fluxed melting of orthogneiss and metasedimentary rocks. (reaction [15]), accompanied by Ms-dehydration melting of metasedimentary rocks.	PT conditions below Bt dehydration melting reaction. Melting lasted 10 m.yr. Melt fraction varies over short distances revealing spatial variation of fluid influx. Fluid source: from dehydration of metapelites.	~ 670°C /7-7.5 kbar	Essentially in situ.	Burri et al. (2005) Berger et al. (2008) Rubatto et al. (2009)
Coast Plutonic Complex, British Columbia, Canada	Bt water-fluxed melting of Hbl-bearing gneisses (melting reactions [16] and [21]).	P_{H_2O} was close to total pressure i.e. presence of free water. Presence of Hbl in leucosome.	675−750°C/ 6−8kbar	Limited partial melting of "andesitic" protoliths explains plutons if melts include some residual material.	Lappin and Hollister (1980)
Central Gneiss Complex, British Columbia, Canada	Bt water-saturated solidus melting of gneisses (reaction [16] and [21]).	Presence of Hbl in leucosome.	≥ 700°C/ ≥ 3 kbar	Essentially in situ.	Kenah and Hollister (1983)
Muskoka Domain migmatites, Grenville Province, Ontario, Canada	Water-fluxed melting of dioritic gneiss by reaction [17] forming stromatic to patchy migmatites.	Volumes of leucosome too large to be derived from Bt-dehydration alone for inferred PT conditions. Granitic leucosome surrounded by Hbl+Pl melanosome.	750-850°C / 9-12kbar	Migmatites interpreted as transfer zone for melts migrating to higher structural levels.	Slagstad et al. (2005) Timmermann et al. (2002)
Gallatin Range, Montana, USA	Incongruent water-fluxed melting of Bt-bearing TTG during pervasive shearing (reaction [15]).	Water influx inferred from melt fraction produced too high for proportion of biotite in source rock and from presence of Hbl in melanosome. Recycling of aqueous fluids causing remelting.	680−730°C /8−10kbar	Granites restricted to vicinity of shear zones that allowed fluid infiltration. Melt was free to rise.	Mogk (1992)
Eseka migmatites, Congo Craton, Cameroon	Melting of TTG gneiss by water-present melting followed by Bt-dehydration.	Neosomes of granodioritic to trondhjemitic composition, rich in peritectic Hbl megacrysts and aggregates (15−45 vol.%), Grt (4−8 vol.%) and scarce Cpx. Small melt volume.	Water-fluxed melting at 700°C. Bt-dehydration at 750°C / 9 kbar.		Nedelec et al. (1993)
Iberian Massif, Spain	Melting of tonalitic orthogneisses by water-fluxed Bt melting (reaction [17a]) followed by Bt-dehydration melting producing stromatic to patchy migmatites.	Water-fluxed melting inferred from presence of peritectic Hbl with Pl+Qtz+Bt inclusions in leucosomes. Ductile shearing related to post-collisional crustal thinning that followed crustal thickening.	Water-fluxed melting at 700°C / 5−10 kbar. Bt-dehydration at 730−750°C / 5−10 kbar	Essentially in situ.	Escuder-Viruete (1999)
Karakoram, Ladakh, NW India	Water-fluxed melting of a calc-alkaline arc sequence and surrounding metasedimentary rocks. (reactions [16] and [17a,b]).	Water-fluxed melting inferred from lack of anhydrous peritectic minerals, presence of peritectic Hbl and biotite remains stable. Melting lasted >5 m.yr.	~670-750°C / 6-8kbar	Water-fluxed melting restricted to the 7−8 km-wide Karakoram Shear Zone. Magma escaped the source.	Reichardt et al. (2010) Reichardt and Weinberg (2012)
Daeijak Island, Korean Peninsula	Water-fluxed disequilibrium melting of dioritic–tonalitic Archean protoliths produced tonalitic–trondhjemitic leucosomes.	P-T conditions based on the hornblende–plagioclase thermobarometry and phase equilibria.	~700–730 °C / 4.7–5.5 kbar	Disequilibrium melting due to rapid extraction.	Lee and Cho (2013)

Chepelare area, Central Rhodopes, Bulgaria	Melting of pelitic gneiss and schist by reaction [17a].	Absence of anhydrous mafic peritectic minerals in leucosome.	>760°C, > 10kbar		Cherneva and Georgieva (2007)
WATER-FLUXED MELTING WITH NOMINALLY ANHYDROUS PERITECTIC PHASES (INCLUDING CRD)					
Damara Belt, Namibia	Felsic orthogneisses melted by incongruent water-fluxed Bt-dehydration melting by reaction [31]. Metasedimentary rocks melted by congruent water-fluxed melting by reaction [4] followed by incongruent water-fluxed Bt melting reactions [25].	Peritectic Grt and Crd in leucosomes. Water presence inferred from low melting T (below onset of dehydration melting reactions), significant amount of melt, and from similarity between leucosomes and experimentally obtained melts. Peritectic Grt composition matches Grt composition predicted from water-present experiments.	700-750°C / 4-5kbar (metasedimentary rocks.), 690−730°C / 5−6kbar (orthogneiss)	Melt extraction from the source.	Ward et al. (2008) Kisters et al. (2009) Jung et al. (2000) Jung et al. (2009)
Cooma Granodiorite, SE Australia	Ms and Bt dehydration melting of metapelites during prograde path followed by congruent water-fluxed melting of metapsammites during cooling (reaction [1]). Ellis and Obata (1992) propose water-fluxed Bt melting already during prograde path (reaction [32]).	Dehydration melting formed Pl-poor leucosomes that crystallized before most or all of the metapsammite water-fluxed melting. The latter occurred along retrograde path, created Pl-rich leucosomes. Water was introduced along high-strain zones.	~650-680°C / 2.5-3.5kbar (water-fluxed melting)	Water-fluxed melts escaped from source, in contrast to dehydration melts that remained essentially in situ	Ellis and Obata (1992) Vernon et al. (2001) Vernon et al. (2003)
Velay anatectic dome, Massif Central, France	Water- fluxed melting first. Change in geothermal gradient induced Bt-dehydration melting.	Bt stable during water-present melting. Peritectic Crd and/or Grt from Bt-dehydration melting.	Water-fluxed melting: < 750°C and > 5bar Bt-dehydration melting: 760−850°C / 4−5kbar.	Water-fluxed melting lead to extensive migmatisation but minor granite bodies. Bt-dehydration led to melt extraction and granite formation.	Montel et al. (1992)
Connemara, Ireland	Extensive water-present melting of metapelites defining a progression from incipient migmatites, to Crd migmatites, to Crd-Grt migmatites (reactions [2, 3, 22, 29, 32]).	Migmatite sequence matches sequence of water-saturated melting reactions in upper amphibolite facies predicted from KFMASH pelite system. Peritectic Crd and/or Grt. Presence of Crd in absence of Kfs suggest water-saturated conditions. Fluid source: water released from crystallized calc-alkaline intrusions. Patchy distribution of aqueous fluid inferred from irregular melt distribution.	650°C-750°C / 4-6kbar		Yardley and Barber (1991a)
Sierra de Comechingones, Central Argentina	Water-fluxed melting (reaction [24]) followed by Bt-dehydration melting of aluminous gneisses.	Water presence inferred from migmatite chemistry. Leucosome and migmatite chemistry similar to experimentally obtained water-fluxed melts. Large melt loss (20-60%).	Water-fluxed melting: ~ 800°C / 7-8kbar. Bt-dehydration melting: > 900°C/7-8kbar		Otamendi and Patiño Douce (2001)
East Greenland Caledonides	Incongruent water-fluxed muscovite melting of metasedimentary rocks (reaction [35] forming Als).	Low Rb/Sr ratios suggest water-present muscovite melting. Aqueous fluids introduced along shear zones.	~750°C / 10-12kbar	Essentially in situ peraluminous leucogranites	Kalsbeek et al. (2001)

Nanga Parbat, Himalaya, Pakistan	Ms-dehydration melting of metapelites in deep crust, followed by localized water-fluxed melting in shallower crustal levels (reaction [33]).	Crd-bearing leucosomes. Water-fluxed melting inferred from geochemical signature (Rb/Sr, Ba). Fluid source: meteoritic water infiltrating along shear zones.	700−720°C. Ms-dehydration melting in >20km depth, water-fluxed melting at 15km depth and above.	Water-fluxing restricted to vicinity of shear zones in intermediate and lower crustal depths	Butler et al. (1997)
Harts Range, Central Australia	Water-fluxed melting of amphibolites (reaction [26]).	Peritectic Grt, Cpx and Ttn. Tonalitic melts.	800-850°C / 8-10kbar		Storkey et al. (2005)
LOW WATER ACTIVITY FLUIDS: MELTING WITH PERITECTIC OPX AND GRT					
Ashuanipi Complex, Labrador, Canada	Grt-Opx-bearing granodiorite diatexites.	Wholesale fusion of biotite-bearing source rocks. CO_2-H_2O mixed fluid (aH_2O < 1) decreased liquidus temperatures and stabilized Opx.	Possibly 850-900°C/3.5-5.5 kbar		Percival (1991)
CONTACT AUREOLES					
Moldanubian zone, Bohemian Massif, Austria	Porphyritic Bt-Hbl granodiorite, generated by regional contact metamorphism around intrusive magmas providing heat and water.	Formation of I-type granitoids by anatexis and generation of secondary granite: "a cool, wet, restite-rich mid-crustal magma".	<750°C/low pressure	Remained close to source	Finger and Clemens (1995)
Eltive Complex, Scotland	Dehydration melting and water-fluxed melting of metapelites and psammites.	Variation in available water at the onset of melting, promoted by focusing of fluid released by dehydration in the middle and outer aureole.	680-800°C/2.2 kbar	Remained close to source	Droop and Brodie (2012) Rigby et al., 2008
Ballachulish Igneous Complex, Scotland	Water-fluxed melting of semipelitic rocks.	PT conditions too low for dehydration melting. Possible water source is underlying Qtz-diorite.	650-700°C/3 kbar	Remained close to source	Pattison and Harte, 1988
OTHER					
Thor-Odin metamorphic core complex, British Columbia, Canada	Water-fluxed melting of metapelites and greywackes aided by Ms-dehydration.	Use and reuse of same water during repeated events of partial melting explaining homogeneity of mineral $\delta^{18}O$ values in the middle continental crust.	>750 °C / 8 kbar		Holk and Taylor Jr. (1997; 2000)

devolatization of metapelites at lower T. Leucosomes in the migmatite zone lack porphyroblasts of anhydrous peritectic minerals, suggesting congruent water-present melting reaction. This conclusion is further supported by up to 40% leucosomes, which requires influx of aqueous fluid at T ~ 700 °C. They suggested anatexis acted as fluid sink and a barrier for further upward fluid migration.

In *St. Malo, France*, Brown (1979) described a core of diatexite surrounded by a rim of metatexite derived from extensive and local anatexis of greywacke at upper amphibolite facies conditions in the presence of water, lacking either peritectic cordierite or garnet (see also Milord et al., 2001). The *Wuluma granite, Central Australia* (Collins et al., 1989), is an example of extensive congruent melting of gneiss during regional retrogression from granulite- to amphibolite–facies as a result of aqueous fluid influx possibly transferred from numerous pegmatite dykes. In the *Trois Seigneurs Massif, France*, water-fluxed melting occurred at shallow crustal levels in the presence of a very steep geothermal gradient in a very hot terrane, where leucogranites stayed close to the source (Wickham, 1987). This is perhaps a unique example where groundwater infiltration (marine fluids) was the source of fluids, as indicated by oxygen isotopes (Wickham and Taylor, 1985).

5.2. Water-fluxed melting with peritectic hornblende

Experiments demonstrated that peritectic Hbl becomes stable in the presence of added water (e.g. Gardien et al., 2000). Reactions producing peritectic Hbl (Fig. 7; Table 2) generally take place at temperatures higher than congruent melt reactions (see Table 2 and Fig. 1a curve 5).

A number of mineral reactions involving a free aqueous fluid phase and producing peritectic Hbl were inferred from petrological field-based studies (Table 2; e.g. Berger et al., 2008; Escuder-Viruete, 1999; Kenah and Hollister, 1983; Lappin and Hollister, 1980; Lee and Cho, 2013; Mogk, 1992; Nedelec et al., 1993; Reichardt and Weinberg, 2012b; Sawyer, 2010; Slagstad et al., 2005).

In the *Central Alps in southern Switzerland*, an orthogneiss melted producing a migmatite with variable volumes of Hbl-bearing leucosome (Berger et al., 2008; Burri et al., 2005; Rubatto et al., 2009). This was accompanied by Ms-dehydration reaction of metapelites. The distribution of partial melts represented by leucosomes is spatially variable in a protolith that was essentially homogeneous (Berger et al., 2008), varying over short distances from leucosome-free gneisses to metatexite and diatexite, revealing spatial variation of fluid influx. Berger et al. (2008) also argued that fluids released by crystallization of the melt in migmatites could trigger further melting, explaining the origin of late pegmatite intrusions. Since such exsolved aqueous fluid may contain appreciable amounts of LILE, they may enhance fertility of the rocks it infiltrates (Aranovich et al., 2013). Zircons from these rocks indicate that melting lasted 10 m.yr. at roughly constant conditions (Rubatto et al., 2009). Rubatto et al. (2009) demonstrated that melting at any point in time was localized, dependent on the availability of water, with rocks side-by-side melting and crystallizing at different times. They suggested also "frequent remelting of the same leucosome under repeated aqueous fluid influx and without changing the mineral assemblage". Thus, water fluxing could melt rocks multiple times during a single and prolonged metamorphic event. These findings imply that melt

productivity was low, explaining the lack of anatectic granitic bodies in the Alps, and that the total volume of leucosomes is not indicative of the melt fraction at any particular time.

Lappin and Hollister (1980) investigated Hbl-bearing migmatitic gneisses from the *Coast Plutonic Complex, British Columbia, Canada*. They documented distinctive textures in three rock types and described three reactions [16, 21a, b] (in Table 2) that account for the production of melt and peritectic Hbl. They estimated that melting took place between 675 °C and 750 °C at 6–8 kbar and that P H₂O was close to total pressure (interpreted here to mean that an aqueous fluid phase had water activity close to unity). They suggested that melting reactions could explain derivation of the tonalitic and granodioritic plutons in the area from limited partial melting of "andesitic" protoliths.

In the *Muskoka Domain migmatites, Grenville Province, Canada*, Slagstad et al. (2005) discussed the origin of coarse-grained hornblende with numerous rounded inclusions of plagioclase, biotite, and quartz resulting from mid-crustal thrusting and high-grade metamorphism. Hbl was considered to be peritectic and a result of reaction [17a], by contrast to the interpretation of Timmermann et al. (2002) who proposed the same reaction but without a free aqueous fluid.

Mogk (1992) described an example of voluminous melting resulting from infiltration of fluids through m-scale anastomosing shear zones into Archean trondhjemite–tonalite–granodiorites (TTGs) at the *Gallatin Range, Montana, USA*. They inferred an incongruent melting reaction [15] and the presence of a free water phase because the protolith had low biotite abundance (low water contents) and because of the presence of Hbl in the melanosome (Naney, 1983). Resulting granites are restricted to the vicinity of the shear zones and the "whole" gneiss was texturally and chemically reworked through cyclic fluid infiltration, melting and melt-enhanced deformation. Melt was free to rise because melting conditions were above Ms-dehydration, approximately 100 °C above the water-saturated solidus and source rocks followed a clockwise P–T path.

Nedelec et al. (1993) described the high T and high P *Eseka migmatites in Cameroon*, where peritectic Hbl was inferred to result from Bt-dehydration at conditions equivalent to the amphibolite–granulite facies boundary. Here, Archaean Bt + Pl + Qtz tonalitic grey gneiss started to melt in the presence of small water volumes below 700 °C and progressed into Bt-dehydration melting at 9 kbar and 750 °C. Melting gave rise to spotted neosomes of granodioritic to trondhjemitic composition, rich in hornblende megacrysts and aggregates, garnet and scarce clinopyroxene. The presence of garnet and hornblende lacking titanite suggest higher P, T conditions supported by experiments of a Bt + Ep + Hbl + Qtz + Pl paragneiss at 10–20 kbar (Skjerlie and Johnston, 1996) indicating that amphiboles may form together with garnet as a result of Bt-dehydration melting reaction. However, this reaction only forms small volumes of melt and occur at temperatures above 850 °C rather than the 750 °C inferred for the Eseka migmatites. As previously mentioned, experimental melting of tonalite at high P–T (Carroll and Wyllie, 1990) shows that with increasing H₂O content the peritectic minerals change from clinopyroxene to garnet and finally to amphibole. Therefore it is possible that the stability of garnet and amphibole may overlap for certain water contents.

Metamorphism of tonalitic orthogneisses in the *Iberian Massif, Spain*, at conditions transitional between amphibolite and granulite facies (Escuder-Viruete, 1999) produced stromatic migmatites, as well as patchy pegmatitic migmatites in the internal parts of the orthogneiss bodies surrounded by ductile shear zones. Leucosomes comprise Qtz + Pl + Kfs + Hbl and sporadic melanosome comprise Bt + Pl ± Hbl ± Ttn. The presence of hornblende with Bt, Pl, Qtz and Ilm inclusions in leucosomes indicates that melting started in the presence of water by reaction [17b]. This reaction produced a small amount of melt and was followed by Bt-dehydration melting.

Collectively examples in Sections 5.1 and 5.2 demonstrate some characteristic features of low-temperature water-fluxed melting. Typically, it generates leucosomes and leucogranites lacking peritectic minerals and melting consumes quartz and feldspars (e.g. Cartwright et al., 1995;

Collins et al., 1989; Sawyer, 1998, 2010), forming melts that plot in the low-temperature field of the normative Q–Ab–Or diagram for water-saturated melt (Fig. 2a; e.g. Kalsbeek et al., 2001). Most significantly, melting and solidification can occur several times during a single tectono-thermal event (Rubatto et al., 2009) and melt volume distribution in the source is heterogeneous depending on water access (Berger et al., 2008; White et al., 2005). Multiple melting events potentially lead to complexities in field relationships between different melt phases, and also to a prolonged history of zircon crystallization (Rubatto et al., 2009, 2013; Weinberg et al., 2013). Small volumes of water influx cause a disproportional increase in melt fraction (Collins et al., 1989; Genier et al., 2008) particularly as temperatures rise during the prograde history of a terrane (Cartwright et al., 1995; White et al., 2005). Whilst water-rich granitic melt is typically unable to rise far from the source (Brown, 1979; Collins et al., 1989; Fornelli et al., 2002; Kalsbeek et al., 2001; Wickham, 1987) there are cases in which this is possible (Prince et al., 2001; Sawyer, 1998). Field observations supported by experiments suggest that peritectic amphibole is indicative of water-present melting. In the absence of water, Bt-dehydration melting generates instead Grt, Crd or Opx as the mafic peritectic minerals. However, a couple of field examples suggest that there may be exceptions to this rule (Eseka migmatites, Nedelec et al., 1993).

5.3. Water-fluxed melting with Crd and nominally anhydrous peritectic phases

Water-fluxed melting that produces Crd and nominally anhydrous phases such as Grt, Opx and Sil are more difficult to recognize in the field, not only because of the nature of the peritectic phases but also because of the concomitant instability of micas. Arguments for the presence of a free aqueous fluid phase revolve around the large volumes of melt produced for a relatively low inferred peak temperature, and composition considerations of the peritectic phases based on experiments or thermodynamic modelling.

Migmatitic metasedimentary rocks of the Pan-African *Damara Belt in Namibia* have leucosomes in extensional sites associated with both cordierite and garnet (Ward et al., 2008). These authors inferred that rocks have undergone water-fluxed biotite melting and have lost approximately 10% melt. They estimated melting conditions to be 750 °C at 5 kbar, lower than the onset of Bt-dehydration melting reactions. They therefore suggested that the incongruent melting reaction [30], which includes an aqueous phase, accounts for the observations. This conclusion is supported by water-present melting experiments that yielded melts and mineral compositions and modal contents that are in general agreement with the observations. Kisters et al. (2009) further detailed how these melts were extracted from the rock mass and together these two papers demonstrate that melt can be extracted from water-fluxed terranes even at a relatively small melt fraction. As we will see below, their ability to rise is likely a result of them being formed at P–T conditions above the water-saturated solidus, so that the melts are water undersaturated and their ascent not inhibited by decompression solidification.

Felsic orthogneisses from the Damara Belt also underwent partial melting through limited influx of water and Bt-dehydration (reaction [31]; Jung et al., 2009). In metapelites, melting was initiated by the congruent melting reaction [4] followed by voluminous partial melting involving the breakdown of biotite to produce a garnet-bearing leucosome and leucogranite via reaction [25] (Jung et al., 2000). Presence of water was inferred from the estimated low peak temperatures and similarities to experimental results.

It has been suggested that cordierite in and around the *Cooma Granodiorite in SE Australia* resulted from water-fluxed melting (Ellis and Obata, 1992). Vernon et al. (2001) used microstructural evidence to argue instead for a two-stage melting. A first melting event consumed muscovite and continued on to consume biotite during prograde

metamorphism in metapelites to produce cordierite, K-feldspar and melt that formed plagioclase-poor leucosomes. Following crystallization of this melt, water influx possibly led to melting of the metapsammites during the cooling path. Leucosomes derived from psammites are plagioclase-rich and zoned, and this is possibly the magma that originated the Cooma Granodiorite, as supported by gradational contacts between metapsammite-derived migmatites and the granitic body. The authors argued for a limited upward migration of the magma away from the source.

Montel et al. (1992) described the opposite order of events in the *Velay anatectic dome, French Massif Central*. They recognized a first melting event characterized by water fluxing with stable biotite. In a few cases where Bt became unstable either garnet or cordierite was formed. This event led to minor granite bodies related to large-scale migmatization. A change in the geothermal gradient, possibly driven by mafic magma intrusions, induced dehydration melting which gave rise to cordierite-bearing granites and late-migmatitic granites.

In *Connemara, Ireland*, metapelites underwent extensive migmatization defining a progression of zones from an incipient migmatite zone, to cordierite migmatites and to cordierite–garnet migmatites (Yardley and Barber, 1991a). These observations match the predicted sequence of H_2O-saturated melting reactions for KFMASH pelite system in upper amphibolite facies. Yardley and Barber (1991a) suggested that the appearance of cordierite or cordierite–garnet in metapelitic migmatites without the appearance of K-feldspar is diagnostic of H_2O-saturated conditions. The crystallization of calc-alkaline intrusions, responsible for regional metamorphism, may have been the source of water. The increased melt production during regional metamorphism caused by water influx buffered the temperatures that could otherwise have reached granulite facies. Like for the Central Alps (Berger et al., 2008), the distribution of aqueous fluid, inferred from leucosome distribution, was patchy and locally buffered by melting reactions.

Otamendi and Patiño Douce (2001) described water-fluxed melting followed by Bt-dehydration melting of aluminous gneisses in the *Sierra de Comechingones, Central Argentina*. The resulting metatexites/diatexites are all strongly melt depleted. They estimated that migmatites that underwent water-fluxed melting at ~800 °C lost around 20% melt and granulites formed by Bt-dehydration melting at ≥ 900 °C, lost ca. 60% melt (Otamendi et al., 1999). Leucosomes resulting from water-fluxed melting have Qtz + Kfs ± Grt ± Crd and were formed at amphibolite to granulite facies conditions following reaction [24]. The presence of an aqueous fluid phase was inferred from migmatite geochemistry.

In the *East Greenland Caledonides*, Kalsbeek et al. (2001) described peraluminous Bt–Ms leucogranite sheets and plutons formed by low-temperature (<800 °C) anatexis of metasedimentary rocks by water-fluxed melting with breakdown of muscovite. Aqueous fluids would have been introduced along shear zones and produced granite as a result of reaction [35], and plutons that did not move great distances.

In summary, water-fluxing at temperatures above water-saturated solidus leads to melting associated with the breakdown of micas and gives rise to water undersaturated melts. A number of reactions have been proposed to account for the different peritectic phases such as Grt, Crd, Als or Cpx (Table 2; e.g. Milord et al., 2001; Storkey et al., 2005). In some cases melts are capable of escaping (e.g. Jung et al., 2000; Kisters et al., 2009; Prince et al., 2001; Sawyer, 1998) whereas in others, melts stayed close to the source (see Table 3; e.g. Collins et al., 1989; Vernon et al., 2001).

5.4. Melting in the presence of low water activity fluids including brines

The composition of the Grt–Opx-bearing diatexites in the *Ashuanipi Complex, Labrador, Canada*, is similar to those of Archean paragneisses in the area, indicating that the diatexites resulted from high-degrees of fusion and mobilization *en masse* of the paragneiss (Percival, 1991). In the absence of fluids, this would require T > 1000 °C, for which there
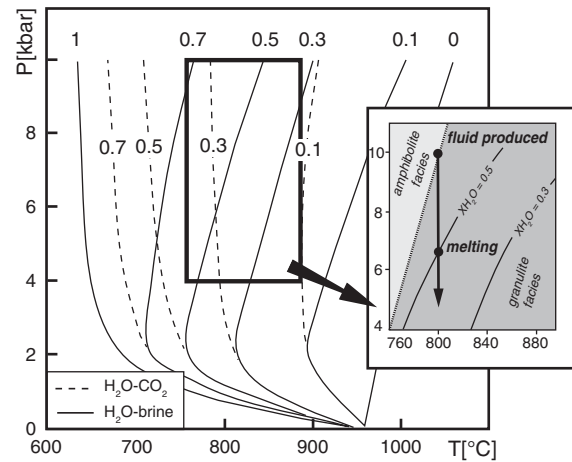

Fig. 8. Comparison between the solidus curves for leucogranites in the presence of $H_2O + CO_2$ solutions (dashed lines, from Ebadi and Johannes, 1991) with those in the presence of brines (solid lines; from Aranovich et al., 2013). XH_2O is the molar proportion of water; used K/K + Na = 2. Curves for brine show increase in solidus T when compared to those of $H_2O + CO_2$ solutions with the equivalent H_2O mole fraction. Strong decrease in water activity of brines with a rise in P is reflected in the positive slope of the solidus curves, instead of negative or vertical. Inset shows the isothermal decompression of a hypothetical brine released at the boundary between amphibolite and granulite facies, with XH_2O of 0.5. This fluid rises and metasomatizes rocks at granulite facies conditions until it intersects the solidus for $XH_2O = 0.5$ where melting starts well within the granulite facies terrane.

is no evidence. Percival (1991) therefore argued for the presence of a CO_2–H_2O mixed fluid ($aH_2O < 1$) capable of decreasing the liquidus temperatures and stabilizing Opx.

Aranovich et al. (2013) recognized melting in the presence of a low water activity fluid as a potentially significant agent of crustal evolution. They found that several examples of granitic terranes were generated by low water activity melting of up to 50 vol.% of the source (Friend, 1983; Percival, 1991; Timmermann et al., 2002). This could not be explained by either water-fluxed or dehydration melting reactions at conditions transitional between amphibolite and granulite facies. Aranovich et al. (2013) expanded on their earlier findings that aqueous brines (alkaline chloride solutions) can have low water activity at high pressures. They carried out experiments with pressures between 4 and 13 kbar and determined the solidus curves using these water-undersaturated brines. Their results (Fig. 8) have significant implications for crustal melting because brines: (a) can stabilize anhydrous phases such as Opx; (b) shift the solidus to higher temperatures due to the great decrease in water activity in brines with increased pressure; (c) can metasomatize and re-fertilize refractory granulite facies terranes; (d) shift the slopes of the water-undersaturated $CO_2 + H_2O$ curves in PT diagrams from negative or vertical, to positive; (e) unlike dehydration melting, brine infiltration has low water activity but no theoretical restrictions on the amount of water that could be available for rock melting; and (f) brines may provide an explanation for K-enrichment of A-type granites. The positive slope of the solidus curves implies that such melts are capable of rising. Furthermore, the low water activity brines are capable of percolating through rocks at granulite facies conditions before causing melting (Fig. 9a). Whilst there are not many sources of brine in the lower and middle crust, degassing gabbros are a potentially important source.

5.5. Archean trondhjemites–tonalites–granodiorites (TTGs), adakites and water-fluxed melting

Many Archean trondhjemites–tonalites–granodiorites (TTGs) terranes record water-fluxed melting (e.g. Mogk, 1992; Nedelec et al., 1993; Table 3). Discussions surrounding the origins of adakites and
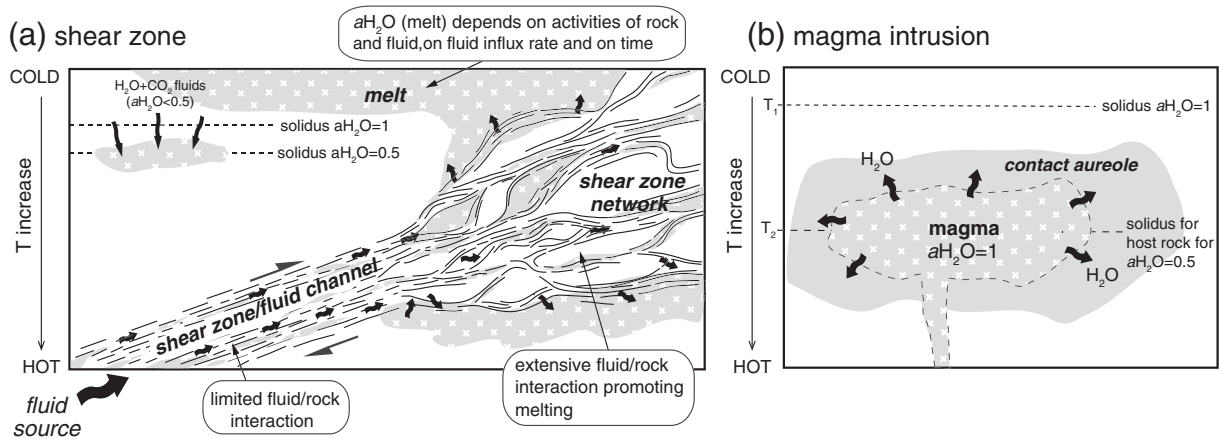
Fig. 9. Structural controls on water fluxing. (a) Shear zone tapping a source of aqueous fluids (such as crystallizing underplated basalt) and providing a channel into a hot terrane. Where the shear zone expands into a network of smaller shear zones, or where fluid migration slows, fluid/rock interaction increases and voluminous melting is promoted by fluids out of equilibrium with surroundings. Melts generated have water activity set by the specific PT conditions, and melt fraction is dictated by the volume of aqueous fluids added, potentially significantly larger than that expected from dehydration melting reactions for peak anatectic conditions (Percival, 1991; Sawyer, 1998). Low water activity fluids, such as CO_2-rich aqueous fluids or brines (top left), migrating up-temperature are also capable of fluxing hot terranes, past the water-saturated solidus, until intersecting the solidus curve for its specific water activity. In either case, melts generated are undersaturated, capable of ascending, and may be associated with anhydrous peritectic minerals. (b) Sketch of a pluton crystallization releasing high water activity fluids to surrounding rocks with water activity established by the metamorphic conditions (T_2) of $aH_2O = 0.5$. Water influx causes extensive aureole melting.

TTGs centre around the nature and conditions of melting of subducted slabs (e.g. Drummond and Defant, 1990; Moyen and Stevens, 2006; Peacock et al., 1994; Prouteau et al., 1999, 2001). There is growing evidence that modern slab melting occurs under low temperature fluid-present conditions (Peacock et al., 1994; Prouteau et al., 1999). Melts generated in this way are of dacitic composition, such as typical adakites and TTGs, and are water rich, which prevents plagioclase from crystallizing early and removing Sr. Dehydration melting of slabs require much higher T and would generate granitic rather than dacitic melts, and lead to early plagioclase crystallization. Furthermore, experiments on water-present melting of mid-ocean ridge basalts show that at T = 900 °C and P = 20 kbar melts generated are depleted in Nb, Ta and Ti (Prouteau et al., 1999). If these melts pervade the asthenosphere and are later recycled during asthenosphere melting, this could explain the negative anomalies of Nb, Ta and Ti that characterize arc magmas. For Archean TTGs, the nature of the primary melts and the conditions at their source, and even whether or not they are related to subduction zones, remain debatable. Due to higher prevailing temperatures, dehydration melting of subducting slabs remains a plausible alternative (e.g. Beard and Lofgren, 1991; Johnson et al., 2014; Moyen and Stevens, 2006; Sen and Dunn, 1994).

6. Structural controls on water-fluxed melting

Active tectonics may lead to perturbations and even inversions of the steady-state geothermal gradient, and thus modify the rate of water production and depth where this occurs (Yardley and Valley, 1997). In this section we summarize examples of water-fluxed melting associated with tectonic activity either related to shear zones or to regions of thermal inversion related to thrust tectonics (Figs. 9 & 10).

6.1. Shear zones

Active shear zones tend to attract regional fluids due to decreased mean pressure (see Mancktelow, 2006 for discussion). This is reflected in the common association between shear zones and quartz veins, migmatites and granitic intrusions. Sawyer (2010) noted that: "Shear zones occur prominently in all examples of granite and orthogneiss for which water-fluxed melting has been proposed. Consequently, shear zones are widely thought to be the pathway along which the aqueous fluids that caused anatexis migrated." Mogk (1992) pointed out that

shear zones serve as channels for both fluid ingress and magma extraction (Fig. 9a) a point that we explore further below.

Genier et al. (2008) described a 500 m wide Variscan shear zone in the *western Alps* in metagreywackes and orthogneisses at amphibolites facies (640–670 °C, 2–4 kbar) where leucosome comprises 20% of outcrop volume. Metapelites at similar P–T conditions, but outside the shear zone did not undergo melting. Using PerpleX pseudosection modelling they estimated that such melt volumes required the presence of 1 wt.% of external water and suggested that a possible source of water was underthrusted units.

The 7–8 km-wide *Karakoram Shear Zone, Ladakh, NW India*, attracted regional fluids which triggered water-fluxed melting inside the shear zone. Pressure gradients within the shear zone not only brought in fluids but also expelled magmas. Magma escape pathways from the source to form the Karakoram batholith are exposed within the length of the shear zone (Hasalová et al., 2011; Reichardt and Weinberg, 2012a, 2012b; Weinberg et al., 2009; Weinberg and Mark, 2008). Anatexis was restricted to the shear zone, where melting of a calc-alkaline batholith produced leucosomes with peritectic Hbl and the surrounding metasedimentary rocks melted without producing anhydrous peritectic phases. Magmas derived from these two different sources shared a single network within the shear zone and hybridized along the way (Hasalová et al., 2011; Reichardt et al., 2010). Like other water-fluxed anatectic terranes, melting in the Karakoram Shear Zone was long-lived and multi-pulsed, lasting ~5 m.yr.

For the *Nanga Parbat, Pakistan*, Butler et al. (1997) documented fluid infiltration to 15 km depth along shear zones where they triggered localized anatexis. Zircon and monazite thermometry indicates
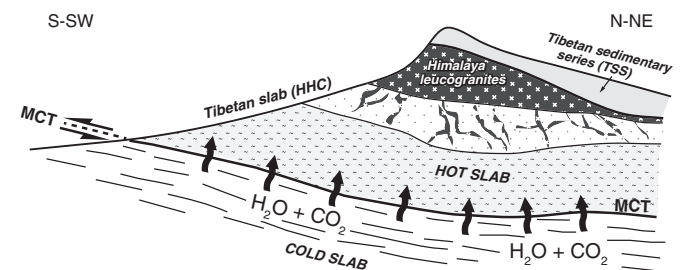
Fig. 10. Origin of Himalayan leucogranites (from Le Fort et al., 1987). Underthrusted cool rocks released water to the hot overlying slab that underwent melting.

leucogranite melt temperatures in the range of 700–720 °C allowing for either "melting during fluid infiltration or fluid-absent anatexis by the incongruent melting of muscovite." Butler et al. (1997) argued that fluid-present melting would not give rise to mobile magmas and used considerations around Rb, Sr and Ba of the leucogranites to conclude that the main phase of leucogranites formed by Ms-dehydration reaction.

6.2. Inverted metamorphic gradient: regional thrusting

Orogenic thrust fronts, where hot slabs are thrust over cold rocks, are key tectonic settings where water-fluxed melting may occur (Fig. 10; e.g. Berger et al., 2008; Finch et al., 2014; Hasalová et al., 2008; Holk and Taylor, 2000; Le Fort et al., 1987; Rubatto et al., 2013; Sawyer, 2010). In this setting, the cold rocks in the footwall heat up and release water through dehydration metamorphic reactions. Water may travel upwards and up-temperature into rocks at or above the water-saturated solidus (discussed in Clemens and Vielzeuf, 1987). In this case, the ascent of cold fluids has to overcome the stable water density gradient and therefore migration must be driven by tectonic pressure gradients (Berger et al., 2008).

England and Thompson (1986) modelled the thermal evolution of a thrust belt, akin to the Himalayas, to investigate conditions appropriate for melt production. They considered that during thrusting, water-rich low-grade crustal rocks are buried and that their metamorphism releases 2–3 wt.% H_2O. They argued that the high porosity resulting from retaining all of the released fluid would be unlikely but that nevertheless, transient high porosity would accompany fluid production.

In the Himalayas, leucogranite formation has been linked to movement on major thrust faults and water-fluxed melting above the Main Central Thrust (Fig. 10; Le Fort et al., 1987; Vidal et al., 1982). Other authors have demonstrated that melting in the Himalayan front is more complex, possibly involving several melting events including both water-fluxing and Ms-dehydration (Finch et al., 2014; Harris et al., 1993; Knesel and Davidson, 2002; Pognante, 1992; Rubatto et al., 2013).

In the High Himalayan Crystallines of Zanskar, NW India, dehydration melting of an orthogneiss was followed by voluminous melting associated with water influx (Pognante, 1992). Melting started during thrusting to the SW, possibly before or around 26 Ma and continued as the shear sense changed to normal movement with top-to-NE shear sense along the South Tibetan Detachment (Finch et al., 2014). Normal movement led to exhumation of the anatectic footwall causing fast cooling and ending the anatectic event by ~20 Ma (Finch et al., 2014). A possible source of fluids in this case is the underthrusted cooler rocks below the Main Central Thrust (as proposed by Le Fort et al., 1987). Voluminous melting associated with water influx (Pognante, 1992) may have been responsible for weakening of the rock mass and initiating normal movement in order to decrease the taper angle (Finch et al., 2014). Similarly, Holk and Taylor (2000) postulated a possible link between water-fluxed anatexis during crustal thickening of the Canadian Cordillera and its subsequent extensional collapse and the exhumation of metamorphic core complexes (see also the Iberian Massif migmatization during ductile shearing related to post-collisional crustal thinning (Escuder-Viruete, 1999)).

In summary, shear zones act both as channels for capturing regional fluids and then for extracting melts, playing a key role in the generation, extraction and emplacement of magmas generated by water-fluxing (Fig. 9a). Thrust belts provide an ideal setting for water-fluxed melting, particularly where the geothermal gradient is inverted and fluids are released at depth by metamorphic reactions (Fig. 10). Melts produced in this setting are free to rise, whether or not they are water-saturated, because they encounter higher temperatures as they rise.

7. Recycling of magmatic fluids

Magmas advect heat and fluids. These fluids may be exsolved and released into the surroundings where they can cause melting (Berger et al., 2008; Collins et al., 1989; Holk and Taylor, 1997, 2000; Yardley and Barber, 1991a) forming the secondary magmas of Finger and Clemens (1995). Mantle-derived magmas formed above subduction zones are typically rich in fluids (Plank et al., 2013; Wallace, 2005). These fluids are expected to go into late-magmatic igneous amphiboles at depth (Davidson et al., 2007), and any excess will go into hydrating surrounding rocks and promoting water-fluxed melting (Annen and Sparks, 2002; Huppert and Sparks, 1988). Given fluctuations in thermal conditions and water fluxing in the interior of arcs, the remelting of magmatic rocks intruded early during arc history is expected to be common (Symington et al., 2014; Tamura and Tatsumi, 2002; Vogel et al., 2004; Weinberg and Dunlap, 2000; White et al., 2011a).

Geochemical modelling of island arc granitoids emplaced in the Norwegian Caledonides suggests they originated from anatexis of a mantle-derived, mafic source rock at the base of the crust, remelted under variable water activity and coexisting with various garnet-bearing residues (Hansen et al., 2002). In this case, mafic magma intrusions were a likely source of heat and volatiles for remelting. Symington et al. (2014) described anatexis of intrusive arc rocks of the St Peter Arc, South Australia that remelted to form migmatites as a result of fluctuations in fluid and thermal influx released by younger intrusions. Here, leucosomes generally lack peritectic phases (congruent melting), except in the vicinity or within diorites, where hornblende is the peritectic phase (Fig. 7).

Davidson et al. (2007) postulated based on REE ratios in arc volcanic rocks that amphibole cumulates form where magmas stall and cool at depth, filtering water out. These rocks could later be remelted producing large volumes of intermediate-silicic hydrous melt. An alternative explanation for the REE ratios they found is that water exsolved from newly intruded juvenile magmas triggers anatexis of slightly older magmatic rocks generating peritectic hornblende, such as in the St. Peter Suite. Separation of anatectic melt from peritectic amphiboles could equally well give rise to fractionated melts with the REE pattern documented by Davidson et al. (2007).

Holk and Taylor (1997, 2000) documented the use and reuse of the same water in metamorphic core complexes of the Canadian Rockies during repeated events of partial melting of fertile rocks, explaining their remarkable homogeneity of mineral $\delta^{18}O$ values. They suggested that melting of metasedimentary rocks began in response to influx of aqueous fluid associated with thrusting and local muscovite breakdown. Water-rich melts ascended and released fluids as they decompressed leading to melting of other fertile rocks.

The Moldanubian zone, Bohemian Massif, is an example from a continental collision. Finger and Clemens (1995) concluded that regional contact metamorphism around intrusive magmas provided the heat and water that generated a secondary Bt–Hbl granodiorite described as "a cool, wet, restite-rich mid-crustal magma that remained close to its site of generation". This granitoid has I-type characteristics, lacking anhydrous peritectic phases.

Local intrusions may cause aureole melting (Fig. 9b; e.g. Ballachulish Igneous Complex or the Eltive granite, both in Scotland; Droop and Brodie, 2012; Pattison and Harte, 1988; Rigby et al., 2008). Importantly, during contact metamorphism, prograde metamorphic reactions are often overstepped, providing a free fluid phase that can be used for melting (e.g. Acosta-Vigil et al., 2010; Brearley and Rubie, 1990; Buick et al., 2004). When melt does not escape, it can result in presence of large amounts of melt at relatively low temperatures.

At a larger scale, the underplating and intraplating of large volumes of mantle-derived, fluid-rich arc magmas may be the regional source of fluids introduced into hot sections of the crust (Finger and Clemens, 1995; Symington et al., 2014; Vernon and Clarke, 2008). These fluids may migrate through relatively narrow channels, such as shear zones, ponding at specific locations such as low pressure or permeability traps causing widespread melting (see Section 8.1).
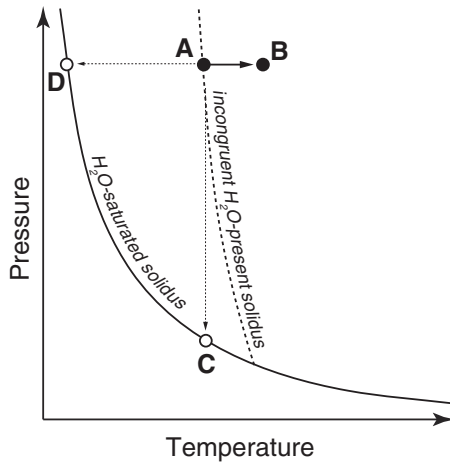
Fig. 11. P–T diagram illustrating the "free-ride layer" or how melts generated by incongruent melting reactions with negative dP/dT are able to rise. Melt produced at point A and heated to point B will crystallize upon cooling back to A if in chemical equilibrium with restitic source. If melt in A is segregated and no longer in chemical contact with restite, its new solidus is the water-saturated solidus, point C, for example, allowing considerable ascent before crystallization. Melt produced in point A is water undersaturated and if it undergoes isobaric cooling, it crystallizes gradually as its water activity increases towards saturation at point D, where the last melt finally solidifies. Adapted from Clemens and Droop (1998).

7.1. Melt extraction and the free-ride layer

Once segregated, granitic melt crystallizes at a lower temperature solidus than the source or residue (Fig. 11; Clemens and Droop, 1998). When melt resulting from incongruent reactions is no longer in chemical equilibrium with the restite, its new solidus is the water-saturated solidus, at lower temperatures than that of the melting reaction that produced the melt. Leitch and Weinberg (2002) explored this feature to explain how magmas chemically segregated from their source are free to rise through solid rocks. This is their free-ride layer, a section of the crust above the anatectic region where magmas can rise pervasively through solid rocks but are not exposed to freezing. As these magmas crystallize they transfer fluids and rehydrate solid crust or trigger melting.

8. How aqueous fluids flow into suprasolidus crust?

The influx of aqueous fluids into a suprasolidus terrane is straightforward when it results from fluids released from intrusive magmas. In some cases, such as in Broken Hill described above (White et al., 2005), fluid is released from dehydration reactions in one rock and consumed in melting reactions in another. There are however many natural examples where metamorphic fluids have flowed into rocks that were above their water-saturated solidus. Just how this happens is less clear. In this section we return to this question first raised in the introduction.

8.1. Shear zones and fracturing

The efficiency of fluid flow in shear zones in triggering melting depends on the degree of fluid–rock interaction (Fig. 9a). If fluid flow is efficient, fluid–rock interaction is minimized with little melting of the surroundings (Clemens and Vielzeuf, 1987). In this case, shear zones become major channels for aqueous fluids that are capable of invading suprasolidus crustal regions when travelling up-temperature. Once in these regions, changes in the nature of the shear zones may promote increased fluid–rock interaction and widespread melting (Fig. 9a).

Fractures in hot terranes may also act as fluid channels (Fig. 12a; Sawyer, 2010). Although the low viscosity of hot rocks, combined with considerable lithostatic pressures, tend to inhibit fracture propagation, high fluid pore pressures or high strain rates can drive fracturing. Ductile fracturing is a possible alternative fracturing process in ductile terranes where water-filled pores interconnect through recrystallization of the surroundings developing shear fractures (Weinberg and Regenauer-Lieb, 2010). Once fluids flow into fractures in suprasolidus terranes, small scale advection and diffusion of water into the surroundings (Acosta-Vigil et al., 2012), driven by a combination of high fluid pressures in microcracks and chemical potential (White and Powell, 2010), lead to melting of the walls (Fig. 12b). In the process, the melt zone widens but this will ultimately hamper further fluid influx because the channel walls may lose their integrity becoming a low viscosity mass that traps fluids (Fig. 12c).
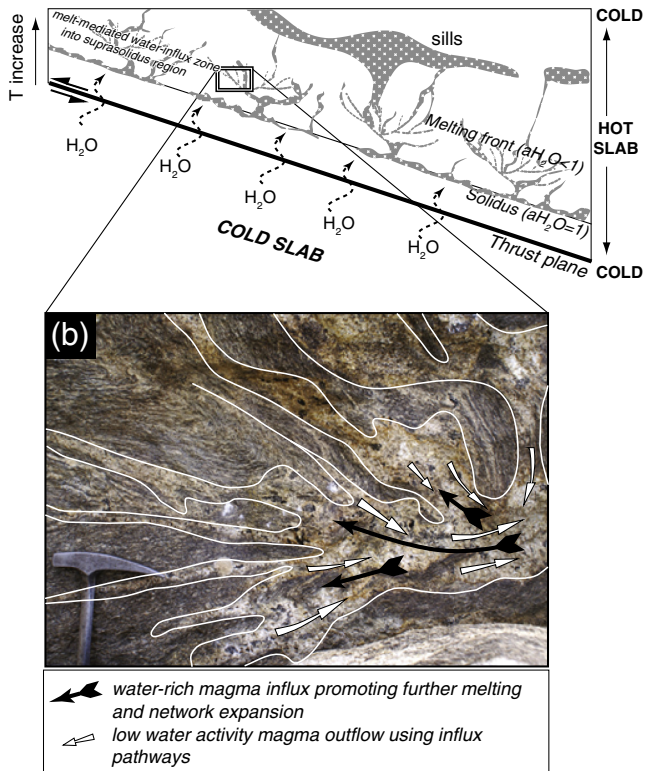
8.2. Regional metamorphic fluids

Whilst fracturing and magma intrusion may explain the ingress of fluids into some suprasolidus terranes, the advection of regional, metamorphic fluids into hot terranes is complicated by the natural barrier represented by the water-saturated solidus (Cartwright and Buick, 1998; Cartwright et al., 1995). Fluids reaching rocks at these conditions promote melting. The volume decrease accompanying water-saturated melting triggers a pressure drop, thus attracting more fluids into the area in a positive feedback. Pressure drop combined with the propensity of water-saturated melts to crystallize upon decompression effectively trap the melts unable to rise. This may have been the case in the Trois Seigneurs area (Wickham, 1987; Wickham and Taylor, 1985) where the downward influx of groundwater fluids stopped at shallow crustal levels above a hotter, dry basement. We have seen above how shear zones and fractures may facilitate the
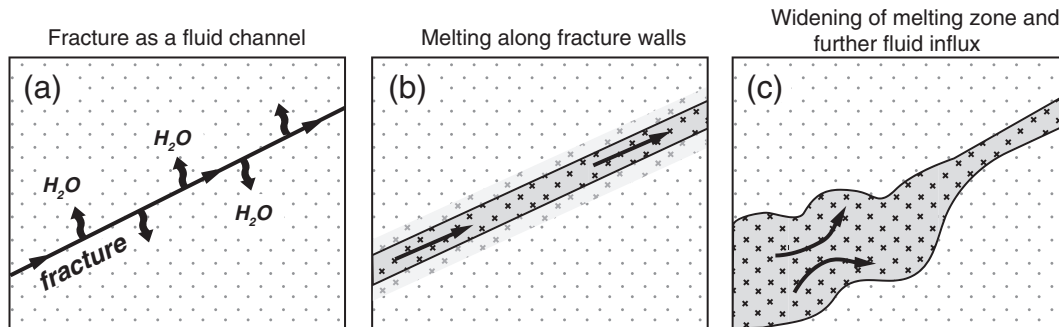
Fig. 12. Aqueous fluid ingress into a terrane at conditions above the water-saturated solidus through a fracture. (a) Fluids trigger water-saturated melting of the surroundings. (b) Melt zone expands outwards from the fracture establishing a water activity gradient from the high activity of the inflowing fluids and the water activity for the melt in equilibrium with the rock at the melt front, dictated by the existing P–T conditions. (c) As melt fraction increases, the fracture walls become ductile, and fluids are no longer able to invade the suprasolidus rocks, and incoming fluid is consumed by rock melting and spreads into an expanding melt pool ((a) and (b) after Sawyer, 2010).
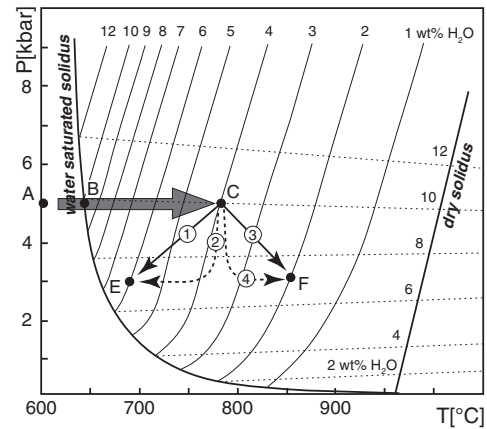
(a) Thrust: inverted thermal gradient

Fig. 14. Evolution of haplogranite undergoing decompression with different T paths. Starting from point C where a haplogranite with 2 wt.% H_2O has a melt fraction of 50% and $aH_2O = 0.4$, we investigate melt decompression paths through a static crust. We envisage pervasive melt migration where melt interacts with the surroundings. In cooling during decompression, melt following path (1) is in thermal equilibrium with the surroundings, and increases its crystal fraction along the way in order to increase its water content to 6% at E and maintain equilibrium. Path (2) indicates a rapid, isothermal magma ascent followed by thermal equilibration to point E. During the isobaric cooling stage to reach point E melt will gradually crystallize, reaching point E with effectively the same melt fraction as magma following path 1. The two paths differ only in the rate of crystallization. Melt undergoing decompression heating (paths 3 and 4) may trigger further melting of the surroundings. Melt travelling rapidly (path 4) reaches point F with 4 wt.% H_2O. Here, it doubles its mass in order to dilute its excess water content to 2 wt.% H_2O, as dictated by the new P–T conditions. Melt following path 3, equilibrates along the way, generating more melt as it progresses, and reaches point F with $aH_2O \sim 0.2$. See main text for details.

Fig. 13. (a) Aqueous fluid influx into a thrusted block with inverted geothermal gradient. Melting starts when fluid reaches water-saturated solidus conditions ($aH_2O = 1$). Magma rises up-temperature and becomes the water-transport agent triggering melting of suprasolidus rocks and decreasing the water activity of the melt, as dictated by the minimum water content curves (Fig. 4). In this way magma migration establishes an upward expanding magma network. Melting is restricted further upwards by the presence of cooler rocks closer to the surface. Beyond the melting front, undersaturated magmas generated by water-fluxing are capable of intruding unmelted rocks. (b) Magma influx pathways may also be magma extraction pathways depending on fluctuations in melt pressure in the system responding to changes in local and regional pressure gradients. If an interconnected melt network already exists in rocks undergoing dehydration melting, this could be exploited and expanded by influx of water-rich magmas. Photograph of Tur-bearing leucosomes in the Higher Himalayan Crystallines from Zanskar, NW India.

ingress of water into hot rocks, and in Section 4.3 we explored the impact of heating on the water content of melts produced (Fig. 4d) and concluded that for rock-dominated systems, water-fluxing will generate water-undersaturated melts capable of rising. In this section, we consider two other processes where regional metamorphic fluids and melt can promote water-fluxed melting in suprasolidus rocks: (i) up-temperature migration of melt (Fig. 13), and (ii) the effects of brines (Figs. 8 and 9a).

8.2.1. Up-temperature migration of melt

Up-temperature migration of fluids and melts (Fig. 13a) is driven by tectonic pressure gradients (Cartwright et al., 1995) required to overwhelm opposing buoyancy effects. This flow may be directed along the same depth, downwards (Petrini and Podladchikov, 2000), or upwards, in the case of inverted geothermal gradients as discussed earlier (Figs. 10 and 13a; e.g. Finch et al., 2014; Genier et al., 2008; Hollister and Crawford, 1986; Le Fort et al., 1987; Pognante, 1992).

Figure 14 contrasts the paths of magma ascent and cooling with those undergoing heating and illustrates how magma may become the melting agent (paths 3 and 4). Magma migrating up-temperature will have water activities out of equilibrium with its surroundings. This promotes

water-fluxed melting in order to decrease the water activity in the magma and reach the value dictated by the liquidus curves. This process gives rise to increased melt volumes and undersaturated, low water activity melts. Because this occurs at conditions above the water-saturated solidus, some breakdown of muscovite and/or biotite may occur simultaneously, generating anhydrous peritectic minerals. These are the migmatites described above which contain low proportions of peritectic phases relative to the volume of leucosome, and large volumes of leucosomes for the estimated peak metamorphic conditions.

Water-fluxed anatexis is ultimately rock-buffered, implying that aqueous fluids added to the rock is consumed in melting reactions. However, there are possible scenarios in which this may not be the case and magmas may have excess water and coexist with aqueous fluids. For example, rapid water influx into a limited volume of rock could raise water content beyond the maximum water content (in Fig. 4c), if only temporarily. Another example is when a melting reaction, taking place at the water-saturated solidus, runs out of one of the solid reactants, for example K-feldspar in a tonalite protolith (Sawyer, 2010). In this case, melting stops until the temperature reaches the higher values required to melt the rock without this reactant. During this period any added fluids may coexist with melt as a separate phase until melting resumes.

8.2.2. Brines

Aranovich et al., (2013) showed how brines have a potent effect on the water activity of aqueous fluids (Fig. 8). Although brines may be a relatively uncommon metamorphic fluid, melting curves of rocks in their presence have a positive slope in PT diagrams, implying that these melts can decompress/rise without solidifying. This could be an efficient way of generating voluminous melts, at relatively low-T by water-undersaturated fluids where anhydrous minerals such as Opx may be stable (Fig. 8). Unlike dehydration melting there is no theoretical limit for the amount of fluids in the system and as described above, low water activity allows brines to permeate into rocks at granulite

facies conditions until it intersects the solidus curve, where it promotes melting (Fig. 8).

8.3. Leucosome networks: influx of water and extraction of magma

In migmatite terranes, channels used to flux the terrane with aqueous fluids are likely to be reused to extract magma generated in situ (Fig. 13b). As discussed in Section 8.2, pervasive migration (Leitch and Weinberg, 2002; Morfin et al., 2013; Weinberg and Searle, 1998) of out-of-equilibrium magma (high water activity) may promote melting of low water activity surroundings, leading to an increase in both melt fraction and permeability. This increases magma throughput, creating a positive feedback effect. For a hot terrane already undergoing dehydration melting, an incipient melt segregation network may be exploited by the ingress of water-rich magma that promotes further melting as it equilibrates with the surrounding.

9. Water activity gradients around fluid sources

We have seen above multiple ways in which water can be transported into terranes at amphibolite and granulite facies. Aqueous fluids or water-rich magmas are driven by pressure gradients and may themselves drive fracturing of hot terranes and promote water-fluxed melting by setting up chemical potential gradients with dry surroundings (White and Powell, 2010).

Figure 15 shows a hypothetical case of the ingress of water into a hot and dry terrane by means of intrusion of a water-saturated magma, similar to the process discussed in Fig. 4d. In this case, an anatectic front develops in the surroundings. If the volume of intruded magma is limited, then the melt front reaches a maximum width and the

Fig. 15. Influx of water-saturated melt through a fracture into a hot terrane. This melt with ~10 wt.% H_2O is out of equilibrium with the surrounding that is comprised of a quartzo-feldspathic rock at 5 kbar and 760 °C. At these conditions, the minimum water content of granitic melts in equilibrium with the rock is ~4.5% dictated by the liquidus curve (see Fig. 4c), So the intruded melt will promote melting of the surroundings. For a limited volume of intruded melt, the melt front will expand until the water content of the intrusive plus in situ anatectic melt reach 4.5 wt.% H_2O.

water content of the intrusive and the new anatectic melts equilibrate and are dictated by the liquidus curve for the prevailing P–T conditions. If melt migrates continuously through the fracture plane, bringing in more fluids, the anatectic front expands into the country rock as a diffusion front with water content and activity within the melt decreasing towards that of the liquidus for the prevailing P–T conditions (Ni and Zhang, 2008). At the front itself melting progresses across a steep and narrow diffusional front.

Considering a range of rock types hosting the intrusion in Fig. 15, such as a layered pelitic–psammitic sequence, different layers may have different solidi and different initial water activities. Some bands may melt preferentially in response to the intrusion and a positive feedback process may be established whereby the presence of melt enhances permeability and the rate of water diffusion (Acosta-Vigil et al., 2006), leading to increased melt fraction. Ultimately such a process of preferential water ingress may lead to stromatic layering.
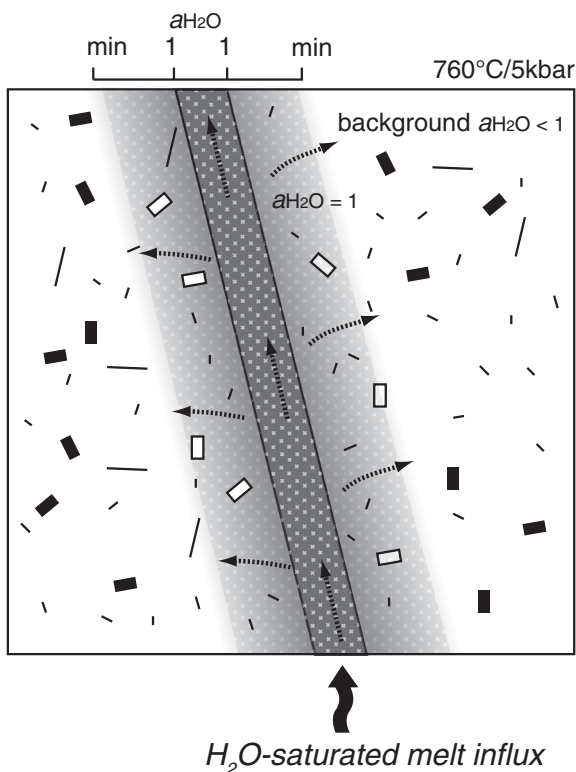
In summary, the influx of aqueous fluids, whether directly or indirectly through water-rich melts, will set up a water activity gradient in the surroundings, with high activities at the point of ingress, decaying with distance and varying as a function of time (Fig. 15). Melting will take place in an evolving water activity environment. Because the volume of fluids in the lower parts of the crust is limited, most water-fluxed anatexis are essentially rock-buffered, and whilst fluid influx raises the water activity temporarily and locally, the system will ultimately equilibrate at the water activity dictated by the P–T conditions (Fig. 4c). Interestingly, and in stark contrast to dehydration melting, a new pulse of aqueous fluids or water-rich melts may cause renewed melting, including remelting of early-formed quartzo-feldspathic leucosomes (Fig. 6, Section 4.7).

There is growing evidence that chemical potential gradients play an important role in partially molten rocks, increasing melt fraction, influencing mineral assemblage and textures developed (e.g. Morgan et al., 2008; Štípská et al., 2014; White and Powell, 2010). White and Powell (2010) demonstrated the important role of chemical potentials between dry residue and wet leucosome in a migmatite. Water diffuses from wet leucosome to restite, promoting crystallization of hydrous phases in the restite and anhydrous phases in the leucosome. Diffusion of water is also accompanied by diffusion of other mobile elements (such as Na, K), which causes change in Qtz, Kfs and Pl proportions in the leucosome and its chemistry. They also suggested that water diffusion away from leucosomes promotes melt crystallization and thus increases the proportion of leucosomes by contrast to the amount of melt crystallized when in chemical isolation (no diffusion gradient). This could potentially enhance melt segregation and allow for expulsion of remaining melt out of the system.

10. Summary and conclusions

Water-fluxed melting is found in diverse crustal environments and varies in scale from local to regional. Water-fluxed melting typically conjures the thought of immobile water-saturated melts when in fact this is a particular case of the more general process of a system that is ultimately rock-dominated, where aqueous fluids, either as a separate phase or dissolved in melts, are consumed to generate large volumes of low water activity melts capable of migrating through the crust.

We have seen that water-fluxed melting is not restricted to the P–T conditions of the water-saturated solidus but range between those of the water-saturated solidus and dehydration melting (Fig. 1). Aqueous fluids can infiltrate suprasolidus rocks in a number of ways and give rise to undersaturated melts. Due to the relatively small volumes of water available in the deeper parts of the crust, anatexis tends to be rock-buffered, so that an aqueous fluid and a hydrous melt only coexist in equilibrium at the water-saturated solidus and aqueous fluids will typically be entirely consumed in melting reactions. The most significant feature of water-fluxed melting is its capacity to produce voluminous melting (Fig. 3), even at amphibolite facies conditions, and in the

absence of significant modal proportions of peritectic phases. This leads to a mismatch between the melt fraction generated and those calculated assuming dehydration melting at peak P–T conditions.

At upper amphibolite facies, water-fluxed melting will typically cause congruent melting and form minimum melts. At higher temperatures, it may be associated with incongruent melting and dehydration melting of micas, associated with the production of hornblende or nominally anhydrous peritectic minerals. A number of incongruent melting reactions have been proposed to account for the paragenesis encountered in water-fluxed suprasolidus terranes (Table 2). These melts are undersaturated in water and capable of rising to form plutons. The influx of even relatively small volumes of fluids early in the prograde path can significantly affect the volumes of melt produced during subsequent dehydration reactions.

Crustal regions at P–T conditions at the water-saturated solidus tend to trap aqueous fluids. Here water is consumed in melting reactions and the negative ΔV of the reaction causes a pressure drop that attracts more fluids from the surroundings and holds the melt in the anatectic region. Nevertheless, there are numerous examples where aqueous fluids have by-passed this trap and reached the core of hot terranes (Table 3). The water-saturated solidus trap may be overcome in two major ways. One way is through the direct influx of fluids by means of efficient fluid channels such as fractures and shear zones (Figs. 9a and 12), intrusion of water-rich magmas (Fig. 9b) or influx of fluids with low water activity, such as brines (Fig. 8). In these cases, the aqueous fluid is initially out of equilibrium with the surroundings, and fluxing generates undersaturated melts that are upwardly mobile and anhydrous peritectic phases in the source. The other way is through up-temperature migration of water-saturated magmas either in regions of inverted geothermal gradient (Figs. 10, 11, 13a) or by lateral or downward migration. In these cases magma migration is unrestricted by decompression crystallization. Pervasive up-temperature magma migration causes water-fluxed melting generating undersaturated (aH$_2$O < 1) melts, with water contents defined by the liquidus curves in Johannes and Holtz (1996) (Figs. 4 and 14). This is a process of water-fluxed melting mediated by water-rich anatectic melts that may be common in anatectic terranes. We conclude that only water-saturated melts that remain in or close to the source will ever record high water activity. All other anatectic melts that are extracted from their immediate source and exposed to interaction with suprasolidus rocks are likely to lose this signature by melting the surroundings and equilibrating at low water activity values.

It is often argued that one of the limiting factors for water-fluxing hot terranes is their expected low porosity and permeability. The combination of deformation, magmatism and metamorphism gives rise to the release of aqueous fluids at depth, and to transient pressure gradients and permeable paths that drive fluid migration. Tectonic activity is responsible for the burial of hydrous rocks, as deep fluid sources, and for maintaining pressure gradients that drive fluid and melt migration, as well as maintaining high permeability channels, and geothermal gradients that favour water-fluxing and melt migration. Water-fluxed melting is controlled by permeable pathways and variable water fluxes lead to heterogeneous melt production from place to place, even at a metre scale, as well as multiple melting events during a single tectono-thermal event, leading to a spread in zircon and monazite ages (Rubatto et al., 2009). Fluid influx sets up a water content gradient in the hot surroundings, rising locally and temporarily the water activity in surrounding rocks and driving melting (Fig. 15).

Water-fluxed melting may impact in the continued development of an orogen. For example for both the Zanskar Himalayas and the Canadian Rocky Mountains, water-fluxed melting may have weakened the core of the orogeny triggering the onset of a period of extension. Furthermore, water-fluxed melting consumes energy buffering peak metamorphic temperatures. Given that the presence of small volumes of an aqueous fluid phase can have a large impact in the volume of melt produced at temperatures above the water-saturated solidus, and given that such undersaturated melts have the capacity to rise, we conclude that water-fluxed melting may have a significant impact on crustal differentiation.

We finish this review by emphasizing that water-fluxing can give rise to a complete range of melts with a range of water activities and generated at P–T conditions anywhere between the water-saturated solidus and the dehydration melting curves. This implies that the difference between water-fluxed and dehydration melting may not always be evident, but may be inferred from careful petrological investigation of migmatites. It is currently difficult to determine whether aqueous fluids were involved in magma genesis when the source is not exposed. We have the impression that the literature tends to assume, implicitly or explicitly, that granitoids generated by crustal anatexis are a result of dehydration melting reactions. This need not be the case and water may have played a significant role in their genesis.

References

Acosta-Vigil, A., London, D., Morgan, G.B., Dewers, T.A., 2003. Solubility of excess alumina in hydrous granitic melts in equilibrium with peraluminous minerals at 700–800 °C and 200 MPa, and applications of the aluminum saturation index. Contribution to Mineralogy and Petrology 146, 100–119.

Acosta-Vigil, A., London, D., Morgan, G.B., 2006. Experiments on the kinetics of partial melting of a leucogranite at 200 MPa H$_2$O and 690–800 °C: Compositional variability of melts during the onset of H$_2$O-saturated crustal anatexis. Contributions to Mineralogy and Petrology 151, 539–557.

Acosta-Vigil, A., Buick, I., Hermann, J., Cesare, B., Rubatto, D., London, D., Morgan VI, G.B., 2010. Mechanisms of crustal anatexis: a geochemical study of partially melted metapelitic enclaves and host dacite, SE Spain. Journal of Petrology 51, 785–821.

Acosta-Vigil, A., London, D., Morgan, G.B., 2012. Chemical diffusion of major components in granitic liquids: Implications for the rates of homogenization of crustal melts. Lithos 153, 308–323.

Aikman, A.B., Harrison, T.M., Hermann, J., 2012. The origin of Eo- and Neo-Himalayan granitoids, Eastern Tibet. Journal of Asian Earth Sciences 58, 143–157.

Alonso Perez, R., Müntener, O., Ulmer, P., 2009. Igneous garnet and amphibolite fractionation in the roots of island arcs: experimental constraints on andesite liquids. Mineralogy and Petrology 157, 541–558.

Annen, C., Sparks, R.S.J., 2002. Effects of repetitive emplacement of basaltic intrusions on thermal evolution and melt generation in the crust. Earth and Planetary Science Letters 203, 937–955.

Aranovich, L.Y., Newton, R.C., Manning, C.E., 2013. Brine-assisted anatexis: Experimental melting in the system haplogranite-H$_2$O–NaCl–KCl at deep-crustal conditions. Earth and Planetary Science Letters 374, 111–120.

Baker, J., 1990. Stable isotopic evidence for fluid–rock interactions in the Ivrea Zone, Italy. Journal of Petrology 31, 243–260.

Barker, F., 1979. Trondhjemite: definition, environment and hypotheses of origin. In: Barker, F. (Ed.), Trondhjemites, dacites, and related rocks. DEV PETROL 6, pp. 1–12.

Bartoli, O., Cesare, B., Poli, S., Acosta-Vigil, A., Esposito, R., Turina, A., Bodnar, R.J., Angel, R.J., Hunter, J., 2013a. Nanogranite inclusions in migmatitic garnet: behavior during piston-cylinder remelting experiments. Geofluids 13, 405–420.

Bartoli, O., Cesare, B., Poli, S., Bodnar, R.J., Acosta-Vigil, A., Frezzotti, M.L., Meli, S., 2013b. Recovering the composition of melt and the fluid regime at the onset of crustal anatexis and S-type granite formation. Geology 41, 115–118.

Beard, J.S., Lofgren, G.E., 1991. Dehydration melting and water-saturated melting of basaltic and andesitic greenstones and amphibolites at 1, 3, and 6. 9 kb. Journal of Petrology 32, 365–401.

Becker, A., Holtz, F., Johannes, W., 1998. Liquidus temperatures and phase compositions in the system Qz–Ab–Or at 5 kbar and very low water activities. Contributions to Mineralogy and Petrology 130, 213–224.

Behrens, H., Nowak, M., 1997. The mechanisms of water diffusion in polymerized silicate melts. Contributions to Mineralogy and Petrology 126, 377–385.

Berger, A., Burri, T., Alt-Epping, P., Engi, M., 2008. Tectonically controlled fluid flow and water-assisted melting in the middle crust: An example from the Central Alps. Lithos 102, 598–615.

Brearley, A.J., Rubie, D.C., 1990. Effects of H$_2$O on the disequilibrium breakdown of muscovite + quartz. Journal of Petrology 31, 925–956.

Brown, M., 1973. The definition of metatexis, diatexis and migmatite. Proceedings of the Geologists' Association 84, 371–382.

Brown, M., 1979. The petrogenesis of the St. Malo migmatite belt, Armorican Massif, France, with particular reference to the diatexites. Neues Jahrbuch für Mineralogie - Abhandlungen 135, 48–74.

Brown, M., 2007. Crustal melting and melt extraction, ascent and emplacement in orogens: Mechanisms and consequences. Journal of the Geological Society 164, 709–730.

Brown, M., 2013. Granite: From genesis to emplacement. Bulletin of the Geological Society of America 125, 1079–1113.

Brown, M., Korhonen, F.J., 2009. Some remarks on melting and extreme metamorphism of crustal rocks. In: Gupta, A.K., Dasgupta, S. (Eds.), Physics and Chemistry of the Earth's Interior. Springer, New Delhi, pp. 67–88.

Brown, M., Averkin, Y.A., McLellan, E.L., Sawyer, E.W., 1995. Melt segregation in migmatites. Journal of Geophysical Research 100 (B8) (15655-11567).

Buick, I.S., Stevens, G., Gibson, R.L., 2004. The role of water retention in the anatexis of metapelites in the Bushveld Complex Aureole, South Africa: An experimental study. Journal of Petrology 45, 1777–1797.

Burri, T., Berger, A., Engi, M., 2005. Tertiary migmatites in the Central Alps: regional distribution, field relations, conditions of formation, and tectonic implications. Schweizerische Mineralogische und Petrographische Mitteilungen 85, 215–232.

Büsch, W., Schneider, G., Mehnert, K.R., 1974. Initial melting at grain boundaries. Part II: melting in rocks of granodioritic, quartz dioritic, and tonalitic composition. Neues Jahrbuch für Mineralogie 8, 345–370.

Butler, R.W.H., Harris, N.B.W., Whittington, A.G., 1997. Interactions between deformation, magmatism and hydrothermal activity during active crustal thickening: A field example from Nanga Parbat, Pakistan Himalayas. Mineralogical Magazine 61, 37–52.

Campbell, I.H., Taylor, S.R., 1983. No water, no granites — no oceans, no continents. Geophysical Research Letters 10, 1061–1064.

Carrington, D.P., Harley, S.L., 1996. Cordierite as a monitor of fluid and melt H_2O contents in the lower crust: an experimental calibration. Geology 24, 647–650.

Carrington, D.P., Watt, G.R., 1995. A geochemical and experimental study of the role of K-feldspar during water-undersaturated melting of metapelites. Chemical Geology 122, 59–76.

Carroll, M.R., Wyllie, P.J., 1990. The system tonalite–H_2O at 15 kbar and the genesis of calc-alkaline magmas. American Mineralogist 75, 345–357.

Cartwright, I., 1994. The two-dimensional pattern of metamorphic fluid flow at Mary Kathleen, Australia: fluid focussing, transverse dispersion, and implications for modelling fluid flow. American Mineralogist 79, 526–535.

Cartwright, I., Buick, I.S., 1998. The link between oxygen isotope resetting, partial melting, and fluid flow in metamorphic terrains. Terra Nova 10, 81–85.

Cartwright, I., Vry, J., Sandiford, M., 1995. Changes in stable isotope ratios of metapelites and marbles during regional metamorphism, Mount Lofty Ranges, South Australia: implications for crustal scale fluid flow. Contributions to Mineralogy and Petrology 120, 292–310.

Castro, A., 2013. Tonalite–granodiorite suites as cotectic systems: A review of experimental studies with applications to granitoid petrogenesis. Earth-Science Reviews 124, 68–95.

Castro, A., Corretge, L.G., El-Biad, M., El-Hmidi, H., Fernandez, C., Patiño Douce, A.E., 2000. Experimental constraints on Hercynian anatexis in the Iberian Massif, Spain. Journal of Petrology 41, 1471–1488.

Cherneva, Z., Georgieva, M., 2007. Amphibole-bearing leucosome from the Chepelare area, Central Rhodopes: P–T conditions of melting and crystallization. Geochemistry, Petrology and Mineralogy 45, 79–95.

Clemens, J.D., 1984. Water contents of silicic to intermediate magmas. Lithos 17, 273–287.

Clemens, J.D., 2009. The message in the bottle: "Melt" inclusions in migmatitic garnets. Geology 37, 671–672.

Clemens, J.D., Droop, G.T.R., 1998. Fluids, P–T paths and the fates of anatectic melts in the Earth's crust. Lithos 44, 21–36.

Clemens, J.D., Petford, N., 1999. Granitic melt viscosity and silicic magma dynamics in contrasting tectonic settings. Journal of the Geological Society, London 156, 1057–1060.

Clemens, J.D., Vielzeuf, D., 1987. Constraints in melting and magma production in the crust. Earth and Planetary Science Letters 86, 287–306.

Clemens, J.D., Wall, V.J., 1981. Origin and crystallization of some peraluminous (S-type) granitic magmas. Canadian Mineralogist 19, 111–131.

Clemens, J.D., Watkins, J.M., 2001. The fluid regime of high-temperature metamorphism during granitoid magma genesis. Contributions to Mineralogy and Petrology 140, 600–606.

Cloos, M., 1984. Landward-dipping reflectors in accretionary wedges: Active dewatering conduits? Geology 12, 519–522.

Collins, W.J., Flood, R.H., Vernon, R.H., Shaw, S.E., 1989. The Wuluma granite, Arunta Block, central Australia: An example of in situ, near-isochemical granite formation in a granulite–facies terrane. Lithos 23, 63–83.

Conrad, W.K., Nicholls, I.A., Wall, V.J., 1988. Water-saturated and -undersaturated melting of metaluminous and peraluminous crustal compositions at 10 kbar: Evidence for the origin of silicic magmas in the Taupo volcanic zone, New Zealand, and other occurrences. Journal of Petrology 29, 765–803.

Davidson, J., Turner, S., Handley, H., Macpherson, C., Dosseto, A., 2007. Amphibole "sponge" in arc crust? Geology 35, 787–790.

Dingwell, D.B., Romano, C., Hess, K.-U., 1996. The effect of water on the viscosity of a haplogranitic melt under P–T–X conditions relevant to silicic volcanism. Contributions to Mineralogy and Petrology 124, 19–28.

Droop, G.T.R., Brodie, K.H., 2012. Anatectic melt volumes in the thermal aureole of the Etive Complex, Scotland: The roles of fluid-present and fluid-absent melting. Journal of Metamorphic Geology 30, 843–864.

Drummond, M.S., Defant, M.J., 1990. A model for trondhjemite–tonalite–dacite genesis and crustal growth via slab melting: Archean to modern comparisons. Journal of Geophysical Research 95, 21,503–21,521.

Ebadi, A., Johannes, W., 1991. Beginning of melting and composition of first melts in the system Qz–Ab–Or–H_2O–CO_2. Contributions to Mineralogy and Petrology 106, 286–295.

Ellis, D.J., Obata, M., 1992. Migmatite and melt segregation at Cooma, New South Wales. Transactions of the Royal Society of Edinburgh: Earth Sciences 83, 95–106.

England, P.C., Thompson, A., 1986. Some thermal and tectonic models for crustal melting in continental collision zones. Geological Society Special Publication 19, 83–94.

Escuder-Viruete, J., 1999. Hornblende-bearing leucosome development during synorogenic crustal extension in the Tormes Gneiss Dome, NW Iberian Massif, Spain. Lithos 46, 751–772.

Ferry, J.M., Watson, E.B., 2007. New thermodynamic models and revised calibrations for the Ti-in-zircon and Zr-in-rutile thermometers. Contributions to Mineralogy and Petrology 154, 429–437.

Finch, M., Hasalová, P., Weinberg, R.F., Fanning, M.C., 2014. Switch from thrusting to extension in the Zanskar Shear Zone, NW Himalaya: Implications for channel flow. Geological Society of America Bulletin 126, 892–924.

Finger, F.C., Clemens, J.D., 1995. Migmatization and "secondary" granitic magmas: effects of emplacement and crystallization of "primary" granitoids in Southern Bohemia, Austria. Contributions to Mineralogy and Petrology 120, 311–326.

Fornelli, A., Piccarreta, G., Del Moro, A., Acquafredda, P., 2002. Multi-stage melting in the lower crust of the Serre (Southern Italy). Journal of Petrology 43, 2191–2217.

Friend, C.R.L., 1983. The link between charnockite formation and granite production: evidence from Kabbaldurga, Karnataka, Southern India. In: Atherton, M.P., Gribble, D.C. (Eds.), Migmatites, Melting and Metamorphism. Nantwich, Shiva, pp. 264–276.

Fyfe, W.S., Price, N.J., Thompson, A.B., 1978. Fluids in the Earth's Crust. Elsevier, Amsterdam.

Gardien, V., Thompson, A.B., Ulmer, P., 2000. Melting of biotite + plagioclase + quartz gneisses; the role of H_2O in the stability of amphibole. Journal of Petrology 41, 651–666.

Genier, F., Bussy, F., Epard, J.L., Baumgartner, L., 2008. Water-assisted migmatization of metagraywackes in a Variscan shear zone, Aiguilles–Rouges massif, western Alps. Lithos 102, 575–597.

Gibbon, D.L., Wyllie, P.J., 1969. Experimental studies of igneous rock series: the Farrington Complex, North Carolina, and the Star Mountain Rhyolite, Texas. Journal of Geology 77, 221–239.

Giordano, D., Romano, C., Dingwell, D.B., Poe, B., Behrens, H., 2004. The combined effects of water and fluorine on the viscosity of silicic magmas. Geochimica et Cosmochimica Acta 68, 5159–5168.

Green, T.H., 1982. Anatexis of mafic crust and high pressure crystallization of andesite. In: Thorpe, R.S. (Ed.), Andesites. John Wiley, London, pp. 465–487.

Hansen, J., Skjerlie, K.P., Pedersen, R.B., De La Rosa, J., 2002. Crustal melting in the lower parts of island arcs: an example from the Bremanger Granitoid Complex, west Norwegian Caledonides. Contributions to Mineralogy and Petrology 143, 316–335.

Harley, S.L., Carrington, D.P., 2001. The distribution of H_2O between cordierite and granitic melt: H_2O incorporation in cordierite and its application to high-grade metamorphism and crustal anatexis. Journal of Petrology 42, 595–1620.

Harris, N.B.W., Inger, S., 1992. Trace element modelling of pelite-derived granites. Contributions to Mineralogy and Petrology 110, 46–56.

Harris, N., Massey, J., Inger, S., 1993. The role of fluids in the formation of High Himalayan leucogranites. Geological Society Special Publication 74, 391–400.

Harrison, T.M., Watson, E.B., Aikman, A.B., 2007. Temperature spectra of zircon crystallization in plutonic rocks. Geology 35, 635–638.

Hasalová, P., Štípská, P., Powell, R., Schulmann, K., Janoušek, V., Lexa, O., 2008. Transforming mylonitic metagranite by open-system interactions during melt flow. Journal of Metamorphic Geology 26, 55–80.

Hasalová, P., Weinberg, R.F., MacRae, C., 2011. Microstructural evidence for magma confluence and reusage of magma pathways: Implications for magma hybridization, Karakoram Shear Zone in NW India. Journal of Metamorphic Geology 29, 875–900.

Hayden, L.A., Watson, E.B., 2007. Rutile saturation in hydrous siliceous melts and its bearing on Ti-thermometry of quartz and zircon. Earth and Planetary Science Letters 258, 561–568.

Hoefs, J., 1980. Stable Isotope Geochemistry. Springer Verlag, Heidelberg.

Holk, G.J., Taylor Jr., H.P., 1997. $^{18}O/^{16}O$ homogenization of the middle crust during anatexis: The Thor-Odin metamorphic core complex, British Columbia. Geology 25, 31–34.

Holk, G.J., Taylor Jr., H.P., 2000. Water as a petrologic catalyst driving $^{18}O/^{16}O$ homogenization and anatexis of the middle crust in the metamorphic core complexes of British Columbia. International Geology Review 42, 97–130.

Höller, W., Hoinkes, G., 1996. Fluid evolution during high-pressure partial melting in the Austroalpine Ulten Zone, Northern, Italy. Mineralogy and Petrology 58, 131–144.

Hollister, L.S., Crawford, M.L., 1986. Melt-enhanced deformation: a major tectonic process. Geology 14, 558–561.

Holtz, F., Barbey, P., 1991. Genesis of peraluminous granites II. mineralogy and chemistry of the tourem complex (North Portugal). sequential melting vs. restite unmixing. Journal of Petrology 32, 959–978.

Holtz, F., Johannes, W., 1991. Genesis of peraluminous granites I. Experimental investigation of melt compositions at 3 and 5 kb and various H_2O activities. Journal of Petrology 32, 935–958.

Holtz, F., Johannes, W., 1994. Maximum and minimum water contents of granitic melts: implications for chemical and physical properties of ascending magmas. Lithos 32, 149–159.

Holtz, F., Johannes, W., Pichavant, M., 1992a. Peraluminous granites: the effect of alumina on melt composition and coexisting minerals. Transactions of the Royal Society of Edinburgh: Earth Sciences 83, 409–416.

Holtz, F., Pichavant, M., Barbey, P., Johannes, W., 1992b. Effects of H_2O on liquidus phase relations in the haplogranite system at 2 and 5 kbar. American Mineralogist 77, 1223–1241.

Holtz, F., Scaillet, B., Behrens, H., Schulze, F., Pichavant, M., 1996. Water content of felsic melts: application to the rheological properties of granitic magmas. Transactions of the Royal Society of Edinburgh: Earth Sciences 87, 57–64.

Holtz, F., Roux, J., Behrens, H., Pichavant, M., 2000. Water solubility in silica and quartzofeldspathic melts. American Mineralogist 85, 682–686.

Holtz, F., Johannes, W., Tamic, N., Behrens, H., 2001. Maximum and minimum water contents of granitic melts generated in the crust: A reevaluation and implications. Lithos 56, 1–14.

Huang, W.L., Wyllie, P.J., 1973. Melting relations of muscovite–granite to 35 kbar as a model for fusion of metamorphosed subducted oceanic sediments. Contributions to Mineralogy and Petrology 42, 1–14.

Huppert, H.E., Sparks, S.J., 1988. The generation of granitic melts by intrusion of basalt into continental crust. Journal of Petrology 29, 599–624.

Icenhower, J., London, D., 1995. An experimental study of element partitioning among biotite, muscovite, and coexisting peraluminous silicic melt at 200 MP (H2O). American Mineralogist 80, 1229–1251.

Ingebritsen, S.E., Manning, C.E., 2010. Permeability of the continental crust: Dynamic variations inferred from seismicity and metamorphism. Geofluids 10, 193–205.

Inger, S., Harris, N., 1993. Geochemical constraints on leucogranite magmatism in the Langtang Valley, Nepal Himalaya. Journal of Petrology 34, 345–368.

Johannes, W., 1985. The significance of experimental studies for the formation of migmatites. In: Ashworth, J.R. (Ed.), Migmatites. Blackie and Son, Glasgow, pp. 36–85.

Johannes, W., Holtz, F., 1990. Formation and composition of H2O-undersaturated granitic melts. In: Asworth, J.R., Brown, M. (Eds.), High-Temperature Metamorphism and Crustal Anatexis. Unwin Hyman, London, pp. 87–104.

Johannes, W., Holtz, F., 1991. Formation and ascent of granitic magmas. Geologische Rundschau 80, 225–231.

Johannes, W., Holtz, F., 1996. Petrogenesis and Experimental Petrology of Granitic Rocks. Springer, (335 pp.).

Johnson, T.E., Hudson, N.F.C., Droop, G.T.R., 2001. Melt segregation structures within the Inzie Head gneisses of the northeastern Dalradian. Scottish Journal of Geology 37, 59–72.

Johnson, T.E., Gibson, R.L., Brown, M., Buick, I.S., Cartwright, I., 2003a. Partial Melting of metapelitic Rocks Beneath the Bushveld Complex, South Africa. Journal of Petrology 44, 789–813.

Johnson, T.E., Brown, M., Solar, G.S., 2003b. Low-pressure subsolidus and suprasolidus phase equilibria in the MnNCKFMASH system: Constraints on conditions of regional metamorphism in western Maine, northern Appalachians. American Mineralogist 88, 624–638.

Johnson, T.E., White, R.W., Powell, R., 2008. Partial melting of metagreywacke: A calculated mineral equilibria study. Journal of Metamorphic Geology 26, 837–853.

Johnson, T.E., Brown, M., Kaus, B.J.P., Vantongeren, J.A., 2014. Delamination and recycling of Archaean crust caused by gravitational instabilities. Nature Geoscience 7, 47–52.

Johnston, A.D., Wyllie, P.J., 1988. Interaction of granitic and basic magmas: experimental observations on contamination processes at 10 kbar with H2O. Contributions to Mineralogy and Petrology 98, 352–362.

Jung, S., Hoernes, S., Mezger, K., 2000. Geochronology and petrology of migmatites from the Proterozoic Damara Belt — importance of episodic fluid-present disequilibrium melting and consequences for granite petrology. Lithos 51, 153–179.

Jung, C., Jung, S., Nebel, O., Hellebrand, E., Masberg, P., Hoffer, E., 2009. Fluid-present melting of meta-igneous rocks and the generation of leucogranites — Constraints from garnet major- and trace element data, Lu–Hf whole rock–garnet ages and whole rock Nd–Sr–Hf–O isotope data. Lithos 111, 220–235.

Kalsbeek, F., Jepsen, H.F., Jones, K.A., 2001. Geochemistry and petrogenesis of S-type granites in the East Greenland Caledonides. Lithos 57, 91–109.

Kenah, C., Hollister, L.S., 1983. Anatexis in the Central Gneiss Complex, British Columbia. In: Atherton, M.P., Gribble, C.D. (Eds.), Migmatites, Melting and Metamorphism. Shiva, Nantwitch, U.K., pp. 142–163.

Kisters, A.F.M., Ward, R.A., Anthonissen, C.J., Vietze, M.E., 2009. Melt segregation and far-field melt transfer in the mid-crust. Journal of the Geological Society, London 166, 905–918.

Knesel, K.M., Davidson, J.P., 2002. Insights into collisional magmatism from isotopic fingerprints of melting reactions. Science 296, 2206–2208.

Koester, E., Pawley, A.R., Fernandes, A.D., Porcher, C.C., Soliani Jr., E., 2002. Experimental melting of cordierite gneiss and the petrogenesis of syntranscurrent peraluminous granites in southern Brazil. Journal of Petrology 43, 1595–1616.

Kohn, M.J., Spear, F.S., Valley, J.W., 1997. Dehydration-melting and fluid recycling during metamorphism. Rangely Formation, New Hampshire, USA. Journal of Petrology 38, 1255–1277.

Kretz, R., 1983. Symbols for rock-forming minerals. American Mineralogist 68, 277–279.

Laporte, D., 1994. Wetting behavior of partial melts during crustal anatexis: the distribution of hydrous silicic melts in polycrystalline aggregates of quartz. Contributions to Mineralogy and Petrology 116, 486–499.

Lappin, A.R., Hollister, L.S., 1980. Partial melting in the Central Gneiss Complex near Prince Rupert, British Columbia. American Journal of Science 280, 518–545.

Le Breton, N., Thompson, A.B., 1988. Fluid-absent (dehydration) melting of biotite in metapelites in the early stages of crustal anatexis. Contributions to Mineralogy and Petrology 99, 226–237.

Le Fort, P., Cuney, M., Deniel, C., France-Lanord, C., Sheppard, S.M.F., Upreti, B.N., Vidal, P., 1987. Crustal generation of the Himalayan leucogranites. Tectonophysics 134, 39–57.

Lee, Y., Cho, M., 2013. Fluid-present disequilibrium melting in Neoarchean arc-related migmatites of Daeijak Island, western Gyeonggi Massif, Korea. Lithos 179, 249–262.

Leitch, A.M., Weinberg, R.F., 2002. Modelling granite migration by mesoscale pervasive flow. Earth and Planetary Science Letters 200, 131–146.

Maaloe, S., Wyllie, P.J., 1975. Water content of a granite magma deduced from the sequence of crystallization determined experimentally with water-undersaturated conditions. Contributions to Mineralogy and Petrology 52, 175–191.

Mancktelow, N.S., 2006. How ductile are ductile shear zones? Geology 34, 345–348.

McDermott, F., Harris, N.B.W., Hawkesworth, C.J., 1996. Geochemical constraints on crustal anatexis: A case study from the Pan-African Damara granitoids of Namibia. Contributions to Mineralogy and Petrology 123, 406–423.

McLellan, E.L., 1988. Migmatite structures in the Central Gneiss Complex, Boca de Quadra, Alaska. Journal of Metamorphic Geology 6, 517–542.

Milord, I., Sawyer, E.W., Brown, M., 2001. Formation of diatexite migmatite and granite magma during anatexis of semi-pelitic metasedimentary rocks: An example from St. Malo, France. Journal of Petrology 42, 487–505.

Mogk, D.W., 1992. Ductile shearing and migmatization at midcrustal levels in an Archean high-grade gneiss belt, Northern Gallatin Range, Montana, USA. Journal of Metamorphic Geology 10, 427–438.

Montel, J.M., Marignac, C., Barbey, P., Pichavant, M., 1992. Thermobarometry and granite genesis: the Hercynian low-P, high-T Velay anatectic dome (French Massif Central). Journal of Metamorphic Geology 10, 1–15.

Morfin, S., Sawyer, E.W., Bandyayera, D., 2013. Large volumes of anatectic melt retained in granulite facies migmatites: An injection complex in northern Quebec. Lithos 168–169, 200–218.

Morgan, G.B., Acosta-Vigil, A., London, D., 2008. Diffusive equilibration between hydrous metaluminous–peraluminous haplogranite liquid couples at 200 MPa (H2O) and alkali transport in granitic liquids. Contributions to Mineralogy and Petrology 155, 257–269.

Moyen, J.-F., Stevens, G., 2006. Experimental Constraints on TTG Petrogenesis: Implications for Archean Geodynamics. In: Benn, K., Mareschal, J.-C., Condie, K.C. (Eds.), Archean Geodynamics and Environments, Monographs. American Geophysical Union, Washington, D. C., pp. 149–178.

Nabelek, P.I., Glascock, M.D., 1995. Ree-depleted leucogranites, black hills, south Dakota: A consequence of disequilibrium melting of monazite-bearing schists. Journal of Petrology 36, 1055–1071.

Naney, M.T., 1983. Phase equilibria of rock-forming ferromagnesian silicates in granitic systems. American Journal of Science 283, 993–1033.

Naney, M.T., Swanson, S.E., 1980. The effect of Fe and Mg on crystallization in granitic systems. American Mineralogist 65, 639–653.

Nedelec, A., Minyem, D., Barbey, P., 1993. High-P-high-T anatexis of Archaean tonalitic grey gneisses: the Eseka migmatites, Cameroon. Precambrian Research 62, 191–205.

Ni, H., Zhang, Y., 2008. H2O diffusion models in rhyolitic melt with new high pressure data. Chemical Geology 250, 68–78.

Nowak, M., Behrens, H., 1997. An experimental investigation on diffusion of water in haplogranitic melts. Contributions to Mineralogy and Petrology 126, 356–376.

Otamendi, J.E., Patiño Douce, A.E., 2001. Partial melting of aluminous metagreywackes in the Northern Sierra de Comechingones, Central Argentina. Journal of Petrology 42, 1751–1772.

Otamendi, J.E., Patiño Douce, A.E., Demichelis, A.H., 1999. Amphibolite to granulite transition in aluminous greywackes from the Sierra de Comechingones, Cordoba, Argentina. Journal of Metamorphic Geology 17, 415–434.

Patiño Douce, A.E., 1996. Effects of pressure and H2O content on the compositions of primary crustal melts. Transactions of the Royal Society of Edinburgh: Earth Sciences 87, 11–21.

Patiño Douce, A.E., 2005. Vapor-absent melting of tonalite at 15–32 kbar. Journal of Petrology 46, 275–290.

Patiño Douce, A.E., Beard, J.S., 1995. Dehydration-melting of biotite gneiss and quartz amphibolite from 3 to 15 kbar. Journal of Petrology 36, 707–738.

Patiño Douce, A.E., Beard, J.S., 1996. Effects of P, f(O2) and Mg/Fe ratio on dehydration melting of model metagreywackes. Journal of Petrology 37, 999–1024.

Patiño Douce, A.E., Harris, N., 1998. Experimental constraints on Himalayan anatexis. Journal of Petrology 39 (4), 689–710.

Patiño Douce, A.E., Johnston, A.D., 1991. Phase equilibria and melt productivity in the pelitic system: implications for the origin of peraluminous granitoids and aluminous granulites. Contributions to Mineralogy and Petrology 107, 202–218.

Pattison, D.R.M., Harte, B., 1988. Evolution of structurally contrasting anatectic migmatites in the 3-kbar Ballachulish aureole, Scotland. Journal of Metamorphic Geology 6, 475–494.

Peacock, S.M., Rushmer, T., Thompson, A.B., 1994. Partial melting of subducting oceanic crust. Earth and Planetary Science Letters 121, 227–244.

Percival, J.A., 1991. Granulite–facies metamorphism and crustal magmatism in the Ashuanipi complex, Quebec–Labrador, Canada. Journal of Petrology 32, 1261–1297.

Peterson, J.W., Newton, R.C., 1989. Reversed experiments on biotite–quartz–feldspar melting in the system KMASH: implications for crustal anatexis. Journal of Geology 97, 465–485.

Pëto, P., 1976. An experimental investigation of melting reactions involving muscovite and paragonite in the silica-saturated portion of the system K2O–Na2O–Al2O3–SiO2–H2O to 15 kbar total pressure: United Kingdom Natural Environment Research Council.

Petrini, R., Podladchikov, Y., 2000. Lithospheric pressure–depth relationship in compressive regions of thickened crust. Journal of Metamorphic Geology 18, 67–77.

Pichavant, M., Holtz, F., McMillan, P.F., 1992. Phase relations and compositional dependence of H2O solubility in quartz–feldspar melts. Chemical Geology 96, 303–319.

Piwinskii, A.J., 1968. Experimental studies of igneous rock series Central Sierra Nevada Batholith, California. Journal of Geology 76, 548–570.

Plank, T., Kelley, K.A., Zimmer, M.M., Hauri, E.H., Wallace, P.J., 2013. Why do mafic arc magmas contain ~4 wt.% water on average? Earth and Planetary Science Letters 364, 168–179.

Pognante, U., 1992. Migmatites and leucogranites of Tertiary age from the High Himalayan Crystallines of Zanskar (NW India): a case history of anatexis of Paleozoic orthogneisses. Mineralogy and Petrology 46, 291–313.

Powell, R., 1983. Processes in granulite–facies metamorphism. In: Atherton, M.P., Gribble, C.D. (Eds.), Migmatites, Melting and Metamorphism. Shiva, Cheshire, pp. 27–139.

Powell, R., Guiraud, M., White, R.W., 2005. Truth and beauty in metamorphic phase equilibrias: Conjugate variables and phase diagrams. Canadian Mineralogist 43, 21–33.

Prince, C., Harris, N., Vance, D., 2001. Fluid-enhanced melting during prograde metamorphism. Journal of the Geological Society 158, 233–242.

Prouteau, G., Scaillet, B., Pichavant, M., Maury, R.C., 1999. Fluid-present melting of ocean crust in subduction zones. Geology 27, 1111–1114.

Prouteau, G., Scaillet, B., Pichavant, M., Maury, R.C., 2001. Evidence for mantle metasomatism by hydrous silicic melts derived from subducted oceanic crust. Nature 410, 197–200.

Ramberg, H., 1952. The Origin of Metamorphic and Metasomatic Rocks. Chicago University, Chicago Press.

Reichardt, H., Weinberg, R.F., 2012a. The dike swarm of the Karakoram shear zone, Ladakh, NW India: Linking granite source to batholith. Geological Society of America Bulletin 124, 89–103.

Reichardt, H., Weinberg, R.F., 2012b. Hornblende chemistry in meta- and diatexites and its retention in the source of leucogranites: An example from the Karakoram shear Zone, NW India. Journal of Petrology 53, 1287–1318.

Reichardt, H., Weinberg, R.F., Andersson, U.B., Fanning, M.C., 2010. Hybridization of granitic magmas in the source: the origin of the Karakoram Batholith, Ladakh, NW India. Lithos 116, 249–272.

Rigby, M.J., Droop, G.T.R., Bromiley, G.D., 2008. Variations in fluid activity across the Etive thermal aureole, Scotland: Evidence from cordierite volatile contents. Journal of Metamorphic Geology 26, 331–346.

Robertson, J.K., Wyllie, P.J., 1971. Rock–water systems, with special refrence to the water-deficient region. American Journal of Science 271, 252–277.

Rubatto, D., Hermann, J., Berger, A., Engi, M., 2009. Protracted fluid-induced melting during Barrovian metamorphism in the Central Alps. Contributions to Mineralogy and Petrology 158, 703–722.

Rubatto, D., Chakraborty, S., Dasgupta, S., 2013. Timescales of crustal melting in the Higher Himalayan Crystallines (Sikkim, Eastern Himalaya) inferred from trace element-constrained monazite and zircon chronology. Contributions to Mineralogy and Petrology 165, 349–372.

Rubie, D.C., 1986. The catalysis of mineral reactions by water and restrictions on the presence of aqueous fluid during metamorphism. Mineralogical Magazine 50, 399–415.

Rushmer, T., 1987. Fluid-absent melting of amphibolite — experimental results at 8 kbar. Terra Cognita 7, 286.

Rushmer, T., 1989. Granulites as residues of partial melting: experimental constrains. Terra Abstracts 1, 302.

Rushmer, T., 1991. Partial melting of two amphibolites: contrasting experimental results under fluid-absent conditions. Contributions to Mineralogy and Petrology 107, 41–59.

Rushmer, T., 2001. Volume change during partial melting reactions: Implications for melt extraction, melt geochemistry and crustal rheology. Tectonophysics 342, 389–405.

Rutter, E.H., Neumann, D.H.K., 1995. Experimental deformation of partially molten Westerly granite under fluid-absent conditions, with implications for the extraction of granitic magmas. Journal of Geophysical Research 100 (B8), 15697–15715.

Rye, R.O., Schuiling, R.D., Rye, D.M., Jansen, J.B.H., 1976. Carbon, hydrogen and oxygen isotope studies of the regional metamorphic complex at Naxos, Greece. Geochimica et Cosmochimica Acta 40, 1031–1049.

Sandiford, M., McLaren, S., 2002. Tectonic feedback and the ordering of heat producing elements within the continental lithosphere. Earth and Planetary Science Letters 204, 133–150.

Sawyer, E.W., 1998. Formation and evolution of granite magmas during crustal reworking: the significance of diatexites. Journal of Petrology 39, 1147–1167.

Sawyer, E.W., 2001. Melt segregation in the continental crust: distribution and movement of melt in anatectic rocks. Journal of Metamorphic Geology 19, 291–309.

Sawyer, E.W., 2008. Atlas of migmatites. Canadian Mineralogist, Special Publication 9. Mineralogical Association of Canada, (386 pp.).

Sawyer, E.W., 2010. Migmatites formed by water-fluxed partial melting of a leucogranodiorite protolith: Microstructures in the residual rocks and source of the fluid. Lithos 116, 273–286.

Scaillet, B., France-Lanord, C., Le Fort, P., 1990. Badrinath–Gangotri plutons (Garhwal, India): petrological and geochemical evidence for fractionation processes in a high Himalayan leucogranite. Journal of Volcanology and Geothermal Research 44, 163–188.

Scaillet, B., Holtz, F., Pichavant, M., Schmidt, M., 1996. Viscosity of Himalayan leucogranites: Implications for mechanisms of granitic magma ascent. Journal of Geophysical Research 101 (B12), 27691–27699.

Schulze, F., Behrens, H., Holtz, F., Roux, J., Johannes, W., 1996. The influence of H_2O on the viscosity of a haplogranitic melt. American Mineralogist 81, 1155–1165.

Sen, C., Dunn, T., 1994. Dehydration melting of a basaltic composition amphibolite at 1.5 and 2.0 GPa: implications for the origin of adakites. Contributions to Mineralogy and Petrology 117, 394–409.

Skjerlie, K.P., Johnston, A.D., 1993. Fluid-absent melting behavior of an F-rich tonalitic gneiss at mid-crustal pressures: Implications for the generation of anorogenic granites. Journal of Petrology 34, 785–815.

Skjerlie, K.P., Johnston, A.D., 1996. Vapour-absent melting from 10 to 20 kbar of crustal rocks that contain multiple hydrous phases: Implications for anatexis in the deep to very deep continental crust and active continental margins. Journal of Petrology 37, 661–691.

Slagstad, T., Jamieson, R.A., Culshaw, N.G., 2005. Formation, crystallization, and migration of melt in the mid-orogenic crust. Muskoka Domain migmatites, Grenville Province, Ontario. Journal of Petrology 46, 893–919.

Spear, F.S., 1993. Metamorphic Phase Equilibria and Pressure–Temperature–Time Paths. Mineralogical Society of America, Washington, D. C. (799 pp.).

Springer, W., Seek, H.A., 1997. Partial fusion of basic granulites at 5 to 15 kbar: Implications for the origin of TTG magmas. Contributions to Mineralogy and Petrology 127, 30–45.

Stevens, G., Clemens, J.D., 1993. Fluid-absent melting and the roles of fluids in the lithosphere: a slanted summary? Chemical Geology 108, 1–17.

Stevens, G., Clemens, J.D., Droop, G.T.R., 1997. Melt production during granulite–facies anatexis: experimental data from "primitive" metasedimentary protoliths. Contributions to Mineralogy and Petrology 128, 352–370.

Štípská, P., Powell, R., Racek, M., Lexa, O., 2014. Intermediate granulite produced by transformation of eclogite at a felsic granulite contact, in Blanský les, Bohemian Massif. Journal of Metamorphic Geology 32, 340–370.

Storkey, A.C., Hermann, J., Hand, M., Buick, I.S., 2005. Using in situ trace-element determinations to monitor partial-melting processes in metabasites. Journal of Petrology 46, 1283–1308.

Storre, B., 1972. Dry melting of muscovite + quartz in the range P = 7 kb to P = 20 kb. Contributions to Mineralogy and Petrology 37, 87–89.

Storre, B., Karotke, E., 1972. Experimental data on melting reactions of muscovite + quartz in the system $K_2O–Al_2O_3–SiO_2–H_2O$ to 20 kbar water pressure. Contributions to Mineralogy and Petrology 36, 343–345.

Symington, N.J., Weinberg, R.F., Hasalová, P., Wolfram, L.C., Raveggi, M., Armstrong, R.A., 2014. Multiple intrusions and remelting-remobilization events in a magmatic arc: The St. Peter Suite, South Australia. Geological Society of America Bulletin 126, 1200–1218.

Symmes, G.H., Ferry, J.M., 1995. Metamorphism, fluid flow and partial melting in pelitic rocks from the Onawa contact aureole, Central Maine, USA. Journal of Petrology 36, 587–612.

Tamura, Y., Tatsumi, Y., 2002. Remelting of an andesitic crust as a possible origin for rhyolitic magma in oceanic arcs: an example from the Izu–Bonin arc. Journal of Petrology 43, 1029–1047.

Tartèse, R., Boulvais, P., Poujol, M., Chevalier, T., Paquette, J.-L., Ireland, T.R., Deloule, E., 2012. Mylonites of the South Armorican Shear Zone: Insights for crustal-scale fluid flow and water–rock interaction processes. Journal of Geodynamics 56–57, 86–107.

Thompson, A.B., 1983. Fluid-absent metamorphism. Journal of the Geological Society 140, 533–547.

Thompson, A.B., 1982. Dehydration melting of pelitic rocks and the generation of h2O-undersaturated liquids. American Journal of Science 282, 1567–1595.

Thompson, A.B., 1990. Heat, fluids, and melting in the granulite facies. In: Vielzeuf, D., Vidal, P. (Eds.), Granulites and Crustal Evolution. Kluwer, Dordrecht-Netherlands, pp. 37–58.

Thompson, A.B., 2001. Clockwise P-T paths for crustal melting and H2O recycling in granite source regions and migmatite terrains. Lithos 56, 33–45.

Thompson, A.B., Connolly, J.A.D., 1995. Melting of the continental crust: some thermal and petrological constraints on anatexis in continental collision zones and other tectonic settings. Journal of Geophysical Research 100 (B8), 15565–15579.

Thompson, A.B., Tracy, R.J., 1979. Model systems for anatexis of pelitic rocks - II. Facies series melting and reactions in the system $CaO–KAlO_2–NaAlO_2–_{Al2O3}–SiO_2–H_2O$. Contributions to Mineralogy and Petrology 70, 429–438.

Timmermann, H., Jamieson, R.A., Parrish, R.R., Culshaw, N.G., 2002. Coeval migmatites and granulites, Muskoka domain, southwestern Grenville Province, Ontario. Canadian Journal of Earth Sciences 39, 239–258.

Tuttle, O.F., Bowen, N.L., 1958. Origin of granite in the light of experimental studies in the system $NaAlSi_3O_8–KAlSi_3O_8–SiO_2–H_2O$. Memoir of the Geological Society of America 74, 1–145.

Valley, J.W., O'Neil, J.R., 1984. Fluid heterogeneity during granulite facies metamorphism in the Adirondacks: stable isotope evidence. Contributions to Mineralogy and Petrology 85, 158–173.

Valley, J.W., Bohlen, S.R., Essene, E.J., Lamb, W., 1990. Metamorphism in the Adirondacks. II. The role of fluids. Journal of Petrology 35, 555–596.

Vernon, R.H., Collins, W.J., Richards, S.W., 2003. Contrasting magmas in metapelitic and metapsammitic migmatites in the Cooma Complex, Australia. Visual Geosciences 8.

Vernon, R.H., 2007. Problems in identifying restite in S-type granites of southeastern Australia, with speculations on sources of magma and enclaves. Canadian Mineralogist 45, 147–178.

Vernon, R.H., Clarke, G.L., 2008. Principles of Metamorphic Petrology. Cambridge University Press, New York.

Vernon, R.H., Richards, S.W., Collins, W.J., 2001. Migmatite–granite relationships: Origin of the Cooma Granodiorite magma, Lachlan Fold Belt, Australia. Physics and Chemistry of the Earth 26, 267–271.

Vidal, P., Cocherie, A., Le Fort, P., 1982. Geochemical investigations of the origin of the Manaslu leucogranite(Himalaya, Nepal). Geochimica et Cosmochimica Acta 46, 2279–2292.

Vielzeuf, D., Clemens, J.D., 1992. The fluid-absent melting of phlogopite + quartz: experiments and models. American Mineralogist 77, 1206–1222.

Vielzeuf, D., Holloway, J.R., 1988. Experimental determination of the fluid-absent melting relations in the pellitic system. Contributions to Mineralogy and Petrology 98, 257–276.

Vielzeuf, D., Montel, J.M., 1994. Partial melting of metagreywackes. Part I. Fluid-absent experiments and phase relationships. Contributions to Mineralogy and Petrology 117, 375–393.

Vielzeuf, D., Schmidt, M.W., 2001. Melting relations in hydrous systems revisited: Application to metapelites, metagreywackes and metabasalts. Contributions to Mineralogy and Petrology 141, 251–267.

Vogel, T.A., Patino, L.C., Alvarado, G.E., Gans, P.B., 2004. Silicic ignimbrites within the Costa Rican volcanic front: evidence for the formation of continental crust. Earth and Planetary Science Letters 226, 149–159.

Wallace, P.J., 2005. Volatiles in subduction zone magmas: Concentrations and fluxes based on melt inclusion and volcanic gas data. Journal of Volcanology and Geothermal Research 140, 217–240.

Ward, R., Stevens, G., Kisters, A., 2008. Fluid and deformation induced partial melting and melt volumes in low-temperature granulite–facies metasediments, Damara Belt, Namibia. Lithos 105, 253–271.

Watkins, J.M., Clemens, J.D., Treloar, P.J., 2007. Archaean TTGs as sources of younger granitic magmas: Melting of sodic metatonalites at 0.6–1.2 GPa. Contributions to Mineralogy and Petrology 154, 91–110.

Watson, E.B., Harrison, T.M., 2005. Zircon Thermometer Reveals Minimum Melting Conditions on Earliest Earth. Science 308, 841–844.

Watt, G.R., Harley, S.L., 1993. Accessory phase controls on the geochemistry of crustal melts and restites produced during water-undersaturated partial melting. Contributions to Mineralogy and Petrology 114, 550–566.

Webb, G., Powell, R., McLaren, S., 2014. The effect of sub-solidus water loss on the melt fertility of crustal source rocks: constraints from phase equilibria modelling. Geophysical Research Abstracts 16, EGU2014–10010-1.

Weinberg, R.F., Dunlap, W.J., 2000. Growth and deformation of the Ladakh Batholith, northwest Himalayas: implications for timing of continental collision and origin of calc-alkaline batholiths. The Journal of Geology 108, 303–320.

Weinberg, R.F., Mark, G., 2008. Magma migration, folding, and disaggregation of migmatites in the Karakoram Shear Zone, Ladakh, NW India. Geological Society of America Bulletin 120, 994–1009.

Weinberg, R.F., Podladchikov, Y., 1994. Diapiric ascent of magmas through power-law crust and mantle. Journal of Geophysical Research 99 (B5), 9543–9559.

Weinberg, R.F., Regenauer-Lieb, K., 2010. Ductile fractures and magma migration from source. Geology 38, 363–366.

Weinberg, R.F., Searle, M.P., 1998. The Pangong Injection Complex, Indian Karakoram: A case of pervasive granite flow through hot viscous crust. Journal of the Geological Society, London 155, 883–891.

Weinberg, R.F., Mark, G., Reichardt, H., 2009. Magma ponding in the Karakoram Shear Zone, Ladakh, NW India. Geological Society of America Bulletin 121, 278–285.

Weinberg, R.F., Hasalová, P., Ward, L., Fanning, M.C., 2013. Interaction between deformation and magma extraction in migmatites: Examples from Kangaroo Island, South Australia. Geological Society of America Bulletin 125, 1282–1300.

White, R.W., Powell, R., 2010. Retrograde melt-residue interaction and the formation of near-anhydrous leucosomes in migmatites. Journal of Metamorphic Geology 28, 579–597.

White, R.W., Pomroy, N.E., Powell, R., 2005. An in situ metatexite–diatexite transition in upper amphibolite facies rocks from Broken Hill, Australia. Journal of Metamorphic Geology 23, 579–602.

White, L.T., Ahmad, T., Ireland, T.R., Lister, G.S., Forster, M.A., 2011a. Deconvolving episodic age spectra from zircons of the Ladakh Batholith, northwest Indian Himalaya. Chemical Geology 289, 179–196.

White, R.W., Stevens, G., Johnson, T.E., 2011b. Is the crucible reproducible? Reconciling melting experiments with thermodynamic calculations. Elements 7, 241–246.

Whittington, A., Richet, P., Behrens, H., Holtz, F., Scaillet, B., 2004. Experimental temperature-$X(H_2O)$-viscosity relationship for leucogranites and comparison with synthetic silicic liquids. Transactions of the Royal Society of Edinburgh: Earth Sciences 95, 59–71.

Wickham, S.M., 1987. The segregation and emplacement of granitic magma. Journal of the Geological Society, London 144, 281–297.

Wickham, S.M., Taylor Jr., H.P., 1985. Stable isotopic evidence for large-scale seawater infiltration in a regional metamorphic terrane; the Trois Seigneurs Massif, Pyrenees, France. Contributions to Mineralogy and Petrology 91, 122–137.

Wolf, M.B., Wyllie, P.J., 1994. Dehydration-melting of amphibolite at 10 kbar: the effects of temperature and time. Contributions to Mineralogy and Petrology 115, 369–383.

Wyllie, P.J., 1977. Crustal anatexis: An experimental review. Tectonophysics 43, 41–71.

Wyllie, P.J., Wolf, M.B., 1993. Amphibolite dehydration-melting: sorting out the solidus. Geological Society Special Publication 76, 405–416.

Wyllie, P.J., Huang, W.L., Stern, C.R., Maaloe, S., 1976. Granitic magmas: possible and impossible sources, water contents, and crystallization sequences. Canadian Journal of Earth Sciences 13, 1007–1019.

Yardley, B.W.D., 2009. The role of water in the evolution of the continental crust. Journal of the Geological Society, London 166, 585–600.

Yardley, B.W.D., Barber, J.P., 1991a. Melting reactions in the Connemara Schists: the role of water infiltration in the formation of amphibolite facies migmatites. American Mineralogist 76, 848–856.

Yardley, B.W.D., Barber, J.P., 1991b. Water availability and partial melting in the Connemara Schists, Ireland. Geologica Carpathica 42, 3–9.

Yardley, B.W.D., Valley, J.W., 1997. The petrologic case for a dry lower crust. Journal of Geophysical Research 102, 12173–12185.

Yoder, H.S., Tilley, C.E., 1962. Origin of basalt magmas: An experimental study of natural and synthetic rock systems. Journal of Petrology 3, 342–532.

Zack, T., Moraes, R., Kronz, A., 2004. Temperature dependence of Zr in rutile: Empirical calibration of a rutile thermometer. Contributions to Mineralogy and Petrology 148, 471–488.

Zamora, D., 2000. Fusion de la croute oceanique subductee: approche experimentale et geochimiquePhD thesis Universite Blaise-Pascal, Clermont-Ferrand.

Zeng, L., Saleeby, J.B., Ducea, M., 2005a. Geochemical characteristics of crustal anatexis during the formation of migmatite at the Southern Sierra Nevada, California. Contributions to Mineralogy and Petrology 150, 386–402.

Zeng, L., Asimow, P.D., Saleeby, J.B., 2005b. Coupling of anatectic reactions and dissolution of accessory phases and the Sr and Nd isotope systematics of anatectic melts from a metasedimentary source. Geochimica et Cosmochimica Acta 69, 3671–3682.